Heidi Öblom

Printing Technologies for Personalization of Dosage Forms

A study in Pharmaceutical Sciences

Åbo Akademi University

Heidi Öblom

Born 1989 in Hangö, Finland

Previous degrees

M.Sc. in Bioscience (Pharmacy), Åbo Akademi University, 2016

B.Sc. in Pharmacy, Åbo Akademi University, 2010

Printing Technologies for Personalization of Dosage Forms

A study in Pharmaceutical Sciences

Heidi Öblom

Pharmaceutical Sciences Laboratory
Faculty of Science and Engineering
Åbo Akademi University
Åbo, Finland, 2021

Supervisors

Main supervisor

Prof. Dr. Niklas Sandler
Pharmaceutical Sciences Laboratory
Åbo Akademi University, Finland

Official assistant supervisor

Associate Prof. Dr. Natalja Genina
Department of Pharmacy
University of Copenhagen, Denmark

External assistant supervisor

Prof. Dr. Jukka Rantanen
Department of Pharmacy
University of Copenhagen, Denmark

Reviewers

Prof. Dr. Clive Roberts
School of Pharmacy
University of Nottingham, United Kingdom

Associate Prof. Dr. João F. Pinto
Faculty of Pharmacy
University of Lisbon, Portugal

Opponent

Prof. Dr. Clive Roberts
Head of School of Pharmacy
University of Nottingham, United Kingdom

ISBN (Print) 978-952-12-4132-1
ISBN (Digital) 978-952-12-4133-8

Painosalama Oy, Åbo, Finland, 2021

Preface

This thesis is based on research conducted at Åbo Akademi University, Finland in the Drug-Delivery and Pharmaceutical Technology Research Group, Pharmaceutical Sciences Laboratory (PSL), Faculty of Science and Engineering in 2016-2019. Additionally, research has been conducted during the one-month external research stay at the Department of Pharmaceutics and Drug Delivery, University of Mississippi, USA in 2016, and the one-year external research stay in the Materials and Manufacturing (M&M) group at the Department of Pharmacy, University of Copenhagen, Denmark in 2019-2020.

Abstract (English)

Along with the recognized advantages of personalized medicine, a demand for new manufacturing technologies that allow for production of such products has emerged. Conventional pharmaceutical manufacturing techniques that have been used for production of dosage forms based on the 'one-size-fits-all' concept are not always suitable for manufacturing personalized dosage forms due to the lack of flexibility. Printing technologies have been explored for this purpose as their precise and flexible nature allows for on-demand printing of a limitless number of product designs with various personalization features, e.g., patient-tailored drug content, drug release profile, and customized functionality.

In this thesis, three different printing technologies, i.e., fused deposition modeling (FDM), semisolid extrusion 3D printing (EXT), and inkjet printing (IJP), were used to prepare personalized solid dosage forms. Although all are printing techniques they require vastly different properties of the starting materials, involving solid, semisolid, and liquid states of matter. The starting materials prepared in this thesis were: drug-loaded filaments for FDM, drug-loaded viscous dispersion for EXT, and drug-loaded ink solutions, as well as drug-free substrates for IJP. In the first study, FDM was utilized to print oral tablets with a personalized dose and tailored drug release of the model active pharmaceutical ingredient (API) isoniazid. This was achieved by modifying the digital design of tablets to be printed enabling printing of various-sized tablets with two different internal infill levels. In the second study, EXT and IJP were successfully used for production of orodispersible films (ODFs) containing 0.1-2 mg warfarin sodium (henceforward called warfarin). Regardless of the technique used to print warfarin, the desired dose was achieved by depositing the drug-containing feedstock material in a single layer. The printed ODFs were shown to have properties on par and even superior in some aspects compared to the oral powders in unit dose sachets (OPSs) compounded at hospital pharmacies today. The ODFs, moreover, offer ease of administration to pediatrics without the need for water. In the third study, IJP was used to prepare personalized data-enriched edible pharmaceuticals (DEEP) containing two cannabinoids. The cannabinoid-containing ink was deposited on a porous solid foam (substrate) in an information-rich pattern (IRP), enabling simultaneous incorporation of information and APIs (cannabinoids) in a single IRP. The dose was tailored by imprinting the solid foam with 1-10 layers of the drug-containing ink. IRPs offer the possibility to incorporate personalized information e.g., for the patient, caregiver, nurse as well as enable traceability and identification of solid dosage forms on a single dosage unit level. This could e.g., be used for improved treatment outcomes, preventing falsified medicines from entering the supply chain, preventing medication errors, or avoiding drug abuse.

This thesis gives an overview of different printing technologies used in the pharmaceutical field and contributes to the understanding of critical

parameters for fabrication of personalized solid oral dosage forms. Moreover, it provides insight into the requirements and possible limitations of the different printing technologies that need to be considered along with the printed API(s) and the desired properties of the final solid oral dosage form. EXT is a versatile method that enables production of both low- and high-dose dosage forms at room temperature. However, EXT typically requires post-processing steps such as drying or curing which adds to the manufacturing time and may cause deformation of the printed solid dosage form. IJP has the benefit of allowing easy incorporation of personalized IRPs on a single dosage unit, as well as the possibility to accurately prepare low-dose solid dosage forms. IJP is typically limited to fabrication of low-dose solid dosage forms as the technique is based on deposition of droplets in the picoliter range. Preparation of high doses by means of IJP would require a large volume of ink to be absorbed into the substrate. FDM has the strength in enabling production of complex inner structures, which e.g., can be used for tailoring of the drug release. One of the recognized drawbacks of the technology is the need for intermediate filaments used as feedstock material. Preparation of printable filaments with a high drug load has been proven challenging.

Abstract (Swedish)

De erkända fördelarna med individanpassad läkemedelsbehandling har resulterat i att det uppstått en efterfrågan på nya metoder som möjliggör tillverkning av sådana läkemedel. Konventionella farmaceutiska tillverkningsmetoder som huvudsakligen använts för tillverkning av läkemedel är baserade på konceptet ”one-size-fits-all” där grundtanken bl.a. är att en eller ett fåtal dosstyrkor av ett visst läkemedel är lämpliga för alla patienter. De konventionella tillverkningsmetoderna är inte alltid ändamålsenliga för tillverkning av individualiserade läkemedel på grund av teknologiernas otillräckliga flexibilitet. Utskriftsteknologier, som till sin natur både är flexibla och exakta, har därför studerats för detta ändamål. De möjliggör vid behov tillverkning av läkemedel i små satser. Läkemedel som framställs med hjälp av utskriftsteknologier kan ha ett obegränsat antal strukturer och mönster vilket möjliggör inkorporering av olika individualiseringsfunktioner, t.ex. patientskräddarsytt läkemedelsinnehåll, dos och läkemedelsfrisättningsprofil samt anpassad funktionalitet.

I denna avhandling användes tre olika utskriftsteknologier, närmare bestämt fused deposition modeling (FDM), semisolid extrusion 3D printing (EXT) och bläckstråleutskrift (IJP), för att tillverka individanpassade orala fasta läkemedel. Startmaterialen som används för de studerade utskriftsteknologierna har varierande egenskaper (material i lösningsform, halvfast form samt fast form) beroende på vilken teknologi som används. Startmaterial som formulerades och framställdes för läkemedelsutskrivning i denna avhandling var läkemedelsinnehållande filament (polymertrådar) för FDM, läkemedelsinnehållande viskös dispersion för EXT och läkemedelsbläck (lösning med låg viskositet) samt läkemedelsfria substrat för IJP. I den första studien användes FDM för att skriva ut orala isoniazid tabletter med individuella doser samt skräddarsydd läkemedelsfrisättning. Detta uppnåddes genom modifiering av den digitala designen av tabletterna som skulle skrivas ut och tabletter med både varierande storlek och infyllnadsnivå tillverkades. I den andra studien användes EXT och IJP framgångsrikt för tillverkning av munsönderfallande filmer innehållande 0,1–2 mg warfarinnatrium (hädanefter kallat warfarin). Oavsett vilken teknik som användes för att skriva ut warfarin uppnåddes den önskade dosen genom att skriva ut läkemedelsbläcket som ett enskilt lager. De utskrivna munsönderfallande filmerna var minst lika bra, men även mer fördelaktiga i vissa avseenden, jämfört med orala pulver i endospåsar som idag rutinmässigt tillverkas på sjukhusapotek. De munsönderfallande filmerna möjliggör dessutom enkel administrering till pediatriska patienter eller till patienter med sväljningssvårigheter, eftersom de kan tas utan vatten. I den tredje studien användes IJP för att tillverka individanpassade, databerikade, ätbara läkemedel (data-enriched edible pharmaceuticals, DEEP) innehållande två cannabinoider. Det cannabinoidhaltiga bläcket skrevs ut i ett informationsrikt mönster på ett poröst fast skum som fungerade som substrat. Detta möjliggjorde samtidig inkorporering av både information och läkemedel

(cannabinoider) i ett enskilt informationsrikt mönster. Dosen skräddarsyddes genom att skriva ut 1–10 lager av läkemedelshaltigt bläck på substratet. Informationsrika mönster som är utskrivna direkt på läkemedlet, istället för exempelvis på förpackningen, erbjuder möjligheten att inkorporera personlig information, t.ex. för patienten, vårdgivaren, vårdpersonalen samt möjliggör spårbarhet av enskilda doser. Detta kan t.ex. tillämpas för att förbättra behandlingsresultaten, förhindra förekomsten av förfalskade läkemedel i leveranskedjan, minska medicineringsfel eller för att undvika läkemedelsmissbruk.

Denna avhandling ger en översikt över olika utskriftsteknologier som används inom det farmaceutiska området och bidrar till förståelsen av kritiska parametrar vid tillverkning av individualiserade orala läkemedel. Dessutom ger avhandlingen insikt i fordringar och eventuella begränsningar hos de olika utskriftsteknologierna som måste beaktas tillsammans med den verksamma substansen och de önskade egenskaperna av den färdiga läkemedelsprodukten. EXT är en mångsidig metod som kan användas vid rumstemperatur för tillverkning av läkemedel innehållande både låga och höga doser av den aktiva substansen. EXT kräver dock vanligtvis efterbehandling såsom torkning eller härdning vilket ökar tillverkningstiden och kan orsaka deformation av det utskrivna läkemedlet. IJP möjliggör enkel inkorporering av ett individuellt informationsrikt mönster på en enskild läkemedelsdos. IJP kan med fördel användas för att tillverka läkemedel innehållande en låg dos och är även vanligtvis begränsat till detta, eftersom teknologin baseras på deponering av droppar av låg volym (pikoliter). Tillverkning av läkemedel innehållande höga doser med hjälp av IJP skulle kräva att en stor volym av bläcket absorberas av substratet. FDM kan användas för att tillverka komplexa inre strukturer, som t.ex. kan utnyttjas för att skräddarsy läkemedelsfrisättningen. En av de identifierade nackdelarna med denna utskriftsteknologi är behovet av filament som används som startmaterial. Framställning av utskrivbara filament innehållande en hög koncentration av aktiv substans har visat sig vara utmanande.

List of original publications

The thesis is based on the following publications, which in the text are referred to by Roman numerals (I–III).

I **Öblom, H.**, Zhang, J., Pimparade, M., Speer, I., Preis, M., Repka, M., Sandler, N., 2019. 3D-Printed Isoniazid Tablets for the Treatment and Prevention of Tuberculosis—Personalized Dosing and Drug Release. AAPS PharmSciTech 20.
https://doi.org/10.1208/s12249-018-1233-7

II **Öblom, H.**, Sjöholm, E., Rautamo, M., Sandler, N., 2019. Towards printed pediatric medicines in hospital pharmacies: Comparison of 2D and 3D-printed orodispersible warfarin films with conventional oral powders in unit dose sachets. Pharmaceutics 11, 334.
https://doi.org/10.3390/pharmaceutics11070334

III **Öblom, H.**, Cornett, C., Bøtker, J., Frokjaer, S., Hansen, H., Rades, T., Rantanen, J., Genina, N., 2020. Data-enriched edible pharmaceuticals (DEEP) of medical cannabis by inkjet printing. Int. J. Pharm. 589, 119866.
https://doi.org/10.1016/j.ijpharm.2020.119866

Contribution of **Heidi Öblom** to the original publications:

I Participation in the study design, performing the experiments, data analysis, and writing the paper.

II Participation in the study design, performing many of the experiments, data analysis, and writing the paper.

III Participation in the study design, performing the experiments, data analysis, and writing the paper.

List of supporting publications

The author has moreover contributed to the following publications that are not included in the thesis:

IV Preis, M., **Öblom, H.**, 2017. 3D-Printed Drugs for Children—Are We Ready Yet? AAPS PharmSciTech 18, 303–308. https://doi.org/10.1208/s12249-016-0704-y

V Xu, W., Pranovich, A., Uppstu, P., Wang, X., Kronlund, D., Hemming, J., **Öblom, H.**, Moritz, N., Preis, M., Sandler, N., Willför, S., Xu, C., 2018. Novel biorenewable composite of wood polysaccharide and polylactic acid for three dimensional printing. Carbohydr. Polym. 187, 51–58. https://doi.org/10.1016/j.carbpol.2018.01.069

VI Tian, Y., Orlu, M., Woerdenbag, H.J., Scarpa, M., Kiefer, O., Kottke, D., Sjöholm, E., **Öblom, H.**, Sandler, N., Hinrichs, W.L.J., Frijlink, H.W., Breitkreutz, J., Visser, J.C., 2019. Oromucosal films: from patient centricity to production by printing techniques. Expert Opin. Drug Deliv. 16, 981–993. https://doi.org/10.1080/17425247.2019.1652595

VII Rosqvist, E., Niemelä, E., Frisk, J., **Öblom, H.**, Koppolu, R., Abdelkader, H., Soto Véliz, D., Mennillo, M., Venu, A.P., Ihalainen, P., Aubert, M., Sandler, N., Wilén, C.E., Toivakka, M., Eriksson, J.E., Österbacka, R., Peltonen, J., 2020. A low-cost paper-based platform for fast and reliable screening of cellular interactions with materials. J. Mater. Chem. B 8, 1146–1156. https://doi.org/10.1039/c9tb01958h

VIII Chao, M., **Öblom, H.,** Cornett, C., Bøtker, J., Rantanen, J., Kälvmark Sporrong, S., Genina, N., 2021. Data-enriched edible pharmaceuticals (DEEP) with bespoke design, dose and drug release kinetics. Pharmaceutics 13, 1866. https://doi.org/10.3390/pharmaceutics13111866

IX Bay Stie, M., **Öblom, H.**, Nørgaard Hansen, A., Jacobsen, J., Chronakis, I., Rantanen, J., Mørck Nielsen, H., Genina, N., 2021. Mucoadhesive nanofiber-on-foam-on-film multi-layered unidirectional release system for systemic peptide delivery. *Submitted.*

Abbreviations

2D	Two-dimensional
3D	Three-dimensional
4D	Four-dimensional
API	Active pharmaceutical ingredient
CBD	Cannabidiol
DEEP	Data-enriched edible pharmaceuticals
DoD	Drop-on-demand
DOS	Drop on solid deposition
DPI	Dots per inch
EMA	European Medicines Agency
EXT	Semisolid extrusion 3D printing
FDA	U.S. Food and Drug Administration
FDM	Fused deposition modeling
HME	Hot-melt extrusion
HPC	Hydroxypropylcellulose
HPLC	High-performance liquid chromatography
HPMC	Hydroxypropylmethylcellulose
IJP	Inkjet printing
IRP	Information-rich pattern
ODF	Orodispersible film
OPS	Oral powders in unit dose sachets
PEG	Polyethylene glycol
PEO	Polyethylene oxide
PG	Propylene glycol
PIJ	Piezoelectric inkjet printing
PLA	Polylactic acid
QR	Quick response
RH	Relative humidity
SLA	Stereolithography
SLM	Selective laser melting
SLS	Selective laser sintering
STL	Stereolithography (file format)
THC	Delta-9-tetrahydrocannabinol
TIJ	Thermal inkjet printing
UPLC	Ultra-performance liquid chromatography

Table of contents

1. Introduction

For a medicine to be effective and safe the active pharmaceutical ingredient (API) needs to be delivered in a desired, safe, and unvarying way to the intended target in the body. Pharmaceutical development aims to define the design space, specifications, and manufacturing requirements to achieve this (European Medicines Agency, 2017). This requires extensive knowledge regarding human physiology along with the API and the manufacturing process. Scientists have during the past century worked on numerous drug delivery strategies to develop safe and effective medicines. The development has mainly been driven by taking into account the physicochemical properties of the API. However, as the benefits of personalized medicine are becoming evident, the conventional way of developing and manufacturing dosage forms needs to be adapted to moreover consider the personalization aspect. This requires a paradigm shift from manufacturing large batches with a fixed drug content to manufacturing processes that allows for easy alteration of the dosage form.

When comparing the development of pharmaceutical manufacturing techniques for oral dosage forms during the last decades to manufacturing in other fields, it is evident that the pharmaceutical field is not moving forward as fast as many other fields (Clarke and Doughty, 2017). This is not to be misinterpreted as the pharmaceutical field not being innovative and forward-thinking but is rather a result of the rigid regulatory framework that pharmaceutical companies need to adhere to in order to ensure the safety and efficacy of the dosage form. Despite this rigidity, there have been recent incentives from the regulatory bodies in the direction of patient-centric drug development and medicines. The European Medicines Agency (EMA) has recently published an ICH reflection paper with the purpose to advance patient-focused drug development (European Medicines Agency, 2021a). Incorporation of the patient's perspective is envisioned to enhance the quality, relevance, safety, and efficiency throughout the drug development process as well as enable more informed regulatory decisions. The U.S. Food and Drug Administration (FDA) has, moreover, encouraged pharmaceutical companies to implement modern and innovative manufacturing technologies and processes as opposed to the fixed procedure and fixed processes parameters used today (Clarke and Doughty, 2017; FDA, 2015).

Today conventional manufacturing methods, e.g., tableting, involve processes that are well understood and have well-established regulatory pathways but lack the flexibility needed for manufacturing personalized dosage forms (Norman et al., 2017). Printing technologies, which are flexible and enable production of advanced dosage forms with high accuracy, have been proposed to solve this unmet need. The ability to manufacture personalized dosage forms is forecasted to advance treatment outcomes by enabling patient-tailored medicines that have improved efficacy, safety, compliance, and accessibility.

To date, the only approved printed dosage form in the world, Spritam®, was approved by FDA in 2015. Spritam® is not a patient-tailored solid oral dosage form, it is merely produced by means of printing to take advantage of the rapid disintegration enabled by the printing technique. However, the printing technique utilized for preparation of Spritam® would additionally allow for production of personalized doses if there was a regulatory framework in place for production of flexible doses. In early 2021, Triastek's T19 solid oral dosage form prepared by melt extrusion deposition (MED™), an automated 3D printing technology, received clearance on their FDA investigational new drug (IND) application (Everett, 2021; Triastek, 2021). Triastek expects to file a new drug application (NDA) for T19 with FDA in 2023. This can be considered as evidence that both the industry and the regulatory bodies find printing technologies advantageous for production of innovative solid oral dosage forms. This thesis investigates the suitability to use 2D- and 3D printing technologies, namely fused deposition modeling (FDM), semisolid extrusion 3D printing (EXT), and inkjet printing (IJP), for production of personalized solid oral dosage forms.

2. Literature overview

2.1. Personalized medicine

Personalized medicine has gained increasing interest as the benefit of personalized approaches has become more apparent. The traditional treatment regime comprises a 'one-size-fits-all' strategy without further considering interpatient variability despite the fact that this treatment approach may result in significantly different therapeutic outcomes among patients. The increased awareness and understanding of personalized medicine is possible due to ongoing development in the field of human genome research. Further advances in the field of pharmacogenomics pave the way for personalized medicines. Providing genetic information on an individual patient level for improved decision-making regarding the right API, dose, and time required for a specific patient results in improved treatment outcomes (European Medicines Agency, 2020a). The EMA defines personalized medicine as a medicine that is targeted to individual patients with regards to their genetic characteristics (European Medicines Agency, 2020b). The concept of personalized medicine further includes both individualized timely and targeted prevention strategies as well as tailoring the best treatment strategies for the right patient at the right time point, based on the characterization of an individual's phenotype and genotype (European Medicines Agency, 2020a). Personalized medicine typically includes at least a medical device for diagnostic purposes and a therapeutic product (US Food and Drug Administration, 2013). Personalized medicine is associated with fewer adverse effects, superior treatment outcomes, improved adherence, and lower risk of sub-therapeutic doses.

In addition to making medical decisions based on patient data and lifestyle factors, personalized medicine can involve taking into account the personal preferences of a specific patient (US Food and Drug Administration, 2013). The concept of personalized medicine is, moreover, moving towards providing special population groups, such as pediatric and geriatric patients, and patients, having swallowing problems, with suitable dosage forms. A solid oral dosage form can be tailored according to personal preferences related to e.g., size, color, shape, and taste, which can be particularly important for acceptability among children (Preis and Öblom, 2017).

To date, the administered dose is typically tailored by manipulation of the marketed formulation by splitting or crushing tablets into smaller pieces or opening capsules (Helmy, 2015). However, such manipulation of solid oral dosage forms is not accurate and may lead to day-to-day variability of the administered dose and thus result in undesired over- or under-dosing (Helmy, 2015; Hill et al., 2016; Madathilethu et al., 2018; Van Riet-Nales et al., 2014; Watson et al., 2018). Manipulations of solid oral dosage forms can also alter the properties of the dosage form with potentially dangerous outcomes such as dose dumping of a sustained release dosage form or destroying the pH-sensitive coating resulting in release of the API at the wrong site in the

gastrointestinal tract. Additional strategies of personalization of the drug dose are utilization of oral liquids or compounding of e.g., oral dose powders or hard capsules in (hospital) pharmacies (Brion et al., 2010). The dosing flexibility is superior for the former, however, oral liquids are associated with drawbacks such as large volumes that need to be administered, limited suitable solvents and excipients (especially for children), and reduced shelf life as compared to solid dosage forms (Öblom et al., 2019a). Especially for pediatrics, also mini-tablets have been explored for personalization purposes as well as for improved acceptability and swallowability (Madathilethu et al., 2018).

Traditional mass production methods such as tableting and capsule filling processes do not allow for easy modification of the prepared solid dosage form, making it impractical and expensive to produce tailored solid dosage forms utilizing these techniques. Mass customization has been proposed as an enabling model for personalized medicine (Govender et al., 2020; Siiskonen et al., 2020). Mass customization builds on the principles of mass production where personalized dosage forms are designed, manufactured, and distributed in an economical fashion. Mass customization is envisioned to be achieved by incorporation of key patient parameters in the manufacturing platform (Govender et al., 2020). It is yet to be fully evaluated how far the mass production platform can be moved towards mass customization and what type of re-engineering is required of the current platforms for this to be achieved. Additionally, the use of printing technologies for production of personalized medicine has been proposed to be the future of personalized medicine (Sandler and Preis, 2016) and has subsequently been comprehensively investigated (Chen et al., 2020; Jamróz et al., 2017a). Pharmacoprinting, i.e., utilization of printing technologies to manufacture pharmaceutical products, is an attractive approach to attain increased personalized drug treatments. Printing technologies are precise and highly flexible enabling easy manipulation of the printed solid dosage form (Sandler and Preis, 2016). Additionally, printing techniques are cost-effective at a small scale and allow for decentralized production (Elkasabgy et al., 2020; Ligon et al., 2017; Park et al., 2019; Shaqour et al., 2020). These factors make printing technologies more suitable as compared to conventional manufacturing methods for production of personalized dosage forms as printing allows for production of small unique batches fabricated based on the need of an individual patient at a specific time. Manufacturing of personalized medicines can be achieved by a shift from centralized mass production facilities to decentralized production facilities such as hospital pharmacies or regional manufacturing facilities. Bringing the production closer to the patient enables short reaction times when changes in the treatment regime are needed.

A recent focus group study among pediatric health care professionals revealed an overall positive attitude towards printed solid oral dosage forms (Rautamo et al., 2020). Personalization of dosage forms and more precise dosing were among the identified attractive features of oral 3D-printed dosage forms. Age-appropriate dosage forms and combination products were further

recognized as areas where printed medicines would be of value. Prerequisites for successful use of printed dosage forms in a hospital setting were also highlighted, e.g., the need for short delivery times of on-demand printed dosage forms in addition to verification and identification possibilities of the printed dosage forms.

There are still hurdles to overcome to make personalized medicines widely available for patients. Medical doctors need to, in an easy way, be able to gather and interpret genomic and other essential data of patients in order to determine suitable personalized treatments. Once this data is available for an individual patient, there needs to be a way to produce the personalized dosage form, which may not always be feasible with conventional manufacturing techniques. Printing technologies could solve this unmet need but further clarity on regulatory requirements and pathways must be established for these innovative on-demand printed dosage forms. This will require close collaboration and dialog with the regulatory bodies and other relevant actors to be able to provide personalized printed dosage forms to patients in the future. Furthermore, it is expected that new distribution models are needed for personalized dosage forms.

2.2. Pharmaceutical printing technologies

This section will give an overview of the most common printing technologies utilized for production of solid oral dosage forms. The classification used for the different printing techniques in this thesis can be seen in Figure 1, where the printing techniques explored in this thesis are shown in black.

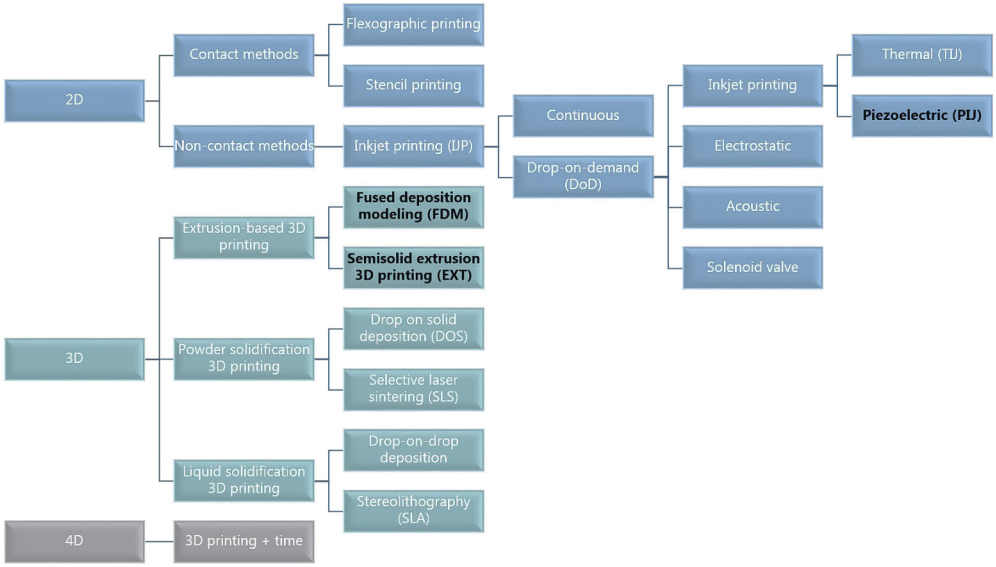

Figure 1. *Overview of printing technologies commonly used for printing of solid oral dosage forms.*

2.2.1. Printing nomenclature

The most commonly used printing technologies can be divided into one-dimensional (1D), two-dimensional (2D), and three-dimensional (3D) printing technologies based on the number of dimensions used for printing an object. In 1D printing, only one dimension is used to print stripe patterns whereas 2D printing utilizes two dimensions, namely the horizontal (X) and vertical (Y). In 3D printing, a third dimension, depth (Z), is added to enable building of 3D objects. A 3D-printed object hence comprises two or more printed layers. In 2013, the concept of four-dimensional (4D) printing was introduced. In 4D printing, the name does not correlate to the number of dimensions used but is rather a progressed version of 3D printing, where either the shape, functionality, or property of the 3D-printed object will change upon time (Momeni et al., 2017). The original definition of 4D printing was simply 3D printing plus time, but as 4D printing increased in popularity, the definition was broadened to: "*4D printing is a targeted evolution of the 3D-printed structure, in terms of shape, property, and functionality. It is capable of achieving self-assembly, multi-functionality, and self-repair. It is time-dependent, printer-independent, and predictable*" (Momeni et al., 2017)". Hence, 4D printing involves 3D printing of an object using stimuli-sensitive materials that when subjected to a stimulus will transform. A 4D-printed object differs from a 3D-printed object as it will evolve as a function of time, whereas the objects fabricated by 3D printing are classified as static.

2.2.2. Perspectives of printed medicine

3D printing enables production of innovative and complex solid oral dosage forms, drug delivery devices, and medical devices with regards to the geometrical shape and complex inner structures that are not easy or impossible to attain with conventional manufacturing methods (Norman et al., 2017; Sandler and Preis, 2016; Vaz and Kumar, 2021). The ease of manipulation of the printed solid dosage form makes 3D printing attractive for use in personalized medicine in comparison to conventional manufacturing processes that do not allow easy in-process adjustments of the final solid oral dosage forms. This limits conventional manufacturing to traditional fixed-dose and fixed-drug combination solid oral dosage forms produced at a large scale rather than fabrication of tailored solid oral dosage forms produced on-demand and in small volumes according to the patients' needs.

The advantages associated with printed medicines are evident and may solve the recognized unmet need for many treatments, which is why FDA encourages continued research within the area (Norman et al., 2017). Printing of medicines is revolutionizing the concept of medicines where conventional drug products typically are simple, uniform in dose, and aim for a shelf life of multiple years. The advantages of personalized printed dosage forms may result in improved treatment outcomes lowering the societal burden associated with poor treatment outcomes that are costly for society. Printing personalized medicines enables taking into consideration an individual patient's preferences, the need

for individual dosing, and characteristics of the dosage forms such as flavor to achieve improved patient-centricity and compliance.

Other investigated applications in the pharmaceutical and medical field for printed products that have gained significant attention and which in some cases already are in clinical use involve fabrication of medical devices such as implants, prostheses, wound dressings, and surgical models as well as bio-based 3D printing for production of e.g., organ-on-chips, 4D printing, and biorobots that imitate biological functions (Jamróz et al., 2018). This thesis focuses exclusively on investigating the use of FDM, EXT, and IJP for manufacturing personalized solid oral dosage forms. Medical devices and other administration routes are thereby outside the scope of this thesis. The printing techniques utilized in the thesis to prepare personalized solid oral dosage forms will be described in more detail in the following sections along with an overview of other printing techniques that have been investigated for this purpose.

2.2.3. 2D printing methods

2D printing methods can be divided into non-contact and contact methods. The contact-based flexographic printing technique has been explored in the pharmaceutical field for manufacturing and coating of dosage forms (ODFs) (Genina et al., 2012; Janßen et al., 2013; Raijada et al., 2013). Flexographic printing is a roll-to-roll printing method consisting of an anilox roll that transfers the printing ink to the printing cylinder equipped with a printing plate that has a predefined pattern (Raijada et al., 2013; Tian et al., 2019). The ink is transferred to the predefined pattern of the printing plate and lastly onto the substrate that is attached to the third roll, i.e., the impression roll. The printing cycle can be repeated to allow transfer of more ink thereby enabling manufacturing of increased doses. Recently, another contact-based printing method, stencil printing, was explored for pharmacoprinting by manufacturing personalized orodispersible discs (Wickström et al., 2020). The conventional impact printing method utilizes semisolid ink to print the design corresponding to the negative pattern on the printing plate. The printing plate is in direct contact with the substrate and a blade is used to spread the ink over the printing plate enabling the design to be printed.

IJP is a non-contact printing technique that has gained recent attention for production of solid oral dosage forms due to its superior dosing precision compared to e.g., flexographic printing (Genina et al., 2012). The 2D printing section in this thesis will focus on IJP and describe the technology in greater detail.

2.2.3.1. Brief history and conceptualization of inkjet printing

IJP is a well-established technique that has been used in the typographical industry since the mid-20th century and is subsequently widely utilized in affordable office printers. IJP is a non-contact printing technique that relies on jetting ink out of one or multiple nozzles onto a specific position according to a premade design. IJP typically involves a substrate upon which the ink is

deposited. The deposited ink can be absorbed into the substrate depending on e.g., the porosity and characteristics of the substrate as well as the interactions of the substrate and ink. The technique is generally classified as 2D but may at times, within the pharmaceutical field, be referred to as 3D printing if more than one layer is printed. Multiple subsequent layers are often printed on top of each other as a measure to increase the amount of the drug-loaded ink that is deposited or to attain a specific geometry.

Using this multilayer approach, solvent-free hot-melt 3D IJP has recently been explored (Kyobula et al., 2017; Lion et al., 2021). This free-form technology builds on the principles of jetting of a hot-melt rather than the traditional solvent-based inks and the 3D geometry is built in a layer-by-layer manner without the need of a substrate (similarly to e.g., FDM). The technology has been used for preparation of tablets possessing complex 3D geometries using a solvent-free hot-melt ink containing beeswax (Kyobula et al., 2017) or the lipid Compritol HD5 ATO (Lion et al., 2021). Hot-melt 3D IJP offers the possibility to print complex geometries with a high resolution where both the macro-structure as well as the micro-structure of the dosage form can be controlled (Lion et al., 2021). This enables preparation of solid dosage forms with tunable drug-release profiles. Further, hot-melt 3D IJP enables printing without the need of traditional solvent-based inks thus eliminating the post-process drying step that typically is required when using solvent-based inks. Potential solvent-related concerns, such as the use of unsuitable solvent(s) for a specific target group, residual solvent(s) in the dosage form, and solvent-related stability issues are also eliminated with this technique. Hot-melt 3D IJP has been proposed to be suitable for drugs that are compatible with lipids and which additionally have a melting point below the used printing temperature (approx. 90 °C). The drug should naturally also be stable at the printing temperature used.

The following IJPs sections in this thesis will concentrate on the traditional solvent-based IJP for production of solid oral dosage forms. This is a manufacturing method where the substrate, ink, process parameters as well as their interplay are critical for attaining reproducible, high-quality dosage forms with the intended characteristics. The important parameters for the components involved in solvent-based 2D printing are discussed in the sections below.

2.2.3.2. Substrate

The ink is deposited on a substrate or a build plate. A release liner can be utilized to provide support during manufacturing of the substrate and/or during the printing step, but it is not a part of the final dosage form. In most cases (however not typically in the case of e.g., hot-melt 3D IJP), a premade substrate is used for production of IJP dosage forms and it has a crucial role in the final dosage form. Various edible films, sheets, solid foams, and tablets are examples of carrier substrates that have been used for such dosage forms (Edinger et al., 2017; Genina et al., 2013b; Iftimi et al., 2019; Thabet et al., 2018a). Substrates are typically prepared by solvent casting, freeze-drying, hot-melt extrusion (HME), electrospinning, and tableting (Borges et al., 2015; Öblom et al., 2020; Palo et al.,

2017; Simões et al., 2019). The substrate properties should be developed with respect to the application and administration route of the dosage form (Raijada et al., 2013). This is typically dictated by the properties of the API, but in some cases also, if realistic, by patient acceptability. The substrate should be able to absorb or hold the amount of deposited ink needed to reach the target dose (Raijada et al., 2013). To avoid loss of the API during printing, transport, and handling, it is typically desired that the ink penetrates into the substrate. Alternatively, the dosage form can be coated to avoid drug loss and to improve stability during post-manufacturing steps such as storage and handling. One or multiple drugs can be loaded in the substrate itself during substrate preparation, where subsequent personalization can be done in the printing step, e.g., by printing of a different drug or by adjusting the dose of the drug(s) already present in the substrate. The substrate should possess properties that are suitable for the printing process as well as the properties desired in the final dosage form to allow for it to be administered via a specific administration route. A flexible substrate that disintegrates rapidly is typically desired for IJP ODFs from a patient acceptability perspective (Hoffmann et al., 2011; Tian et al., 2019). Improved flexibility and disintegration can be achieved e.g., by introduction of plasticizers and superdisintegrants in the substrate formulation. Another approach to alter the properties of the final dosage form is the inclusion of ingredients that acts as e.g., plasticizers in the printing ink that will interact with the substrate. For IJP (and other printed) buccal dosage forms, mucoadhesive polymers can be introduced in or on the substrate and may further be combined with a water-impermeable backing layer to enable unidirectional drug release (Eleftheriadis et al., 2019). Finally, it should be ensured that the deposited ink does not dissolve or disintegrate the substrate which for instance can be avoided by imprinting a water-soluble and ethanol-insoluble substrate with an ethanol-based ink (Raijada et al., 2013; Tian et al., 2019).

2.2.3.3. Ink

The amount of the API incorporated in a single dosage form can be controlled by factors such as the drug concentration in the ink, printed resolution, i.e., dots per inch (DPI), printed area, and the droplet volume, which is obtained by a camera incorporated in the printer close to the nozzles. The number of subsequent layers printed on top of each other can, furthermore, be utilized to adjust the dose. In order to successfully IJP dosage forms that contain the intended content of API(s) with a good print edge definition, special attention must be paid to the printability of the ink to ensure stable jetting and unvarying physical dimensions of the droplets during the printing process. Certain ink properties are required to achieve stable jetting without leaking of the ink from the nozzle or accumulation of the ink in the nozzle. As for all printing technologies, the rheological properties of the ink or other starting material play a vital role for printability and the print result. The most important parameters of an IJP ink are viscosity and surface tension as they affect the droplet formation as well the ink flow in the small tubings that feed the nozzle(s). Optimal surface tension and

viscosity have been proposed to be in the range of 25–50 mN/m and 1–30 mPa·s, respectively (Huang et al., 2012; Raijada et al., 2013; Sun et al., 2012). If an ink fails to be within the mentioned range, there is an increased risk that the ink is not printable as a result of unsuccessful droplet formation. In case the surface tension and viscosity are too low it can result in leaking of the ink or splashing of the droplets. To obtain suitable ink properties, pharmaceutical inks are typically formulated with pharmaceutically approved solvents, co-solvent, a humectant, and one or multiple APIs. The solvent(s) in the ink should, in addition to the previously mentioned aspects, be selected based on the solubility of the API and take into account possible limitations for use in the target population such as pediatrics. Viscosity- and surface tension modifiers, as well as humectants (hygroscopic substances), are typically added to the ink to obtain a printable ink and to avoid evaporation of the solvent(s).

The Z-value (Eq. 1) has been proposed as a prediction of printability (Jang et al., 2009), i.e., a measure of whether the developed ink will be printable in the printer used. The Z-value is a dimensionless number that is the inverse Ohnesorge number (Oh) (Eq. 2), which in turn is based on the Reynolds (Re) (Eq. 3) and Weber (We) (Eq. 4) numbers. These equations (Eq. 1-4) describe the various relationships between density (ρ), surface tension (γ), and viscosity (η) of the ink, in addition to the nozzle radius (d) and average velocity (V) in the used system.

$$Z = \frac{\sqrt{d\rho\gamma}}{\eta} \qquad \textbf{Eq. 1}$$

$$Oh = \frac{\eta}{\sqrt{d\rho\gamma}} \qquad \textbf{Eq. 2}$$

$$Re = \frac{\mathrm{d}\rho V}{\eta} \qquad \textbf{Eq. 3}$$

$$We = \frac{d\rho V^2}{\gamma} \qquad \textbf{Eq. 4}$$

The Z-value does not take into account the fluid velocity and it is important to note that the predictions made with Eq. 1-4 apply to Newtonian fluids only. Therefore, for more complex inks e.g., non-newtonian suspensions and polymer solutions printability predictions can be inaccurate (Clasen et al., 2011). Despite these considerations, the Z-value is a good starting point for developing an ink, and inks with a Z-value between 1–10 (Derby and Reis, 2003) or 4–14 (Jang et al., 2009) have previously been reported as printable.

IJP is a precise manufacturing technique due to jetting of droplets in the picoliter range, which in turn also is a drawback of the technique. Relatively

small volumes of the drug are deposited per printing pass, which is why IJP is usually utilized for printing low-dose dosage forms. As the substrate has a limited absorption capacity and in order to reduce the printing time required the concentration of the ink should be as high as possible. The drug present in the ink should however ideally be below the solubility limit to minimize recrystallization and subsequent clogging of the nozzles. Clogging is a problem frequently reported for IJP of dosage forms and can be caused by various reasons. Nozzle clogging can be seen as a major drawback as it results in variability in the printing process affecting the print quality and fluctuation in the amount of drug present in the dosage form. If the formulated ink is a suspension-type and not solution-type, it is important that the suspension is colloidally stable and that the particles present in the suspension are small enough to prevent clogging. Nanosuspensions have been explored for IJP when the API has poor solubility in pharmaceutically approved solvents to obtain a high enough drug load in the ink (Cheow et al., 2015; Pardeike et al., 2011; Wickström et al., 2017a).

2.2.3.4. Inkjet printing

IJP can be divided into continuous and drop-on-demand (DoD) techniques. In the former, the ink droplets are continuously ejected out of the printhead, whereas in the latter the droplets are only ejected when desired. DoD techniques include piezoelectric (PIJ), thermal (TIJ), solenoid valve, electrostatic, and acoustic inkjet printing (Le, 1998), differing in the methods utilized for droplet formation. Research in the area of 2D pharmacoprinting has mainly focused on PIJ and TIJ (Tian et al., 2019). In both PIJ and TIJ the ink container is connected to a transducer that is coupled to one or multiple nozzles and the techniques only differ in the type of transducer utilized (Figure 2). TIJ uses a thermal transducer element that locally heats the ink when a current is applied, causing the volatile solvent(s) present in the ink to form a vapor bubble that quickly expands and collapses enabling the ejection of droplets (Goole and Amighi, 2016; Tian et al., 2019). The rapid collapse of the bubble and reduction in the ink volume allows the nozzle to be refilled with ink. As TIJ requires the presence of volatile solvents in the ink, there is a limitation to which solvents may be used for pharmaceutical applications. As it is desired to formulate inks with high concentrations of the APIs, the solubility of the APIs would further define the choice of the solvent thereby limiting the number of APIs that can be printed using this technique. A small possibility of thermal degradation of the ink caused by rapidly applying heat (up to 300 °C) also needs to be considered. This makes PIJ operable at room temperature with a wider range of solvents more applicable for pharmacoprinting (Park et al., 2019; Scoutaris et al., 2011). PIJ, which is the IJP technique used in this thesis, differs mainly from TIJ by the transducer utilized for droplet formation. PIJ uses a piezoelectric element that deforms when a voltage is applied. The deformation of the piezoelectric material results in a droplet being ejected from the nozzle. Stopping the current allows the piezoelectric element to return to the initial shape and refilling the nozzle with

ink from the ink container. The droplet ejection process is repeated until the desired amount of drug is deposited.

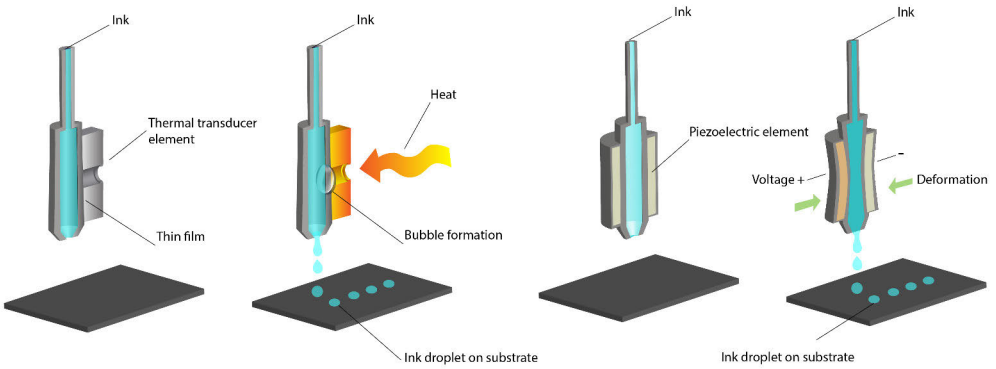

Figure 2. *Schematic overview of thermal- (left) and piezoelectric inkjet printing (right).*

IJP is an interesting technique for manufacturing personalized dosage forms as it allows for accurate deposition of the desired volume of the drug-loaded ink onto an edible substrate. Especially APIs with a low dose or a narrow therapeutic window are favorably prepared by IJP, as droplets in the picoliter range can be jetted from the nozzle(s). The printed pattern can easily be modified enabling personalization of the dosage form. Personalization features can include tailoring of the drug dose and/or incorporation of information in the form of an IRP (see section 2.3.3), which is readable by a standard smartphone or other similar devices. IJP is commonly explored for fabrication of orodispersible films (ODFs), which according to Ph. Eur. are defined as single- or multilayer sheets of suitable materials, to be placed in the mouth where they disperse rapidly (European Pharmacopoeia Commission, 2020a). Batch production is common for dosage forms prepared by means of IJP, but continuous manufacturing has also been explored (Thabet et al., 2018a).

2.2.3.5. Liquid dispensing technologies

Various micro-dispensing techniques have been investigated to manufacture dosage forms. Typically the nozzle diameter is larger for liquid dispensing technologies making them an alternative to IJP in cases where the ink has a higher viscosity and/or includes larger particles (Tian et al., 2019). A commercial continuous liquid dispensing technology developed by GlaxoSmithKline is suitable for production of high volumes (up to 2 million tablets a day) of low-dose drugs in the range of 1 µg to 5 mg (GlaxoSmithKline, 2021). The potent API is formulated as a solution or suspension and subsequently deposited on placebo tablets for production of immediate-release tablets in a safe and reproducible manner. The process further includes a drying, imaging, and coating step before real time release of the tablet. The main difference between liquid dispensing technology and IJP is that liquid dispensing technology deposits the whole drug-

dose in a single droplet, i.e., the droplet volume can be varied between 4–25 µl, whereas in IJP the dose is achieved by printing multiple droplets that typically have a volume in the picoliter range (Clarke and Doughty, 2017). This technique is thus not suitable e.g., for incorporation of IRPs in the same way as IJP.

2.2.4. 3D printing methods

2.2.4.1. Brief history and conceptualization

The concept of 3D printing was already presented in the 1970s by Pierre Ciraud when he described that each layer of applied powdered material could be solidified using a high-energy beam (Jamróz et al., 2018). Charles Hull is accredited for developing the first working 3D printer based on selective solidification (SLA) technology in 1984, which was brought to the market by 3D Systems in 1989 (Horvath, 2014). The same year (1989) fused deposition modeling (FDM) was patented by Stratasys Ltd, and the technology was trademarked (FDM™) (Awad et al., 2018; Horvath, 2014). Along with the expiration of many key patents for various printing techniques the interest in utilizing 3D printing for innovative purposes arose both in academia and the commercial space.

3D printing, also referred to as additive manufacturing or solid freeform fabrication, is a collective term for numerous rapid prototyping techniques, which can be divided into (i) extrusion-based, (ii) powder solidification, and (iii) liquid solidification techniques depending on the principles of the technology (Jamróz et al., 2018). Irrespective of the variety of 3D printing techniques utilizing different materials and methods to build the 3D object, all techniques have some common steps essential for production of a printed object. All methods require a computer-aided design of the 3D object, which is exported in a format that is readable by the printer, e.g., stereolithography (STL). In the STL format, the triangulated surface geometry of the 3D object is registered (Jamróz et al., 2017a). The STL file is imported to the printing software where the 3D design is sliced into layers with a defined thickness that will be printed. This information is provided as data in the form of XYZ coordinates for the printer and the designed object is fabricated in a layer-by-layer deposition procedure according to the given coordinates. The used layer height will affect the quality of the printed object as well as the production time (Jamróz et al., 2018).

2.2.4.2. Extrusion-based 3D printing

Extrusion-based 3D printing techniques include fused deposition modeling (FDM) and semisolid extrusion 3D printing (EXT), utilizing a solid and semisolid starting material, respectively (Figure 3). Amid all printing technologies used for pharmacoprinting, extrusion-based techniques have gained the most attention. These techniques are affordable and enable e.g., printing with a variety of polymers, tailoring the drug release properties by modifying the geometry or the used excipients, and printing of hollow objects that can be used for fabrication of gastro-floating tablets (Goyanes et al., 2014). FDM and EXT are the printing

technologies used for production of tailored dosage forms in this thesis and will be discussed in greater detail in sections 2.2.4.2.1 and 2.2.4.2.2 below.

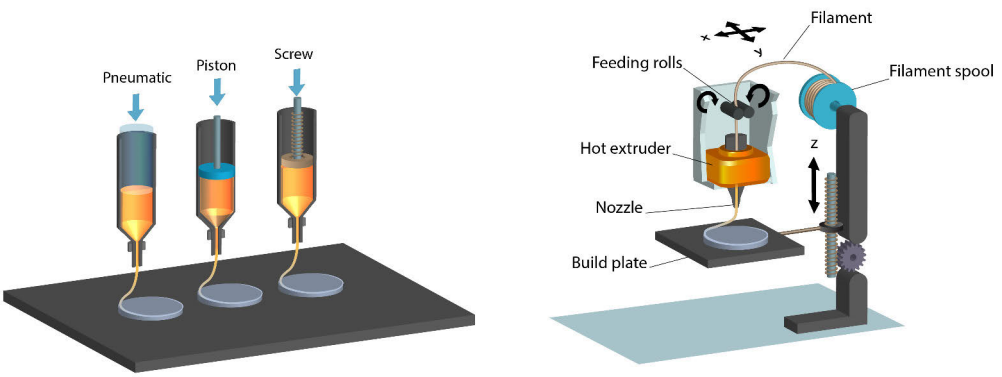

Figure 3. *Schematic overview of semisolid extrusion 3D printing (EXT) (left) and fused deposition modeling(FDM) (right).*

2.2.4.2.1. Fused deposition modeling

During the past decade, researchers have extensively explored the potential use of FDM, also known as fused filament fabrication, within the healthcare sector (Shaqour et al., 2020). For pharmaceutical applications, FDM is one of the printing techniques that has gained the most attention (Öblom et al., 2019a). The suitability to utilize FDM for personalization of the dose, tailoring of the drug release, as well as the combination of different drugs and polymers in the same dosage form, are some of the features that have been investigated. FDM uses a thermoplastic drug-polymer filament as feedstock material, which typically is produced by hot-melt extrusion (HME). In the printing step, the filament is heated above the glass transition temperature of the formulation in order to transform the solid filament to a semisolid or molten state before it is extruded through the printhead nozzle. The extruded material is deposited in a layer-by-layer manner on the build plate while the printhead moves along the X and Y-axes and the build plate moves in the Z direction to fabricate the designed 3D object. The thickness of the printed layer, typically in the range of 100-300 µm, directly impacts the resolution of FDM printed objects (Rahman et al., 2018). In addition, the number of outlines as well as the infill type and ratio used for printing the dosage form will affect the mechanical properties (Jamróz et al., 2018) as well as the drug release properties.

As FDM technology requires heat it may be unsuitable for formulations containing thermolabile API, polymers, and excipients (Awad et al., 2018; Rahman et al., 2018). The thermal properties of the formulation, as well as the rheological properties of the melt, will have an impact on the required printing temperature, which in turn will affect the quality and mechanical properties of the printed dosage form (Yang et al., 2018). In addition to the requirement of heat, other reported FDM drawbacks are associated with the printability of the

prepared HME filaments. Printability issues may for example originate from variation in the diameter of the circular filament and its properties related to brittleness, stiffness, moisture content, and melt rheology (Fuenmayor et al., 2018; Jamróz et al., 2018; Öblom et al., 2019b). To overcome the difficulties associated with production and subsequent printing of drug-loaded filaments, hot-melt ram-extrusion directly coupled to the 3D printer and hot-melt pneumatic 3D printing have been explored for the production of 3D-printed ODFs eliminating the need for filaments (Musazzi et al., 2018; Oh et al., 2020). Similarly, single-screw direct powder extrusion 3D printing has been used to prepare tablets in a single step avoiding the use of filaments (Goyanes et al., 2019). A final limitation of FDM is the availability of suitable pharmaceutical-grade thermoplastic polymers with properties suitable for both the printing process as well as the desired properties in the final dosage form (Rahman et al., 2018).

2.2.4.2.2 Semisolid extrusion 3D printing

Semisolid extrusion 3D printing (EXT), also called pressure-assisted microsyringe printing method or extrusion-based bioprinting, is an additive manufacturing technique where the semisolid starting material such as a gel or paste is extruded through a nozzle onto a build plate with the help of pressurized air, a syringe plunger, or a rotating screw to produce the solid dosage form (El Aita et al., 2019; Goole and Amighi, 2016; Tian et al., 2019). The object is built in a similar manner as described for FDM, where subsequent layers are printed when the printhead moves according to coordinates in the X and Y space and the build plate moves in the Z-direction.

The technique utilizes both disposable syringes and nozzle tips thus eliminating the risk of cross-contamination as the drug formulation is not in contact with the printer. A recognized advantage is that dosage forms with a high drug load can be fabricated using EXT (Khaled et al., 2018a). An additional benefit as compared to FDM is that EXT allows for printing of thermolabile drug formulations as elevated heat is not required, however, solidification of the dosage form after the printing step is typically needed increasing the production time (Aita et al., 2020; Khaled et al., 2015a, 2015b). Solidification can involve drying in specific conditions or curing of cross-linkable materials utilizing heat or light (e.g., visible or ultraviolet light), which may result in undesired effects like shrinkage and deformation upon drying (Azad et al., 2020; Holländer et al., 2018).

2.2.4.3. Powder solidification 3D printing

Drop on solid deposition (DOS), selective laser sintering (SLS), and selective laser melting (SLM) are powder solidification 3D printing techniques. In DOS, also named powder bed jetting, ink droplets acting as a binding material are jetted according to the digital design onto a thin layer of powdered material (Figure 4). The process is repeated with spreading of a new thin layer of powder with a defined thickness and subsequent deposition of droplets adhering to the

previous layer until the designed geometry is formed. The unbound particles act as support material for the geometry as the subsequent layers are being built. The API as well as the desired excipient(s) can be present in the ink or blended in the powder. The only FDA-approved 3D-printed tablet to date, Spritam® (approved in 2015) is prepared by DOS (Zieverink J., 2015). Spritam® uses Aprecia's proprietary ZipDose® technology platform to fabricate fixed-dose tablets with a high drug load that due to the porous structure achievable with DOS offers rapid disintegration for patients with administration or swallowing problems (Aprecia, 2020). Both tablets with modified release and linear release properties have been fabricated using DOS (Jamróz et al., 2018). Similar to DOS, SLS and SLM utilize solidification of subsequent powder layers to build the dosage form. However, instead of the ink used in DOS, a beam of high energy is used to solidify the powder by heating the material close to or above the melting point of the powder blend (Jamróz et al., 2018). SLS is an attractive method for production of dosage forms ranging from porous fast disintegrating dosage forms to dosage forms with a prolonged drug release without the use of binding agents. Nevertheless, degradation of one or more components in the formulation, due to the use of a high-energy beam, is a concern for dosage forms fabricated by SLS and SLM.

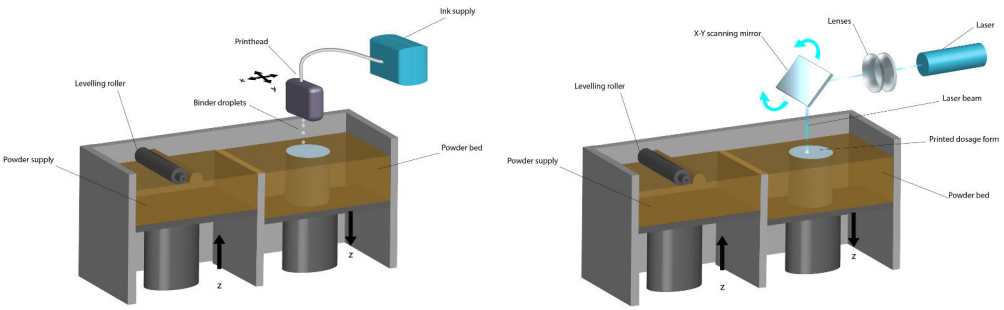

Figure 4. *Schematic overview of drop on solid deposition (left) and selective laser sintering (right).*

2.2.4.4. Liquid solidification 3D printing

Liquid solidification printing techniques comprise drop-on-drop deposition and stereolithography (SLA), which are similar to powder solidification techniques. Drop-on-drop deposition is similar to DOS, but instead of jetting a liquid on a solid material, droplets are ejected on top of each other to form a solid object. As a result of the small droplet size (approx. 100 µm in diameter), DOS is a precise method that enables fabrication of microscopic dosage forms with flexible geometries (Park et al., 2019). SLA, being the most precise 3D printing method, uses computer-controlled laser light or digital light projector to solidify liquid photosensitive polymers (resins) to a predefined depth (Jamróz et al., 2017a; Melchels et al., 2010). Subsequent layers are solidified according to the premade design to generate a solid 3D object. The cross-linked surface is recoated with and a new layer of liquid resin, equal to the thickness of one layer by either moving the build plate up or down along the Z-axis depending on the position of

the light source. The high-energy light source can be located either on the top or the bottom (inverted SLA) of the resin tank. Post-processing such as removal of excess resin and post-curing for improved mechanical properties is typically required for SLA adding to the manufacturing time (Melchels et al., 2010). As a result of the limited availability of nontoxic resins as well as the use of UV-light, the use of SLA for production of dosage forms is not as common as the extrusion-based 3D printing techniques.

2.3. Printed solid oral dosage forms

Compared to conventional manufacturing techniques utilized for production of oral dosage forms, the benefits of printing technologies are specifically related to increased product complexity, personalization, suitability of on-demand manufacturing, (Norman et al., 2017) as well as incorporation of data on a single dosage unit (Edinger et al., 2018a; Öblom et al., 2019a, 2020). Conventional manufacturing methods for solid oral dosage forms such as tablets typically involve multiple process steps such as mixing, wet or dry granulation, drying, size reduction, tablet compaction, and coating (Hemanth et al., 2021). The printing process on the other hand commonly involves preparation of feedstock material, printing, and depending on the printing method utilized potential post-processing such as drying or curing. Opposed to the flexibility attainable for printed dosage forms, the size and the shape of conventionally manufactured tablets are limited to geometries manufacturable using stainless steel punches.

Further, printed dosage forms could be used for manufacturing orphan drugs that are characterized by small patient populations. Orphan dosage forms are manufactured in smaller batches and personalization is often required making conventional manufacturing techniques less cost-efficient for these types of products. Similarly, printing technologies may be used to manufacture dosage forms for clinical trials. In specific first in human studies where there is a need for rapid production of dosage forms with flexible dosing (Hemanth et al., 2021). Another application where printed solid dosage forms have been explored is for veterinary use (Sjöholm et al., 2020). Today, there is only a limited number of approved veterinary dosage forms available on the market, which is why manipulation of marketed dosage forms or extemporaneous manufacturing is required. Printed veterinary dosage forms, which can be produced in small batches, have been proposed to solve the need for flexible doses needed due to great differences in e.g., the body mass of animals as well as variabilities in pharmacokinetic factors between different species.

Pharmacoprinting has mainly been explored for manufacturing of solid oral dosage forms, such as tablets, capsules, orodispersible tablets, and orodispersible films with various properties (Jamróz et al., 2017a). This is expected as the oral administration route still remains favored compared to other administration routes due to ease of administration resulting in improved patient acceptability and compliance (Alhnan et al., 2016; Homayun et al., 2019).

2.3.1. Complexity

Pharmacoprinting, especially 3D printing, enables fabrication of complex geometries that are not possible with conventional tableting or molding techniques. This is due to the flexibility of the technique achieved by a layer-by-layer approach and digital control of the deposition of the printed material (Norman et al., 2017). These features are attractive in the development and manufacturing of dosage forms in cases where modification of the drug release kinetics and drug targeting is desired. Dosage forms with e.g., immediate (Khaled et al., 2018a, 2015b; Öblom et al., 2019b; Pietrzak et al., 2015; Sadia et al., 2016), sustained (Goyanes et al., 2015a; Khaled et al., 2015b; Yang et al., 2018), controlled (Khaled et al., 2014; Öblom et al., 2019b; Zhang et al., 2017a), extended (Khaled et al., 2015a; Pietrzak et al., 2015; Skowyra et al., 2015), modified (Goyanes et al., 2017), delayed (Okwuosa et al., 2017), and pulsatile (Lion et al., 2021) release profiles have been prepared by pharmacoprinting. Moreover, osmotic pumps have been 3D-printed resulting in zero order release of the drug (Khaled et al., 2018b, 2015a). These different release characteristics are achieved by e.g., changing the geometry (Goyanes et al., 2015b; Khaled et al., 2018b), internal/external structure (Öblom et al., 2019b; Sadia et al., 2018; Tagami et al., 2018; Yang et al., 2018; Zhang et al., 2017b), or composition (Alhijjaj et al., 2016; Öblom et al., 2019b) of the dosage form. Tailoring of the surface area to volume ratio of printed dosage forms, which is easily achievable with printing of complex shapes has been shown to affect the drug release kinetics, which is why the geometrical design of the dosage form needs to be carefully selected (Goyanes et al., 2015b). A large surface area has been explored to facilitate faster disintegration of the dosage form and an increased drug release rate (Arafat et al., 2018; Jamróz et al., 2017a; Zieverink J., 2015). 3D printing has also been utilized to alter the inner structure of dosage forms to produce gastro-floating tablets with prolonged gastric residence time required for APIs with e.g., pH-dependent solubility or with an absorption window in the stomach. This has been achieved by printing low-density or hollow dosage forms that allow for entrapment of air (Chai et al., 2017; Huanbutta and Sangnim, 2019; Li et al., 2018; Wen et al., 2019). In addition dosage forms containing multiple APIs have been explored to increase the compliance of multimorbidity patients (Pereira et al., 2019; Robles-Martinez et al., 2019). 3D printing enables fabrication of multi-compartment oral dosage forms, where the various APIs loaded in a single dosage form can be spatially separated in case of incompatibility, which also allows for tailoring of the drug release kinetics for each incorporated API (Genina et al., 2017; Khaled et al., 2015a; Robles-Martinez et al., 2019).

2.3.2. Personalization

Pharmacoprinting of dosage forms enables printing of endless different shapes and geometries using the same printer. This allows for personalization of the dose without the need for splitting and/or crushing fixed-dose strength tablets or the use of liquid dosage forms often resulting in inaccurate doses being

administered (Alomari et al., 2015). Manipulation of dosage forms is moreover perceived as inconvenient by the patient (Chen et al., 2020). Personalization is especially useful for tailoring the dose of potent drugs or for children that undergo physiological changes (e.g., mass and metabolism) during the treatment. Pharmacoprinting can be utilized for tailoring the dosage form to possess drug release characteristics based on the patient's physiological factors such as anatomy, metabolism, elimination, and genetics.

Tailored solid oral dosage forms have been explored e.g., by FDM printing tablets with personalized drug dose combined with tailored release profiles originating from the polymer composition as well as the infill percentage of the printed tablet (Öblom et al., 2019b). Personalization of the dosage form has also been studied by printing so-called 'polypills' that contain the patient's medications combined in a single dosage unit (Gioumouxouzis et al., 2018; Khaled et al., 2015a; Pereira et al., 2019; Robles-Martinez et al., 2019). This benefits many patients, especially geriatric patients that commonly are on complex treatment regimens requiring that the patient take multiple dosage forms several times a day leading to medication errors and poor adherence in many cases (Chen et al., 2020). As many as 80% of the reported adverse effects are associated with inappropriate dosing or dose combinations (Cohen, 1999), which is why personalized therapies may improve adherence, the effectiveness, and success of the treatment (Breitkreutz and Boos, 2007; Preis and Öblom, 2017). Personalized dosage forms are especially desired for children and elderly as the deviation from what is considered normal physiological factors are greatest in these populations (Breitkreutz and Boos, 2007). These population groups may have difficulties swallowing conventional dosage forms, which is why e.g., personalization of orodispersible films and tablets employing printing have been explored (Elbl et al., 2020; Jamróz et al., 2017b; Musazzi et al., 2018; Öblom et al., 2019a; Sjöholm and Sandler, 2019). Pharmacoprinting can further tailor the dosage form to suit the patient's individual preferences regarding e.g., size, color, taste, and shape, which all are factors that may affect patient acceptability (Fastø et al., 2019; Preis and Öblom, 2017). An example to increase acceptance in the pediatric population is 3D printing of chewable taste-masked dosage forms with shapes imitating commercially available sweets (Scoutaris et al., 2018).

Printing technologies aid printing of various geometries and sizes by changing the digital design rather than the complex and costly process of modifying/exchanging the physical equipment e.g., punches in the tableting machines. This is one reason why printing technologies are superior and cost-effective when manufacturing small batches or single dosage units. In comparison, conventional manufacturing methods are more cost-effective for large-scale production of dosage forms of the same dose and size (Goyanes et al., 2015a; Park et al., 2019; Zema et al., 2017). Personalized dosage forms are typically produced in small batches based on the patient's need at a specific time, which is why personalized medicine is envisioned to be prepared on-demand close to the patient.

2.3.3. Information-rich dosage forms

Falsified, substandard, and unregistered/unlicensed medical products entering the global supply chain remains a huge problem accounting for as much as 10.5% of medical products in the supply chain in low- and middle-income countries (WHO, 2019). As a result, 30.5 billion USD is spent annually on unsafe medicines with unpredictable treatment outcomes causing increased socioeconomic cost, failed treatment outcomes, and potential death. IRPs are being explored to prevent these potentially hazardous medical products from entering the supply chains by increasing traceability of dosage forms on a dosage unit level enabling safe medicines and improved treatment outcomes.

The increased availability and popularity of small medical devices, often in combination with smartphones, are foreseen to have a great impact on improving healthcare and treatment outcomes (Accenture, 2017; Haluza and Jungwirth, 2018; Wac, 2012). Combining these devices with information-rich dosage forms enables the possibility to identify and trace a patient's dosage forms thereby advancing drug safety and patient adherence (Mira et al., 2015; Tseng and Wu, 2014), preventing the distribution of falsified medicines (European Commission, 2019), and reducing the number of physical visits to healthcare professionals (Rathbone and Prescott, 2017). To allow tracing, IRPs such as quick response (QR) codes are being explored. These codes can be read by both inexpensive smartphones equipped with a camera and more sophisticated devices.

IRPs are already being used in pharmaceutical products on a packaging level. Since 2019 all European Union (EU) member states should comply with supplement 2016/161 to the EU directive 2011/62/EU stating that machine-readable unique identifiers (in a form of a 2D matrix) are mandatory on a packaging level for traceability and preventing falsified medicines from entering the supply chain (European Commission, 2015). Another guideline published by EMA (European Medicines Agency, 2015) concerns IRP readable by mobile technologies to be found on the packaging or the leaflet to provide further information for health care professionals and/or the end-users. More novel track and trace barcodes have been explored as a measure to circumvent falsified (fake medicines that deliberately and dishonestly pass themselves off as real, authorized medicines (European Medicines Agency, 2021b)) and counterfeit medicines (medicines that do not comply with intellectual-property rights or that infringe trademark law (European Medicines Agency, 2021b)) by printing a barcode visible only in a specific light at a position of the package so that it would be broken in case the package is opened (Zhang et al., 2020). However, IRPs included on the packaging still allow for exchanging the authentic medicine inside the package, which is why in-drug labeling of every dosage unit would be more sufficient in combating falsified products from entering the supply chain. QR-encoded dosage units could be incorporated in a blockchain environment enabling immutable traceability since the dosage unit would be registered once manufactured and deregistered from the blockchain ledger when the patient

scans the QR code prior to administration (Figure 5). This would allow tracing of a single dosage unit along the entire supply chain (Nørfeldt et al., 2019). IRPs used today on a packaging level contribute to generic information for the patient, but do not provide personalized information.

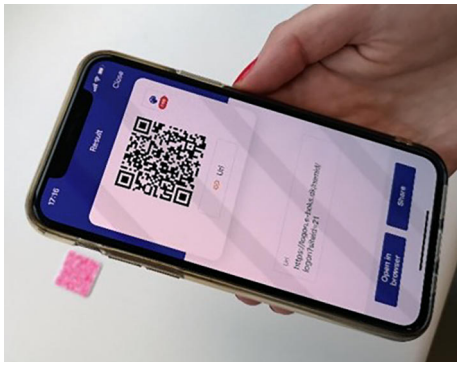

Figure 5. *Scanning of an IJP pink dosage form prior to administration. The dosage form contains a personalized dose and an IRP readable with a smartphone. Unpublished picture.*

To enhance the benefits of IRPs, individualized QR-encoded dosage forms, also called data-enriched edible pharmaceuticals (DEEP) have been explored. DEEP have the possibility to combine personalized dosing with the incorporation of data relevant to different stakeholders (Figure 6). Manufacturing of such advanced dosage forms has been proposed by IJP QR codes with a drug-loaded ink (Edinger et al., 2018a; Öblom et al., 2020) or drug-free ink (Öblom et al., 2019a). Although typically printed by IJP, IRPs have also been investigated using hot-melt pneumatic extrusion technology (Oh et al., 2020) and a combination of different printing technologies together with IJP. QR-encoded dosage forms have been fabricated both to prevent falsified medicines and for identification purposes. This has been achieved by using e.g., fluorescent inks (Logue et al., 2015; You et al., 2016), drug-free biodegradable QR codes (Trenfield et al., 2019), and traceable fluorescent micro-tags to be inserted in a capsule (Han et al., 2012).

Figure 6. *Concept of data-enriched edible pharmaceuticals (DEEP), exemplifying the potential use for medical cannabinoids. Reproduced with permission from* (Öblom et al., 2020).

The use of personalized IRP on a single dosage unit opens up immense opportunities for improved and safer medications. The objective for encoding the dosage units with tailored information may be numerous. It may, for example, be related to the nature of the API (e.g., API with abuse potential or challenging dosing regimens) or the environment where the treatment is given (e.g., support correct administration in hospitals, patient's home, or nursing home as well as administration to the right patient in a hospital ward). The incorporated information would thus be based on the actual need for using such advanced dosage forms.

2.3.4. On-demand manufacturing

In addition to the personalized aspect of on-demand manufacturing, it enables printing at the point-of-care. This is beneficial for dosage forms and formulations with short shelf life and can facilitate bringing APIs to market that otherwise could not be developed (Norman et al., 2017). The suitability of low-cost 3D printers as reactors for synthesis of molecules has been investigated and could potentially eliminate the stability problems associated with certain APIs (Kitson et al., 2013; Symes et al., 2012). Additionally, printing technologies can be used in drug product development, where the simple modification of the digital design enables cost-efficient and fast optimization of the drug product. This can decrease the time required to bring a new drug product to the market. Printing technologies can furthermore be utilized for on-demand low-cost screening purposes (Rosqvist et al., 2020) and drug discovery.

2.3.5. Analytical methods

When exploring the suitability to manufacture printed oral dosage forms a variety of conventional analytical methods are used to gain an understanding of the formulation, processes, and properties of the final dosage form. The analytical methods used to investigate final dosage forms are typically destructive, expensive, require skilled operators, and involve time-consuming analysis of the results. Before printing of dosage forms can become a reality, especially for small personalized batches, there is a need for fast, reliable, and robust analytical methods that can quantify the content of API present in the printed dosage form (Edinger et al., 2018b). Conventional, sampling-based destructive analytical methods (e.g., HPLC and UV-Vis spectroscopy) for quantification of the API used for batch release are not suitable for personalized dosage forms printed in small batches. Traditional pharmacopoeia methods require analysis of multiple samples for each analytical test making personalization of dosage form by printing too expensive and slow with the printers available today. This highlights the need for real time non-destructive analytical methods suitable for printed dosage forms to ensure that the fabricated dosage form complies with the specifications and can be released ideally with a real time release testing approach (European Medicines Agency, 2012a). The analytical equipment used for quantification and/or qualitative aspects of the printed dosage forms, e.g., in a pharmacy setting, should be fast

and small in size (Edinger et al., 2018b) to enable integration in the printing process or preferable handheld if the printed dosage forms are manually analyzed after the printing process. The most commonly proposed non-destructive analytical methods for the final printed dosage forms are Raman, near-infrared (NIR), and infrared (IR) spectroscopy (Boetker et al., 2016; Edinger et al., 2018b; Scoutaris et al., 2018; Trenfield et al., 2020, 2018; Vakili et al., 2017). Moreover, colorimetry, which is an indirect technique for quantification of the API in the printed dosage forms has been used. Colorimetry analyzes the color density in the dosage from printed with a colored drug-containing ink and the color density is correlated to the drug content (Vakili et al., 2016; Wickström et al., 2017b). Additionally, analytical balances are being incorporated in the printers for quality control purposes.

3. Aims of the thesis

The overall objective of the research conducted in this thesis was to explore printing-based manufacturing of personalized solid oral dosage forms, more specifically to investigate the use of FDM, EXT, and IJP. The thesis mainly focuses on printed dosage forms for challenging patient populations, i.e., pediatrics and patients who benefit from increased traceability, as these target groups potentially would profit most from personalized dosage forms. It is hypothesized that printed dosage forms for these populations groups would be superior to the currently marketed products in aspects of personalization of the dose, age-appropriateness as well as incorporation of data on a single dosage unit. Such dosage forms likely result in improved treatment outcomes thereby contributing to a net positive societal impact.

The specific aims of the thesis were to:

- Produce HME filaments with a sufficient drug load consisting of pharmaceutical-grade polymers that can be used for printing of dosage forms with various drug release characteristics (I).
- Evaluate the content uniformity and dosing flexibility of printing technologies for oral dosage forms (I-III).
- Investigate the printability of the prepared filaments and inks (I, III).
- Compare printed dosage forms with a conventional manufacturing technique utilized at hospital pharmacies (II).
- Fabricate DEEP, allowing for simultaneous personalization of the dose and incorporation of desired data in the form of an IRP at a single dosage unit level (III).

4. Materials

An overview of the materials used in the studies included in the thesis is described in the sections below. A more detailed description can be found in the respective original publications (I-III).

4.1. Active pharmaceutical ingredients (I-III)

The active pharmaceutical ingredients (APIs) used as model drugs were all selected based on one or numerous personalization needs. The different APIs used for printing of personalized dosage forms were isoniazid (>98%, TCI America, Portland, OR, USA) (I), warfarin sodium (henceforward called warfarin) (Sigma-Aldrich, St. Louis, MO, USA) (II), and cannabidiol (CBD) and delta-9-tetrahydrocannabinol (THC) present in Sativex® (GW Pharmaceuticals, Cambridge, UK) (III).

4.2. Filaments (I)

Pharmaceutical grade polymers and excipients, namely hydroxypropylmethylcellulose (HPMC, Benecel™ grade E5 Pharm and K100M Pharm, Ashland, Covington, KY, USA), hydroxypropylcellulose (HPC, Klucel™ grade EF Pharm, MW 80,000 and HF Pharm, MW 1,150,000, Ashland, Covington, KY, USA), polyethylene oxide (PEO, Sentry™ Polyox™ WSR N-80 NF, MW ~200,000, and Sentry™ Polyox™ WSR N-750 NF, MW ~300,000, Dow Chemical Company, Midland, MI, USA), Eudragit® RS PO, RL PO and L 100 (Evonik Industries AG, Essen, Germany), triethyl citrate ≥99% (TEC) (Sigma-Aldrich, Darmstadt, Germany), and Kolliphor® TPGS (vitamin E polyethylene glycol succinate, D-alpha-tocopherol content min 250 mg/g, BASF, Ludwigshafen, Germany) were utilized for the production of isoniazid-loaded filaments for FDM. Commercially available polylactic acid (PLA) filament (PLA natural, MakerBot Industries, Brooklyn, NY, USA) with a diameter of 1.75 mm was used as reference material to the prepared drug-loaded filaments.

4.3. Inks (II-III)

Drug-loaded inks with suitable properties for EXT as well as IJP were prepared. The EXT ink contained warfarin, HPC (Klucel™ EXF, MW 80,000, Ashland, Schaffhausen, Switzerland) and a mixture of ethanol (≥94%, Etax A, Altia, Helsinki, Finland), and purified water (Milli-Q water, Millipore SA-67120, Millipore, Molsheim, France) (II).

The warfarin containing ink for IJP was formulated in a mixture of ethanol (≥94%, Etax A, Altia), purified water (Milli-Q water, Millipore SA-67120, Millipore), and propylene glycol (PG) (≥99.5%, Sigma-Aldrich, St. Louis, MO, USA). The colorant quinoline yellow (Sigma-Aldrich, Bangalore, India) was added to the ink for visualization purposes (II).

The THC- and CBD-containing commercial product, Sativex® (GW Pharmaceuticals, Cambridge, UK), with the added colorant erythrosine B (90%

dye content, Sigma-Aldrich, Bangalore, India) was used as ink for IJP of personalized cannabinoid dosage forms (III).

4.4. Substrates (II-III)

Substrates for IJP were prepared by dissolving the film-forming polymer HPC (Klucel™ EXF, MW 80,000, Ashland) in a mixture of ethanol (≥94%, Etax A, Altia) and purified water (Milli-Q water, Millipore SA-67120, Millipore) (II).

Freeze-dried porous substrates for IJP were fabricated from a mixture of hydroxypropylmethylcellulose (HPMC, Metolose 60SH-4000, Shin-Etsu, Tokyo, Japan) polyethylene glycol 4000 (PEG 4000, Emprove, Darmstadt, Merck KGaA, Germany), polysorbate 20 (Tween 20, Emprove, Merck KGaA, Fontenay-sous-Bois Cedex, France), glycerol (≥99%) (Sigma, Petaling Jaya, Malaysia), and poloxamer 188 (Lutrol F68, Sigma, Steinheim, Germany) together with purified water (MilliQ-water, Purelab flex 4, ELGA LabWater, High Wycombe, UK) (III).

5. Methods

An overview of the methods used in the studies included in the thesis is described in the sections below. A more detailed description can be found in the respective original publications (I-III).

5.1. Preparation

5.1.1. Filaments for fused deposition modeling (I)

Various formulations containing 30% (w/w) isoniazid and pharmaceutical grade polymers and excipients possessing different characteristics were formulated into filaments used as feedstock material for FDM (Table 1). The formulations were mixed using a Maxiblend (GlobePharma, New Brunswick, NJ, USA) at 25 rpm for a minimum of 20 min before being extruded utilizing a co-rotating twin-screw extruder (Thermo Fisher Process 11 mm, Waltham, MA, USA) equipped with a standard factory screw assembly and a circular die (⌀ 2 mm). The various formulations were subjected to a constant screw speed of 50 rpm and a barrel temperature between 100 and 155 °C depending on the formulation. A conveyor belt was in addition to cooling the filament also utilized for adjusting the filament diameter by changing the speed of the conveyor belt.

Table 1. *Process temperatures for the hot-melt extruded formulations as well as subsequently applied temperatures during the printing step. All formulations contained 30% (w/w) isoniazid. F = Formulation, HME = hot-melt extrusion, T = temperature. Modified and reproduced with permission from* (Öblom et al., 2019b)*.*

F	Polymer(s) and plasticizer(s)	HME T (^{0}C)	Print T (^{0}C)
1	50% HPC EF + 20% HPMC E5	150	185
2	70% PEO N80	140	185
3	65% HPC EF + 5% PEO N80	140	190
4	60% HPMC E5 + 10% PEO N80	140	—
5	40% HPC EF + 30% PEO N80	140	195
6	40% HPMC K100 + 20% PEO N80 + 10% TPGS	120	—
7	40% HPMC K100 + 30% PEO N750	155	—
8	45% HPC HF + 25% PEO N750	130	185*
9	20% RS PO + 20% RL PO +30% PEO N750	140	—
10	60% HPC EF + 10% PEO N80	130	185
11	20% RS PO + 20% RL PO +27.5% PEO N750 + 2.5% TEC	100	165
12	40% HPC HF + 30% L100	130	170
13	40% HPC HF + 30% E PO	130	175

**Showed day-to-day variability regarding the printability and should therefore be considered as non-printable.*

5.1.2. Inks for semisolid extrusion 3D printing (II)

The drug-loaded printing solution was prepared by dissolving 1.5% (w/w) warfarin and 15% (w/w) HPC in a 1:1 mixture of ethanol and purified water. The placebo solution for EXT was prepared similarly without the addition of warfarin.

5.1.3. Inks for inkjet printing (II-III)

Various inks for IJP, both drug-loaded and drug-free placebo formulations for analytical purposes, were prepared. More precisely, an inkjet printable ink solution was prepared by dissolving 100 mg/g warfarin in the ink base consisting of a mixture of 5% purified water (w/w), 27% PG (w/w), and 57.99% ethanol (w/w). 0.01% of quinoline yellow (w/w) was added to the ink for improved visualization of the printed area (Table 2). A placebo ink was prepared in a similar manner with a composition of 5% (w/w) purified water, 27% (w/w) PG, 67.99% (w/w) ethanol, and 0.01% (w/w) quinoline yellow (II).

To obtain an inkjet printable cannabinoid ink, the colorant erythrosine B was added to the commercial product Sativex® containing 25 mg/ml CBD and 27 mg/ml THC, respectively, and a 1:1 (v/v) mixture of PG and anhydrous ethanol with a small amount of peppermint oil for improved taste (Table 2) (III). The printability of the commercial oil-based cannabinoid product, Stenocare®, containing 12.5 mg/ml of both CBD and THC was also investigated.

Table 2. *Composition of the drug-loaded inks used for IJP of oral dosage forms in studies II and III.*

Study	Ink base	API(s)	Concentration (mg/ml)	Colorant
II	Ethanol, PG, purified water	Warfarin	100	Quinoline yellow
III	1:1 (v/v) ethanol* and PG	CBD THC	25 27	Erythrosine B

**Anhydrous ethanol*

5.1.4. Substrates for inkjet printing (II-III)

HPC-based substrates for IJP, prepared from a solution containing 15% (w/w) HPC and a 1:1 mixture of ethanol and purified water, were solvent cast utilizing a film applicator (Multicator 411, Erichsen, Hemer, Germany). The polymeric solution was cast on top of transparency sheets (clear transparent X-10.0, Folex, Germany) with a wet thickness of 600 µm and the cast substrates were allowed to dry in ambient conditions overnight before imprinting of the drug (II).

Porous substrates, i.e., solid foams, for IJP were fabricated by solvent casting and subsequent freeze-drying. Briefly, the polymer solution was prepared by dispersing 2.5% (w/v) of HPMC, 0.0825% (w/v) of Lutrol, and 0.25% (w/v) of PEG, Tween 20, and glycerol in purified water. An in-house 3D-printed casting knife was utilized to cast the HPMC-based solution on top of transparency sheets (type A paperbacked laser/copier transparencies, Xerox, Norwalk, CT, USA). The cast film was immediately freeze-dried using an Epsilon 2-4 LSC shelf freeze-dryer (Martin Christ, Germany). The freeze-drying cycle consisted of freezing to –30 °C over 3 h and retaining the temperature at –30 °C for the next 3 h. After the freezing step, the pressure was reduced to 0.12 mbar over 10 min whereafter the temperature was increased to 0 °C over 1 h 20 min. The temperature (0 °C) and pressure (0.12 mbar) were kept constant during the following primary drying for 16.5 h. Additionally, the HPMC-based solvent cast films prepared similarly without freeze-drying were dried at ambient conditions for three days. The air-dried film and commercially available potato starch substrate (wafer paper) (AB Marketing GmbH, Germany) were used as reference materials for the freeze-dried foam.

5.1.5. Oral powders in unit dose sachets (II)

Oral powders in unit dose sachets (OPSs) that were used as a comparator to the printed dosage forms were extemporaneously prepared according to the standard operating procedure at the hospital pharmacy of Helsinki University Hospital (HUS) in batches of 30 or 120 OPSs. Commercially available Marevan forte® 5 mg tablets (Orion Pharma, Espoo, Finland) were crushed in a mortar and ground with a pestle to a fine powder. Lactose monohydrate was added in geometric amounts to receive the final concentration needed for each dose and

batch size. 200 mg of the prepared powder blend was weighed (analytical balance, MettlerToledo XP204, Greifensee, Switzerland) into waxed powder papers (Herra Järvisen Verstas Oy, Helsinki, Finland). The OPSs were finally labeled and further packed in plastic ziplock bags.

5.2. Printing

5.2.1. Fused deposition modeling (I)

Various sized tablets (6, 8, or 10 mm in diameter and 2.5 mm in height), as well as replicates of the HME filament geometry (cylinders 40 mm long and 1.75 mm in diameter), were designed in the Rhinoceros software (version 4.0). The 3D designs were saved as STL files and imported into the MakerBot Desktop software (version 3.7.0.108) where the printing parameters were determined. The 3D designs were subsequently printed using a MakerBot Replicator 2 (MakerBot Industries, Brooklyn, NY, USA) equipped with a custom-made air-cooled printhead. The different HME filaments were printed at temperatures ranging from 165 to 195 °C using a layer height of 0.05 mm, two printed outlines, and printing and traveling speeds of 90 mm/s and 150 mm/s, respectively. To obtain tablets with different porosities, infill levels of 15% and 90% were used for printing the tablets.

5.2.2. Semisolid extrusion 3D printing (II)

ODFs were prepared by means of EXT. The HPC-based solution was inserted into 10 ml single-use syringes equipped with a disposable 25 G electro-polished tip (1/4" Techcon TE Needle, Ellsworth adhesives, Norsborg, Sweden). The Biobots 1 (Biobot, Philadelphia, PA, USA) EXT coupled to an air compressor was used to print both drug-free ODFs and ODFs containing warfarin. The ODFs were printed one at a time on top of transparency sheets. They were fabricated with a layer height of 0.1 mm, a printing speed of 8 mm/s, and a pressure of 25 PSI.

5.2.3. Inkjet printing (II-III)

ODFs were prepared by imprinting the prefabricated HPC substrates with the warfarin ink according to a premade digital design made in PowerPoint (II). A PixDro LP50 piezoelectric printer (Roth and Rau, Eindhoven, Netherlands) equipped with a 128-nozzle printhead (SL-128 AA, Fujifilm, Tokyo, Japan) and a camera for visualization of the jetted droplets was used for preparation of personalized warfarin doses. The prepared ink (drug or drug-free) was filtered (0.45 µm polypropylene membrane syringe filter, VWR International, Radnor, PA, USA) prior to printing. The used printing resolution was 720 DPI and the IJP was conducted with a jetting frequency of 1400 Hz, a voltage of 80 V, an ink pressure of –18 mbar, and a pulse shape of 3-16-5 µs. One printing pass resulted in 32 ODFs, which were allowed to dry in ambient conditions overnight before manually being cut into the final size using a scalpel and an in-house designed cutting template.

DEEP, combining personalization aspects both regarding the dose as well as incorporation of desired data in a single step, were prepared by IJP (III). The cannabinoid ink was loaded into an empty disposable ink cartridge and the ink was deposited on the prepared porous substrates according to the pre-generated QR code (2 x 2 cm) utilizing a low-cost Epson XP-8500 desktop piezoelectric inkjet printer (Seiko Epson Corporation, Nagano, Japan). The QR code was generated using a free online QR generator (goQR.me, Foundata GmbH, Karlsruhe, Germany). Personalized doses were achieved by subjecting the printed area to various numbers of subsequent printing passes. The printed DEEP were allowed to dry at ambient conditions overnight and the final size of the DEEP was attained by manual cutting with scissors.

5.3. Characterization

5.3.1. Hot-melt extruded filaments (I)

The HME filaments used for FDM were studied with regards to their mechanical properties (n = 10) utilizing a three-point bend test with a TA-XT2i texture analyzer (Texture Technologies, Hamilton, MA, USA) to get a deeper understanding of factors influencing the printability. Filament pieces (45 mm) were cut from the filament strand and placed on the three-bend rig sample holder (TA-95N, Texture technologies) with a set gap of 25 mm. The measurement was conducted at 10 mm/s and recording started when the trigger force of 5.0 g was exceeded. The endpoint was defined as a 15 mm downward movement of the upper probe. Data analysis was performed using the Exponent software (version 6.1.5.0, Stable Micro Systems, Godalming, UK).

To further evaluate factors affecting the printability, dynamic vapor sorption analysis of the HME filaments was performed using the SPS11 (ProUmid, Ulm, Germany) to get insight regarding the moisture uptake of the prepared filaments. The analysis started with drying of the samples at 0% relative humidity (RH), whereafter the RH automatically was increased to 90% RH in steps of 10% RH after reaching equilibrium (0.0100%/30 min) at the previous cycle. The weight was determined every 10 min, and the minimum and maximum time at each climate cycle was 60 min and 72 h, respectively.

The drug content uniformity of the prepared filaments was evaluated by determining the drug content (n = 10) in filament pieces (150 ± 6 mg) cut from random sections of the extruded filament. The filament pieces were immersed in 100 ml of purified water and shaken at 120 rpm (Multi-shaker PSU 20, Biosan, Latvia) for 24 h. Dilutions were performed when needed and the drug content was determined by utilizing a UV-Vis spectrophotometer (Lambda 35, PerkinElmer, Singapore) at 263 nm. Moreover, the drug release profiles (n = 3) of the HME filaments in 900 ml phosphate buffer (pH 7.4) at 37 ± 0.5 °C with paddles rotating at 100 rpm were investigated using an automated setup (Sotax AT 7smart, Basel, Switzerland). At predetermined time points samples were automatically withdrawn using a pump (Sotax CY 6, Basel, Switzerland) and filtered (glass microfiber filter GF/B, GE Healthcare Life Sciences, UK), prior to

measuring the absorbance at 263 nm utilizing an online UV-Vis spectrophotometer (Lambda 35, PerkinElmer, Singapore). For calculations of drug release at various time points, the theoretical drug content of 30% (w/w) present in the samples was used.

The thermal properties of the prepared drug-loaded filaments were investigated by differential scanning calorimetry (DSC 1, Mettler Toledo, Columbus, OH, USA) to get an understanding of how the different processing steps affected the formulation. Samples weighing 3 to 6 mg were placed in pierced aluminum pans that were subjected to a heat-cool-heat cycle from − 20 to 250 °C with a heating and cooling rate of 10 °C/min and 20 °C/min, respectively. The data was analyzed using the STARe software (Version 9.20, Mettler Toledo).

5.3.2. Printing inks (III)

The printability of the investigated cannabinoid inks was evaluated by determining the density, dynamic viscosity, and surface tension of the formulations in order to formulate a printing ink with suitable properties to be jetted out of the nozzles in the used printer. The density was attained by accurately weighing 1 ml of the ink at ambient conditions (n = 5), whereas the viscosity of the inks was determined by using a Discovery HR-3 Rheometer (TA Instruments Ltd, New Castle, DE, USA) with a cone (angle 1.002°) and plate (ø 40 mm) setup at 25 °C. The ink was pipetted onto the plate and a 60 s soaking time was used before starting the measurement using a shear stress ramp from 0.01 to 1000 s^{-1} with 4 points per decade and a maximum equilibration time of 60 s. The average viscosity at 1000 s^{-1} (n = 3) was defined as the viscosity of the ink. The Trios software (version 4.0.1.29891, TA Instruments) was used to acquire the data. Furthermore, a DSA100 Drop shape analyzer (Krüss GmbH, Hamburg, Germany) was used to determine the surface tension of the inks (n = 6) at ambient conditions. The surface tension of an ink droplet was attained with a 5 s interval over 1 min. The average of all measured droplets was used as the surface tension for the ink.

To further predict the printability of the cannabinoid inks in the used printer the Z-value was calculated according to equation 1 (see section 2.2.3.3), which comprises the following parameters: nozzle diameter of the printer, density, surface tension, and viscosity of the ink.

5.3.3. Substrates and printed solid oral dosage forms (I-III)

5.3.3.1. Weight, thickness, and appearance (I-III)

The appearance of the prepared filaments for FDM (I), substrates for IJP (II-III), as well as the printed dosage forms (I-III) were evaluated visually. Moreover, the weight of the dosage forms was determined using an analytical balance (AND GH-252, A and D Instruments Ltd., Tokyo, Japan) (I-II) and the thickness of the substrates and printed dosage forms was determined using a digital caliper (CD-6”CX, Mitutoyo, Kawasaki, Japan) (n = 10 and n = 3 for study II and III, respectively).

5.3.3.2. Absorption capacity (III)

The absorption capacity (n = 6) of the prepared substrates was evaluated by immersing 1 x 1 cm pieces of the substrates in paraffin oil for 24 h in a desiccator with an applied vacuum (III). After 24 h, excess oil from the surface of the substrates was removed by carefully wiping the substrates with Kimwipes (Kimberly Clark Worldwide Inc., Irving, TX, USA). The absorption capacity was calculated according to equation 5, where w_t represents the weight after immersion in paraffin oil and w_0 represents the initial weight.

$$Absorption\ capacity\ (\%) = \frac{w_t - w_0}{w_0} * 100\% \qquad \textbf{Eq. 5}$$

5.3.3.3. Microscopic analysis (III)

The morphology of the surface and the cross-section of the freeze-dried, air-dried, and commercial potato starch substrates, as well as the DEEP (drug imprinted freeze-dried substrate) (III), were analyzed utilizing a tabletop TM3030 scanning electron microscope (SEM) (Hitachi, Tokyo, Japan) applying different levels of magnifications at 5 kV. Before analysis, small pieces of the substrates were cut and gold-coated for 30 s using the 108 Auto sputter coater (Cressington Scientific Instruments, Watford, UK). The TM3030 software (version 01-02, Hitachi) was used to acquire the SEM images.

5.3.3.4. Texture analysis (II-III)

Various mechanical properties of the prepared substrates and the printed dosage forms were studied using a TA-XTplus (Stable Micro Systems, Godalming, UK) texture analyzer equipped with either a 5 kg or 10 kg load cell utilizing different setups.

The burst strength and elongation at break of the drug-free and drug-loaded ODFs (n = 5) prepared in study II were investigated using a film puncture setup conducted at ambient conditions. The setup consisted of a perspex film support platform and an aluminum circular top plate (film support rig HDP/FSR, Stable Micro Systems) clamping the ODF in place as well as a spherical probe (ø 5 mm, SMS P/5S, Stable Micro Systems) that was used to puncture the ODF. The acquisition of data was initiated when the trigger force of 0.049 N was reached and the measurement was conducted at a constant speed of 1 mm/s until reaching the target distance of 5 mm (EXT films) or 15 mm (IJP films). The maximum applied force (N) and penetration depth (mm) into the film before rupturing was recorded.

The mechanical properties of the freeze-dried, air-dried, and commercially available potato starch substrates, as well as DEEP (drug imprinted freeze-dried substrates), were studied in tension mode (n = 3) (III). The samples were cut into rectangular samples (40 mm x 10 mm) and fixed to the tensile grips (A/TG tensile grips, Stable Micro Systems) with a distance of 20 mm between the two grips. The acquisition of data started when the trigger force of 0.049 N was reached and the analysis was performed at a constant speed of 2 mm/s until the

upper grip had moved 40 mm. The attained data included the change in length (% strain) of the sample versus the applied force divided by the cross-section area (stress, N/mm^2).

5.3.3.5. Surface pH (II)

The surface pH of the ODFs prepared by means of EXT, IJP (drug-loaded and placebo), and OPSs were analyzed by addition of 1 ml of purified water to a small glass vial containing the ODF or OPS (n = 3). The pH of the media was determined at room temperature at 1 min and 15 min utilizing a pH meter (Mettler Toledo FE20, Mettler Toledo AG, Greifensee, Switzerland).

5.3.3.6. Moisture content (II)

The moisture present in the fabricated ODFs (drug-loaded and placebo, n = 3) was evaluated using a moisture analyzer (Radwag Mac 50/NH, Radom, Poland). Samples were placed in an aluminum pan and heated up to 120 °C while the weight loss measured in mass % (i.e., moisture evaporation) was recorded. The measurement was completed when the difference in mass was lower than 1 mg/min.

5.3.3.7. Disintegration (II-III)

The disintegration time of the substrates and printed dosage forms was studied using a static Petri dish disintegration test. The substrates and drug-loaded ODFs were placed in a Petri dish (plastic, ø = 10 cm) prefilled with 10 ml of purified water (II). Similarly, the substrates and subsequently printed DEEP were added to a Petri dish (glass, ø = 6 cm) prefilled with 5 ml of purified water (III). The time for the samples to fully rupture into smaller fragments was recorded and defined as the endpoint of the static test.

5.3.3.8. Drug content (I-III)

The drug content for the 3D-printed tablets was calculated from the data attained in the *in vitro* dissolution study (section 6.1.4.7) (I). Briefly, the drug content was determined by calculating the mean drug content of five subsequent time points in the dissolution study once the drug release had reached 100% drug release (n = 3).

The drug content in the prepared dosage forms was studied by dissolving the ODFs or OPSs (the comparator formulation) in 100 ml of purified water while agitated at 50 rpm on a Multi-shaker PSU 20 (Biosan, Riga, Latvia) for a minimum of 3 h (n = 10) (II). The drug present in the fabricated dosage forms was subsequently determined using a spectrophotometer (Lambda 35, PerkinElmer) measuring the absorbance at 207 nm and samples were diluted when required. Uniformity of content of single-dose preparations (UC) was calculated according to the European Pharmacopoeia (Ph. Eur. 9.0) 2.9.6, test B (European Pharmacopoeia Commission, 2017). Furthermore, the uniformity of dosage units was determined as defined in Ph. Eur. 2.9.40. The acceptability constant k = 2.4 (n = 10) and T = 100% were used to calculate the acceptance values (AV). In the

conducted study, the compliance with the stated limits for UC and AV were based on 10 replicates, an additional 20 dosage forms were not analyzed.

The drug content in the IJP DEEP containing cannabinoids was determined using ultra-performance liquid chromatography (UPLC) (III). DEEP imprinted with various layers of the cannabinoid containing ink were dissolved in 3 ml of a mixture of acetonitrile and purified water (70:30 v/v) (n = 3). The samples were vortexed until fully dissolved and subsequently centrifuged at 5000 rpm for 10 min (Hettich EBA20, Tuttlingen, Germany) whereafter the supernatant was analyzed or diluted if needed prior to analysis on an Ultimate 3000 (Thermo Scientific, Waltham, MA, USA). The UPLC was equipped with a Kinetex C18 LC column (1.7 µm, 100 Å, 150 x 2.1 mm, Phenomenex), a vacuum degasser, a temperature-controlled column compartment, and an autosampler compartment, kept at 30 °C and 8 °C, respectively. The mobile phases used to elute the sample comprised of 0.1% (v/v) formic acid in both acetonitrile (A) and purified water (B). A multistep gradient program as described by Öblom et al. (2020) was used. 10 µl of the sample was injected and analyzed at 228 nm with a flow rate of 0.4 ml/min. The chromatograms were acquired and analyzed in the Thermo Xcalibur software (version 3.0.63).

5.3.3.9. In vitro drug release (I-III)

The 3D-printed tablets were placed in capsule sinkers and the drug release characteristics of the various printed formulations were determined utilizing the same method as previously described for the filaments (section 5.3.1) (I).

The drug release behavior of the printed ODFs was determined in 10 ml of purified water at 37 °C under continuous shaking at 50 rpm (n = 3) (II). The ODFs were placed in dissolution baskets to avoid sticking to the glass. At predetermined sampling times, 3 ml samples were manually withdrawn and replaced with 3 ml of preheated media. The absorbance of the withdrawn samples was measured at 207 nm utilizing a UV–Vis spectrophotometer (Lambda 35, PerkinElmer, Singapore). In parallel to the manual dissolution study, the ODFs containing the highest amount of drug were analyzed with an automated setup (Sotax AT 7smart, Basel, Switzerland) in 500 ml of purified water at 37 ± 0.5 °C (n = 3). The ODFs were placed in dissolution baskets, which rotated at 50 rpm and samples of the release media were automatically withdrawn using a pump (Sotax CY 6, Basel, Switzerland), subsequently filtered (glass microfiber filter GF/B, GE Healthcare Life Sciences, Little Chalfont, UK), and analyzed using an on-line UV–Vis spectrophotometer at 207 nm (Lambda 35, PerkinElmer, Singapore). The percent of drug released at the different time points in both setups was calculated based on the data attained from the drug content analysis.

The drug release from the 10 layers imprinted DEEP (n = 3) was determined in 6 ml of simulated saliva (pH 6.8) prepared according to (Palo et al., 2017) and to which 0.5% (v/v) polysorbate 20 was added (III). The experiment was conducted at 37 °C and the dissolution media was continuously stirred at 60 rpm utilizing a magnetic stirrer. Manual sampling at each time point consisted of

withdrawal of 200 µl of the sample and addition of 200 µl of the preheated simulated saliva. The withdrawn samples were centrifuged at 10,000 rpm for 10 min at 4 °C, and the supernatant was transferred into silanized high-performance liquid chromatography (HPLC) vial inserts (450 µl, Phenomenex), whereafter the drug content was determined using the UPLC method previously described in the drug content section (5.3.3.8).

5.3.3.10. Thermal properties (I-II)

The thermal properties of the 3D-printed tablets, ODFs (drug-loaded and placebo) as well as OPSs were investigated using differential scanning calorimetry (DSC). The thermograms for the 3D-printed tablets were attained using the method described for thermal analysis of the filaments in section 5.3.1 (I).

In study II, the samples (n = 2-3) were placed in sealed Tzero aluminum pans and analyzed from –20 to 230 °C with a heating rate of 10 °C/min using the Q2000 (TA Instruments, New Castle, DE, USA) with a nitrogen purge gas flow of 50 ml/min. The TA Universal Analysis software (version 4.5A, TA Instruments) was used to acquire and analyze the data.

5.3.3.11. Infrared spectroscopy (II)

Attenuated total reflectance fourier transform infrared (ATR-FTIR) spectroscopy (Spectrum Two, PerkinElmer Inc., Beaconsfield, UK) equipped with a diamond was used to determine the infrared spectra of the prepared ODFs (drug-loaded and placebo) and the OPSs (n = 2-3). The samples were subjected to an applied force of 75 N and analyzed from 4000 to 400 cm^{-1} with four accumulations at a resolution of 4 cm^{-1}. The data was acquired using the Spectrum software (version 10.03.02, PerkinElmer). The same software was further used for data treatment (baseline correction, normalization, and data tune-up) and analysis.

5.3.3.12. Stability (II-III)

The stability of the fabricated ODFs and OPSs stored in ambient conditions in the dark was investigated with regards to visual appearance, mechanical properties (texture analysis), drug content (UV-Vis spectroscopy), thermal properties (DSC), and chemical interactions (ATR-FTIR) (II). The samples were analyzed on days 1, 7, 14, 21, and 28.

The stability of the IJP DEEP was studied with regards to the readability of the printed QR code as well as the drug content after 1 day, 1 week, 2 weeks, and 8 weeks (n = 3) (III). The readability was evaluated using a QR code scanner app for iPhone 11 Pro (QR-kod, App Store) and the drug content was investigated by UPLC according to the method described in the drug content section (5.3.3.8). The stability of the IJP DEEP was investigated in two different storage conditions, namely, accelerated stability conditions (40 °C/75% RH) as well as cold and dry storage conditions (4 °C, in a desiccator with silica).

6. Results and discussion

In the thesis, three different printing techniques were successfully used to produce personalized dosage forms. APIs with a specific need for personalization and/or traceability were formulated into printed solid oral dosage forms, namely tablets and ODFs. An overview of the different manufacturing methods and APIs used to prepare the oral dosage forms is listed in Table 3.

Table 3. *Overview of the manufacturing methods and APIs used in the different studies.*

Study	Manufacturing method	API	Feedstock material(s)	Dosage form
I	FDM	Isoniazid	Filament	Tablet
II	EXT	Warfarin	Viscous ink	ODF
	IJP		Substrate & low-viscous ink	ODF
	Tablet manipulation		Commercial tablet	OPS
III	IJP	CBD	Substrate & low-viscous ink	DEEP
		THC		

6.1. Preparation and characterization

6.1.1. Hot-melt extruded filaments (I)

HME, an established method used in the pharmaceutical industry, was utilized to prepare 13 drug-loaded filaments with various compositions. These filaments were subsequently used as feedstock materials for FDM. The filaments contained 30% (w/w) isoniazid and various combinations of pharmaceutical-grade polymers and excipients (Table 1). To investigate the release behavior based on the specific formulations a fixed drug load was used, thereby eliminating the effect originating from the drug load, which is known to alter the drug release behavior (Boetker et al., 2016; Water et al., 2015). The use of one specific drug load further supported the concept that personalized medicines can be fabricated on-demand in e.g., a hospital pharmacy utilizing premade filaments with a fixed drug load, thus, highlighting that personalization of the dosage form could be achieved utilizing FDM.

A total of eight out of the thirteen filaments formulations prepared were printable. Out of these eight printable formulations, six were HPC-based formulations indicating good printability of HPC. In comparison filaments containing a high amount of HPMC were unprintable. For successful printing, the filament should possess sufficient flexibility without being too soft (Smith et al., 2018). A brittle filament will break from the pressure from the driving gears that the filament is subjected to during the feeding step, while a filament that is too

soft is prone to feeding problems as it is deformed under the pressure (Fuenmayor et al., 2018; Zhang et al., 2017a). To get an understanding regarding the printability of the prepared filaments a 3-point bend test was utilized to study the mechanical properties. Commercially available PLA filaments with ideal properties for printing were used as a reference. The test revealed that filaments possessing a higher breaking distance (i.e., tougher filaments) typically were printable compared to filaments with a breaking distance below 1.5 mm. These were too brittle and failed to load into the 3D printer, which is in line with what has been previously reported in the literature (Korte and Quodbach, 2018; Zhang et al., 2017a). However, the printability of filaments is complex and cannot be fully understood by only one mechanical parameter. Some filaments with adequate breaking distance were found too soft to be printable and other filaments were subjected to wear, both resulting in failed feeding of the filament. Therefore, other mechanical properties of the material should be evaluated, such as column strength, Young's modulus, and softness to get a deeper understanding of the filaments and their printability.

In addition to the mechanical properties, moisture uptake of the filament is of importance as the ambient RH can vary greatly. Moisture uptake by the filament has been associated with poor print quality and printing failures as a result of the materials' ability to absorb moisture from the air (Duran et al., 2015). The absorption process depends on e.g., the RH, temperature, affinity between the surface of the material and the water molecules as well as the surface area (Airaksinen, 2005). When water is taken up by the filament it may cause an increase in the diameter of the filament by swelling and alter the glass transition temperature of the formulation, both resulting in unpredictable printing performance and day-to-day variability in the printability of the filament (Halidi and Abdullah, 2012). Therefore, printing should be performed in a controlled humidity environment to achieve repeatable results.

All the prepared filaments showed moisture uptake in a sigmoidal manner, revealing low moisture uptake at low humidity and high uptake at higher RH as expected for cellulose- and starch-based polymers (Szakonyi and Zelkó, 2012). Based on the results obtained from the analyzed filaments it can be concluded that filaments with a high overall moisture uptake were more likely to be unprintable. No clear correlation could be made between printability and moisture uptake at low RH, which is the typical condition during printing. Future studies are thus needed to get a full understanding of how moisture uptake affects printability.

6.1.2. Printing inks (III)

Understanding the ink properties is imperative in order to have a robust printing process that enables production of high-quality dosage forms. A suitable ink for IJP shows stable ink jetting, which is needed for a content uniformity of the API(s) that is within the specified limits as well as a good print edge definition required for decoding of printed IRPs. The most important parameters of a printable ink are described in section 2.2.3.3.

The printability of the printing ink containing the two cannabinoids, CBD and THC, was evaluated by determining the viscosity, surface tension, and density of the ink. In addition, the Z-value was calculated and used to predict printability in the used printer (Table 4). The same was done for various placebo formulations to get an understanding of how the ink composition could be modified, if needed, to achieve a printable ink.

Table 4. *Measured properties of the cannabinoid-containing inks and the placebo ethanol-propylene glycol (PG)-based inks (% v/v) as well as the calculated Z-value as a predictor of printability. Data are presented as average ± SD, n = 5, 3, and 6 for density, viscosity, and surface tension, respectively. Reproduced with permission from* (Öblom et al., 2020).

Formulation	Density (g/ml)	Viscosity (mPa·s)	Surface tension (mN/m)	Z-value
Sativex®	0.907 ± 0.002	11.0 ± 0.1	26.5 ± 0.2	1.4
Stenocare®	0.933 ± 0.003	29.2 ± 0.1	24.0 ± 1.8	0.5
EtOH/PG 0/100	1.030 ± 0.011	40.9 ± 0.5	30.6 ± 0.3	0.4
EtOH/PG 20/80	0.993 ± 0.004	24.9 ± 0.4	29.7 ± 0.1	0.7
EtOH/PG 40/60	0.937 ± 0.002	12.9 ± 0.7	27.8 ± 0.0	1.3
EtOH/PG 50/50	0.902 ± 0.001	8.3 ± 0.2	26.3 ± 0.0	1.9
EtOH/PG 60/40	0.877 ± 0.008	3.6 ± 0.2 [a, b]	25.2 ± 0.0	4.1
EtOH/PG 80/20	0.829 ± 0.008	N/A [a]	23.2 ± 0.1	N/A
EtOH/PG 100/0	0.773 ± 0.008	1.162 [a, c]	21.9 ± 0.1	12.9

[a] *Could not be measured with the used setup due to too low viscosity and solvent evaporation.*
[b] *Viscosity at 30 °C for the ink taken from* (Genina et al., 2013a).
[c] *Viscosity value at 20 °C taken from* (Krüss GmbH, 2019).

6.1.3. Substrates (III)

Personalized IJP dosage forms are commonly prepared by imprinting solvent cast substrates, but other substrates such as tablets (Edinger et al., 2017) and electrospun fibrous substrates (Palo et al., 2017) have been explored. Successful IJP of dosage forms requires high-quality substrates that have the capacity to absorb a sufficient amount of the drug-loaded ink. For the purpose of incorporation of IRPs, the substrate further needs to absorb the ink without spreading of the ink as a high print edge definition of the printed IRP is required to enable decoding after drying. Polymeric solutions that are solvent cast to form orodispersible substrates are typically thin and non-porous and can therefore absorb only a limited amount of deposited ink. To overcome this limitation substrates containing mesoporous silica and porous substrates, also referred to as solid foams, have been developed (Edinger et al., 2018a; Iftimi et al., 2019). Solid foams have improved absorption capacity due to the porous structure and can retain the ink in the foam while drying so that it is not easily smeared off (Iftimi et al., 2019).

In study III porous substrates were prepared by freeze-drying in a similar manner as previously described (Iftimi et al., 2019), however, the substrates were solvent cast prior to freeze-drying to achieve thinner substrates that could be fed into the printer. The porous substrates were white with a thickness of 0.78 ± 0.03 mm, while the air-dried films prepared as comparator were transparent and only 0.06 ± 0.01 mm thick despite being cast with the same wet thickness. Commercially available white potato starch substrates with a thickness of 0.32 ± 0.02 mm commonly used for food printing were included as a second comparison.

Microscopic analysis of the substrates with SEM revealed differences in porosity. The air-dried film was non-porous (Figure 7 A-B), the potato starch substrate showed some heterogeneous pores (Figure 7 C-E), while the foam had a homogenous network of open pores (Figure 7 F-H). The cross-section of the foam confirmed that the porous structure was present throughout the substrate, not only on the surface.

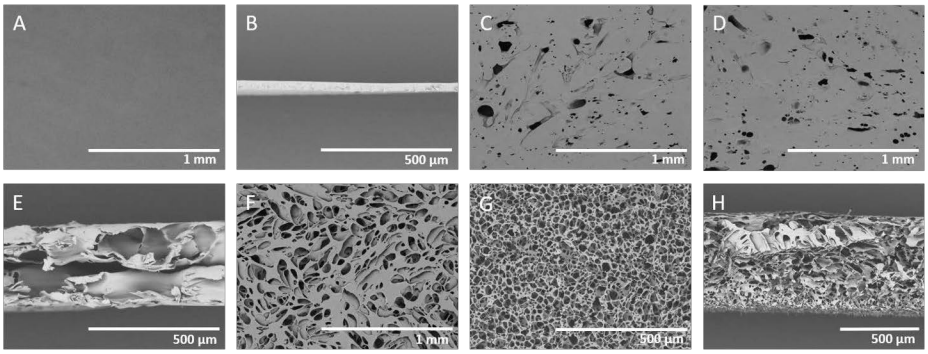

Figure 7. *Scanning electron microscopy images of the A) top surface of the non-porous air-dried film and B) cross-section of the non-porous air-dried film C) rough surface of the commercial potato starch substrate, D) smooth surface of the commercial potato starch substrate, and E) cross-section of the commercial potato starch substrate F) top surface of the freeze-dried solid foam, G) bottom surface of the freeze-dried solid foam, and H) cross-section of the freeze-dried solid foam.* Modified and reproduced with permission from *(Öblom et al., 2020)*.

The oil absorption study revealed a greatly improved absorption for the foam (freeze-dried) as compared to the film (air-dried), with absorption capacities of 1620 ± 101% (w/w) and 10 ± 4% (w/w), respectively. These findings indicate that the porous foams have improved drug-loading capacity compared to conventionally prepared films as the foam can absorb more of the ink deposited during printing.

6.1.4. Printed solid oral dosage forms (I-III)

6.1.4.1. Physical appearance (I-III)

In study I, the FDM 3D-printed tablets were pale yellow to yellow, similar to the HME filaments, depending on the formulation. The shape of the different sized tablets complied with the premade design (Figure 8 A), except for some smaller

imperfections for several of the formulations resulting in not completely round tablets. Some formulations had a rough surface (Figure 8 C-D) on the tablet side that was not in contact with the build plate while other formulations had a desired smoother (Figure 8 A-B) top surface. This indicates that the printing parameters would require fine-tuning to achieve a smoother finish of the printed tablets. All formulations were printed with identical printing parameters that were initially optimized for PLA. Since the formulations likely possess different melt-flow properties this should be accounted for when choosing the printing parameters. It has been reported that the melt flow behavior of a formulation, which changes with temperature, impacts both the printability and the final quality of the 3D-printed object (Fuenmayor et al., 2018; Wang et al., 2018). Investigation of the polymer melt properties could have assisted in the selection of the optimal process parameters thereby improving quality (Aho et al., 2015).

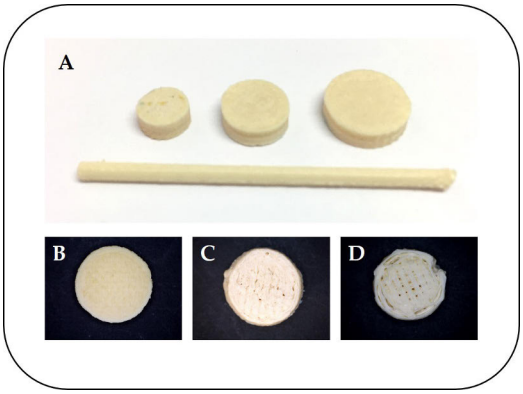

Figure 8. *FDM 3D-printed tablets. A) Photograph of the various sized 3D-printed tablets and cylinder rod replicating the HME filament as well as the top surface visualized with a digital microscope of the tablets printed with B) formulation 2 (smooth tablet surface) C) formulation 1 (rough tablet surface with small holes) and D) formulation 8 (poor print quality). Modified with permission from* (Öblom et al., 2019b) *and unpublished pictures.*

The ODFs and OPSs prepared in study II are presented in Figure 9. EXT ODFs were transparent with a slightly wavy structure that was observed upon close inspection. In comparison, the IJP ODFs were pale yellow as a result of the colored ink that was deposited on the transparent solvent cast substrate. In both cases the printed ODFs were thin and flexible. The powder in the OPSs had a pink color consisting of a mixture of larger ground pink tablet particles and smaller white lactose particles.

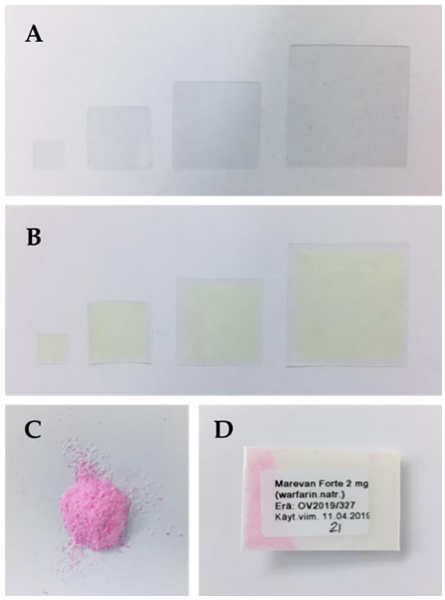

Figure 9. *Photographs of the prepared dosage forms A) EXT ODFs B) IJP ODFs C) oral dose powder, and D) OPS. Reproduced with permission from* (Öblom et al., 2019a).

The DEEP prepared in study III were imprinted with a pink QR code on the white slightly shiny substrate (solid foam) (Figure 10 A-C). Part of the DEEP was noticed to be compressed during the printing process as a result of the feeding roll compressing the porous structure of the substrate (Figure 10 C). This was more pronounced the more consecutive layers that were printed as this subjected the substrate to further printing passes and thus further compression by the feeding rolls in the printer.

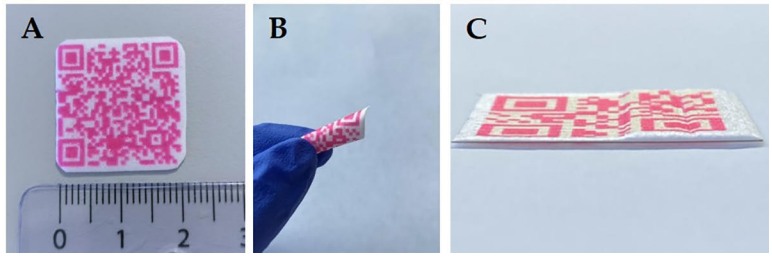

Figure 10. *Photographs of printed DEEP showing the A) size, B) flexibility, and C) compressed part of the DEEP originating from the printing process. Modified with permission from (Öblom et al., 2020) and unpublished picture.*

6.1.4.2. Mechanical testing (II-III)

According to Ph. Eur. ODFs should possess suitable mechanical strength to resist handling without being damaged (European Pharmacopoeia Commission, 2020a). To date, no standardized test method or acceptable limits for mechanical properties are provided in the guidelines making it hard to compare results from different studies. The DIN EN ISO 527 tensile test, originally developed for foil,

has been utilized to determine the mechanical stress (also referred to as tensile or breaking strength) for ODFs, buccal dosage forms, and substrates used for pharmaceutical purposes (DIN, 2003, 1996; Garsuch and Breitkreutz, 2009; Hoffmann et al., 2011; Jamróz et al., 2017b; Preis et al., 2014). However, the method has low sensitivity and originally required an 80 mm bone-shaped specimen (DIN, 1996). ODFs are generally smaller in size and have a less complex geometry, e.g., rectangular or square shaped thus deviating from the standard. It is challenging to perform mechanical testing on thin films due to their fragile nature and the drastic decrease in the cross-sectional area during testing (Pryor, 2021). Today most used standards for testing thin films used as packing material, but also in optical coatings, various electronics, batteries, etc. are ASTM Standard D882 usually used in the US and ISO 527-3 typically favored in Europe and Asia. The ISO 527-3 is aiming at films that are less than 1 mm in thickness and does not require the common bone-shaped specimens but rather a rectangular shape making it more suitable for testing of thin films compared to ISO 527-1. Due to the challenges described above and the lack of standardized tensile test methods for pharmaceuticals like ODFs, various other mechanical testing methods have been used. These tests aim to determine the mechanical strength in order to ensure that ODFs are not damaged during any of the steps involved prior to administration, i.e., manufacturing, distribution, and handling by the patient.

In this thesis, a texture analyzer was utilized to investigate the burst strength (N) (i.e., the maximum tolerated force on the ODF before rupturing) and the burst distance (mm) (i.e., the flexibility of the ODF) (II) as well as Young's modulus (an indication of stiffness of a material), ultimate tensile strength (UTS) (the maximum stress that a material can withstand before breaking), and elongation at break (the ability for the material to stretch before breaking) for the prepared substrates and subsequently imprinted DEEP (III).

Different manufacturing techniques revealed differences in the mechanical properties of the ODFs (II). Placebo IJP ODFs were found to be more than twice as strong as compared to the placebo EXT ODFs, which may be partly explained by the thicker placebo IJP ODFs and by the structure of the ODF. The placebo IJP ODF (solvent cast) was completely flat whereas the placebo EXT ODF had a slightly wavy structure originating from the line-by-line fabrication of the film during the printing process. Incorporation of the drug in the EXT ODFs resulted in a slight decrease in strength and a decreased burst distance. These ODFs were also the most brittle assessed in the study (II). In comparison drug-loaded IJP ODFs had the greatest flexibility, over twice as much as compared to the placebo IJP ODFs (i.e., the printing substrate for IJP). This can be explained by the introduction of plasticizers, e.g., moisture and PG, which both have a plasticizing effect. The addition of plasticizers typically increases the polymer chain mobility by interaction with these polymer chains resulting in a decreased glass transition temperature and improved mechanical properties, which are important for ODFs, such as plastic and elastic properties (Boateng et al., 2009). This study indicates that the thickness of the prepared ODF, the printing technique itself including differences in the involved process steps, and additional liquid serving

as a plasticizer for IJP ODFs may all affect the mechanical properties. The mechanical properties did not change drastically during the one-month stability study except for a trending decrease in strength and flexibility for the drug-loaded EXT ODFs during the first week. This is an indication that the ODFs may have contained residual moisture upon initiation of the study or that the properties changed due to changes in the ambient RH.

Mechanical analysis of the substrates and imprinted DEEP revealed that all formulations showed more brittle than ductile characteristics, apart from some minor necking for the air-dried film substrates (III). Similar to what was observed in the previous study, the manufacturing method affected the resulting mechanical properties. The air-dried film was the strongest and stiffest substrate revealing much higher UTS and Young's modulus values compared to the freeze-dried porous foam. The UTS of the commercially available potato starch substrate was between the other two substrates and displayed a higher Young's modulus than the foam. The imprinted DEEP (foam imprinted with lipophilic cannabinoid ink) was stiffer and stronger as compared to the foam. This may be explained by the porous structure of the foam being partly damaged during the printing process (Figure 10 C and Figure 11 C-D). The feeding rolls in the desktop printer caused observable compression of the foam thereby affecting the mechanical properties. This resulted in a higher UTS attributed to a decreased stress area of the compressed foam. In addition, deposition of the ink was seen to change the surface structure by dissolving the surface of the foam resulting in a non-porous layer where the ink was deposited (Figure 11 A-B). The foam substrate exhibited the greatest ability to stretch, which further improved after printing. Similar to the findings in study II, imprinting the substrate with ink resulted in improved elongation at break (for 3 and 5 layers imprinted DEEP). This can also in this case be attributed to the introduction of an additional plasticizer (PG) present in the ink. Studying the mechanical properties of the substrates and DEEP revealed that the printed DEEP possess a slightly increased UTS, Young's modulus, and elongation at break compared to the foam. The mechanical compression observed during printing resulted in a heterogeneous structure of the printed DEEP and therefore also variability in the results.

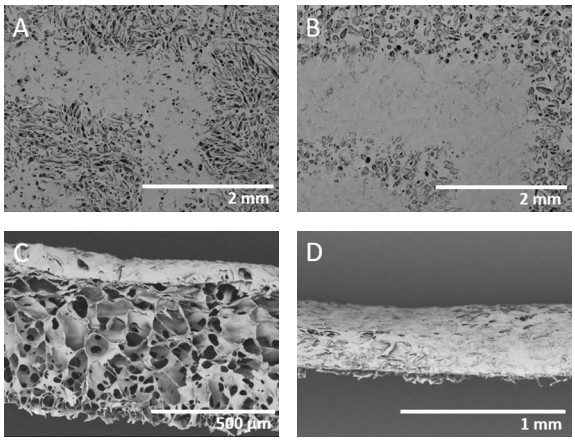

Figure 11. *Scanning electron microscopy images of A) 1 layer imprinted DEEP, and B) 10 layers imprinted DEEP showing the different surface structure of the printed and unprinted area of the DEEP C) cross-section of 10 layers imprinted DEEP, and D) cross-section of the compressed part of the 10 layers imprinted DEEP. Reproduced with permission from* (Öblom et al., 2020)*.*

All the prepared ODFs (II) and DEEP (III) could be handled without breaking and thus complying with the European Pharmacopoeia (European Pharmacopoeia Commission, 2020a). If desired, the mechanical properties of the prepared ODFs and DEEP could be further altered by addition of plasticizers such as PG, PEG, sorbitol, citrates, and low molecular weight macrogols to the formulation (Hoffmann et al., 2011; Liew et al., 2014).

6.1.4.3. Surface pH and moisture content (II)

For ODFs that are administered without water in the oral cavity, the pH must be in the range of physiological saliva (pH 5.8-7.4) to avoid potential local irritation of the mucosa and discomfort to the patient upon administration (Pechová et al., 2018). All the ODFs prepared revealed pH in the preferred range, indicating that no local irritation at the administration site should occur (Table 5) (II). The OPSs were found to initially (after 1 min) be slightly alkaline, but in the neutral range when allowed to further dissolve/disperse (15 min). This suggests that OPSs preferably should not be administered immediately after dispersion in water to avoid possible local irritation if they are administered directly in the oral cavity with a low volume of water without any other delivery vehicle.

Table 5. *Surface pH and moisture content of the printed drug-loaded and placebo ODFs, as well as OPSs prepared in the hospital pharmacy. Data presented as average ± SD, n = 3. Modified and reproduced with permission from* (Öblom et al., 2019a).

Sample	Surface pH		Moisture content
	1 min	15 min	Mass loss (%)
EXT ODF	7.1 ± 0.1	7.1 ± 0.1	9.4 ± 2.5
EXT placebo	6.9 ± 0.1	6.4 ± 0.3	10.5 ± 2.5
IJP ODF	7.4 ± 0.3	7.1 ± 0.0	12.4 ± 1.7
IJP placebo	7.0 ± 0.2	6.4 ± 0.2	9.1 ± 4.1
OPS	9.4 ± 1.6	7.3 ± 0.2	2.4 ± 0.3

The moisture content of pharmaceutical products is of interest as it is known to affect various properties of the dosage form, such as the physicochemical, chemical, and microbiological stability (Szakonyi and Zelkó, 2012). ODFs with high moisture content are typically sticky making them more difficult to administer. However, a little residual moisture is typically desired due to its plasticizing effect. Dry films are usually brittle and may break during handling. To evaluate the moisture content in the printed ODFs and the prepared OPSs a moisture analyzer was utilized (II).

As expected, the OPSs showed lower moisture content (2.4 ± 0.3%) compared to the drug-loaded EXT ODFs (9.4 ± 2.5%) and IJP ODFs (12.4 ± 1.7%) as the printing technologies introduce moisture during the manufacturing processes. The drug-free EXT ODFs revealed a moisture content (10.5 ± 2.5%) comparable to the drug-loaded ODFs, whereas the drug-free IJP ODFs displayed a lower moisture content (9.1 ± 4.1%). The difference in moisture content for the drug-free and drug-loaded IJP ODFs was a result of additional moisture and plasticizers being introduced during IJP as compared to only solvent casting. The ODFs and OPSs were stored in ambient conditions allowing the hygroscopic components in the ODFs (e.g., HPC) to absorb moisture from the air. It has been proposed that ODFs should have a moisture content lower than 5% (Nair et al., 2013). All printed ODFs showed higher moisture contents but were still easy to handle and non-sticky. Only the IJP ODFs were observed to slightly stick to each other upon storage, which suggests that an increased drying time or drying in an oven would be beneficial due to additional plasticizers present after IJP.

6.1.4.4. Disintegration (II-III)

Fast disintegration upon administration is required for orodispersible formulations in the oral cavity to allow for convenient administration of the dosage form. To date, there are no disintegration limits to comply with in the Ph. Eur for ODFs (European Pharmacopoeia Commission, 2020b). This has led scientists exploring novel ODFs to adopt the disintegration limit for orodispersible tablets, which states that disintegration should take place within 180 s (Thabet et al., 2018b).

The prepared ODFs (II) and DEEP (III) can be administered sublingually or elsewhere in the oral cavity such as on the tongue, where they either partly or fully disintegrate before subsequent swallowing without the need for water. An increased

disintegration time for the drug-imprinted substrates was reported in both studies for all the analyzed formulations (Table 6).

Table 6. *Disintegration times for IJP substrates, placebo ODF (EXT), and drug-loaded printed oral dosage forms (ODFs and DEEP) using a similar static disintegration method. The samples shown for study II are the largest-sized ODFs from the study with a target dose of 2 mg. Data are presented as average ± SD, n = 3. EXT = semisolid extrusion-based 3D printing, IJP = inkjet printing, ODF = orodispersible film, DEEP = data-enriched edible pharmaceuticals.*

Study	Printing	Sample	Thickness (mm)	Disintegration (s)
II	EXT	Placebo ODF	0.04 ± 0.00	28 ± 9
II	EXT	Warfarin ODF	0.04 ± 0.00	39 ± 4
II	IJP	Film substrate[a]	0.05 ± 0.00	90 ± 1
II	IJP	Warfarin ODF	0.05 ± 0.00	123 ± 5
III	IJP	Film substrate[a]	0.05 ± 0.02	58 ± 3
III	IJP	Foam substrate[b]	0.76 ± 0.08	10 ± 2
III	IJP	DEEP 1L[c]	0.58 ± 0.11	157 ± 39
III	IJP	DEEP 3L[c]	0.55 ± 0.06	> 180
III	IJP	DEEP 5L[c]	0.54 ± 0.12	> 180

a = air-dried solvent cast substrate, b = freeze-dried solvent cast substrate, c = 1, 3, and 5 layers imprinted foam with cannabinoids

In study II, all the ODFs disintegrated within 180 s, thus complying with the limit stated in the pharmacopeia for orodispersible tablets. The ODFs prepared by EXT disintegrated faster (> 40 s) than the corresponding IJP ODFs (> 130 s) (Table 6). This can be explained by an increased thickness for the IJP substrate and subsequently printed ODF as well as a difference in the surface structure of the ODFs. EXT ODFs revealed a wavy structure originating from the rectilinear infill utilized for printing thereby slightly increasing the surface area resulting in faster wetting as compared to the flat IJP substrate and ODF, although probably not significantly. Similar findings have previously been reported where FDM ODFs were shown to possess faster disintegration compared to conventional solvent cast ODFs (Jamróz et al., 2017b). Incorporating the drug in the ODFs resulted in a slightly increased disintegration time irrespective of the used printing method. An increase in the disintegration time has also previously been reported for drug-loaded ODFs prepared by conventional solvent casting (Garsuch and Breitkreutz, 2010). The OPSs were not successfully analyzed applying this method due to the nature of the comparator formulation and thus could not be compared to the printed ODFs.

As in study II, the unprinted substrates showed the fastest disintegration, where the foam (freeze-dried) disintegrated considerably faster than the corresponding film (air-dried) (III). This can be explained by the differences in the structure of the two substrates. The foam is a porous substrate (Figure 7 F-H), thus allowing for faster wetting than the corresponding non-porous film (Figure 7 A-B). Imprinting the foam with the drug-loaded ink resulted in slower

disintegration, as also found for the imprinted ODFs in study II. In addition to imprinting the foam with lipophilic cannabinoids resulting in a slower wetting process of the DEEP, the porous structure of the foam was partly destroyed during the printing process. The feeding rolls in the used printer were seen to compress the porous foam (Figure 10 C and Figure 11 C-D) leading to loss of the porous structure thus also contributing to the slower wetting of the DEEP. The compression of the foam resulted in a foam with higher density and properties similar to the dense air-dried film.

The lack of a harmonized Ph. Eur. disintegration test makes it hard to compare disintegration results from different studies displaying the need to develop a biorelevant dynamic disintegration test for ODFs. The disintegration method used in studies II and III is static. A setup that allows controlled movement such as shaking will likely result in much faster disintegration, which needs to be taken into account if comparing results to other studies. The used method further only allows wetting of the ODF from one side, which is expected to further contribute to a slower disintegration time. Nonetheless, the used method has an easy setup where the ODF does not stick to the side of the Petri dish and is therefore well suitable for comparing the different ODFs in these two studies. However, a disintegration setup that better could mimic the conditions in the oral cavity would deepen the understanding of the disintegration behavior and aid the development of improved ODFs.

6.1.4.5. Solid-state analysis (I-II)

The solid-state properties of the raw materials, physical mixtures, intermediate products, and final dosage forms were investigated to gain an understanding of whether the process alters changes in the formulation.

In study I, the filament thermograms obtained by DSC were similar to the printed tablets, suggesting that no apparent changes occur during the printing process that involves brief reheating of the prepared thermoplastic filament. No evident drug degradation was thus observed for the printed tablets. None of the HME filaments or subsequently printed tablets were found to be completely amorphous. Due to the high water-solubility of isoniazid, an amorphous formulation is not required and HME was merely used to produce the filaments for FDM. HME of the physical mixture of the formulations into filaments typically resulted in a small melting point depression along with a broadened endothermic peak. A further lowering of the melting point was observed for some of the 3D-printed tablets. This is likely originating from further dispersion or dissolving of the drug in the polymer when the formulation is reheated close to the melting point of the drug resulting in a reduction of the chemical potential of the system. Other endothermic events on the thermograms could be attributed to either the drug, polymers, or dehydration of the formulation.

The results from the DSC in study II showed similarities to the results found in study I. A small melting point depression for IJP ODFs and also a broadening of the peak attributed to HPC were observed for the drug-loaded ODFs as compared to the printed placebo ODF or substrate containing only HPC. In the case of the IJP ODFs this can be attributed to the additional materials present in

the ODFs originating from the printing ink, such as PG acting as a plasticizer. The endothermic events were generally small for the ODFs. No evident melting point for the drug was observed for the ODFs, indicating that the drug was present in the amorphous state, while the polymer was semi-crystalline. As in study I, other endothermic events could be attributed to HPC or dehydration of the hygroscopic HPC. The OPSs showed a sharp endothermic event (peak onset 142 °C) with subsequent decomposition. This can be attributed to lactose monohydrate that was present in the formulation as a filler. It has been reported that the crystallization water present in lactose monohydrate is lost at temperatures above 100 °C resulting in the anhydrous form (DFE Pharma, 2019). Decomposition of the material occurs at approximately 140 °C when all the water is removed. No further conclusions could be made regarding warfarin in the formulation as the decomposition occurred before melting of warfarin, which according to the pure drug was expected to melt around 178 °C (peak onset).

In study II, ATR-IR was further used to investigate the dosage forms and starting materials. The attained spectra for the drug-free ODFs, namely placebo EXT ODF and the substrate used for IJP, were identical. This was expected as the formulations also were identical and only the manufacturing process, i.e., EXT at room temperature and solvent casting, was different. When the IJP substrate was imprinted with the drug-loaded ink the spectra remained unchanged, although new materials (PG and colorant) were introduced in the IJP ODFs. The drug-loaded EXT ODFs, however, differed from the drug-loaded IJP ODF, suggesting that the differences originated from interactions between the drug and the ink. Characteristic bands for warfarin were present at 759 cm^{-1} and 700 cm^{-1}. As lactose monohydrate was present in a greater ratio than the drug in the OPSs, it was challenging to draw any conclusions from the spectra. One characteristic band for warfarin was found at 760 cm^{-1}, although this band also was seen in the spectra for pure lactose monohydrate. The spectrum for the commercial product Marevan® was very similar to the OPSs prepared in this study, which can be attributed mainly to the presence of lactose monohydrate in a much larger ratio than the drug.

According to these studies, it appears that EXT and IJP are methods that will not likely have a big impact on the formulation during the printing process, whereas FDM that is performed at elevated temperatures may cause formulation changes during the printing step. This was, however, not seen to a larger extent in study I.

6.1.4.6. Drug content (I-III)

Study I

In study I, all the HME filaments and thus also the subsequently printed tablets had a target drug load of 30% (w/w). Both the filaments and the tablets printed from the filaments showed a similar drug content in the range of 27.9 ± 2.6 to 31.7 ± 0.2% (including 8 different filaments formulations) and 27.5 ± 1.1% to 34.7 ± 0.2% (including 48 different tablets), respectively (Table 7). This

indicates that degradation of isoniazid does not occur when processed into tablets by FDM that utilizes heat. The drug was found to be homogenously distributed throughout the filaments, although they showed a slightly higher standard deviation than the further processed 3D-printed tablets. This is likely because the filament pieces analyzed were cut from various places of the filament strand whereas the tablets were printed with a short piece of the filament.

Table 7. *Drug content (%) of the hot-melt extruded filaments (feedstock material) and the subsequently 3D-printed tablets (three different sizes and two different infill levels) for the different formulations (F). Data presented as average ± SD, n = 10 (filaments) and 3 (tablets), respectively. Modified and reproduced with permission from (Öblom et al., 2019b).*

F	% API in 3D-printed tablets and hot-melt extruded filament (w/w)						
	6 mm, 15%	6 mm, 90%	8 mm, 15%	8 mm, 90%	10 mm, 15%	10 mm, 90%	Filament
1	31.6 ± 0.2	28.0 ± 1.7	30.4 ± 0.2	31.2 ± 1.4	27.5 ± 1.1	29.9 ± 1.3	27.9 ± 2.6
2	30.6 ± 0.3	30.8 ± 0.1	30.1 ± 0.7	30.9 ± 0.0	30.4 ± 0.1	30.6 ± 0.1	30.2 ± 1.0
3	31.0 ± 0.1	30.9 ± 0.1	31.1 ± 0.1	31.0 ± 0.0	30.9 ± 0.1	30.7 ± 0.1	31.7 ± 0.2
5	30.3 ± 0.5	30.5 ± 0.1	30.6 ± 0.2	30.8 ± 0.0	31.3 ± 0.0	30.7 ± 0.1	29.6 ± 1.2
10	34.7 ± 0.2	34.6 ± 0.1	32.8 ± 0.4	33.4 ± 0.4	34.3 ± 0.1	30.4 ± 0.4	31.3 ± 1.8
11	31.8 ± 0.1	32.1 ± 0.1	31.6 ± 0.0	30.9 ± 0.0	31.2 ± 0.1	31.0 ± 0.1	31.0 ± 0.3
12	30.2 ± 0.4	30.9 ± 0.1	31.1 ± 0.1	30.3 ± 0.0	30.4 ± 0.1	30.7 ± 0.1	29.7 ± 1.1
13	31.1 ± 0.1	30.8 ± 0.3	30.8 ± 0.1	30.8 ± 0.2	30.9 ± 0.0	30.3 ± 0.1	30.2 ± 0.6

The weight of the 3D-printed tablets of a specific size and infill level varied depending on the printed formulation (Table 8). The mass variation of the printed tablets is likely a result of the different melt flow properties of the formulations at the utilized printing temperature. As melt flow has been identified as a parameter that affects the printability as well as the quality of the printed object (Fuenmayor et al., 2018; Wang et al., 2018) it would be beneficial to determine the melt flow behavior of the material prior to printing to enable optimization of the printing parameters (e.g., printing speed). Although there were weight differences between the printed formulations, a correlation between the tablet size and weight for an individual formulation was >0.99 for all formulations except formulation 12 with an infill level of 15%. This is at the same level as for PLA, which indicates that the printing process for a specific formulation is robust, thus enabling printing of targeted personalized doses.

Table 8. *Weight and correlation of printed isoniazid tablets with various sizes and infill. Reprinted from Öblom et al., 2019b.*

	6 mm, 15% (mg)	6 mm, 90% (mg)	8 mm, 15% (mg)	8 mm, 90% (mg)	10 mm, 15% (mg)	10 mm, 90% (mg)	R^2, 15%	R^2, 90%
PLA	76.4 ± 0.6	83.9 ± 0.5	135.8 ± 0.2	150.1 ± 1.1	210.3 ± 1.3	235.1 ± 2.7	0.9958	0.9948
1	88.7 ± 2.7	77.7 ± 3.4	141.2 ± 4.5	145.2 ± 1.0	181.5 ± 2.2	220.8 ± 4.5	0.9942	0.9989
2	61.6 ± 0.7	65.3 ± 0.6	107.6 ± 1.3	116.2 ± 5.3	143.8 ± 1.2	170.0 ± 0.8	0.9952	0.9997
3	59.2 ± 0.5	69.4 ± 5.3	133.2 ± 0.4	141.4 ± 2.0	195.0 ± 7.2	192.0 ± 8.1	0.9973	0.9900
5	59.2 ± 1.7	67.8 ± 2.2	140.0 ± 3.4	144.5 ± 4.1	203.6 ± 12.6	236.7 ± 3.1	0.9996	0.9972
10	70.8 ± 1.0	73.5 ± 0.9	121.5 ± 2.4	130.1 ± 2.1	193.4 ± 5.2	205.9 ± 1.7	0.9902	0.9930
11	66.1 ± 1.2	73.7 ± 2.1	141.4 ± 4.9	136.5 ± 0.6	208.3 ± 10.0	222.5 ± 1.9	0.9988	0.9920
12	68.1 ± 2.6	74.7 ± 0.7	115.9 ± 1.8	133.4 ± 4.8	196.5 ± 8.1	214.8 ± 4.7	0.9786	0.9913
13	64.5 ± 0.7	73.6 ± 2.6	130.0 ± 3.7	143.4 ± 5.4	163.1 ± 2.1	165.7 ± 0.9	0.9651	0.9182

To achieve therapeutic serum concentrations of isoniazid (approx. 3 µg/ml for a duration of minimum 6 h) in children over 3 months the World Health Organization (WHO) recommends doses of 10 (10-15) mg/kg (European Medicines Agency, 2012b). Clinical data shows that especially younger children and fast acetylators of isoniazid require an increased dose compared to adults to achieve this. Theoretically, a patient weighing 10 kg would thus need a dose of 100 mg. The 10 mm (ø) tablets prepared in study I weighed roughly 200 mg, thus, containing around 60 mg of isoniazid. To obtain higher doses by FDM, the drug content in the filaments or the tablet size could be increased, ideally the former to achieve better patient acceptability.

Study II

In study II, child-friendly dosage forms, i.e., ODFs and OPSs, with therapeutic doses of warfarin were prepared. Ten dosage forms of each dose (0.1, 0.5, 1, and 2 mg), prepared batch, and preparation method were analyzed to determine the uniformity of content of single-dose preparations (UC) and the acceptance value (AV) as described in the Ph. Eur. All dosage forms with a target dose of 1 or 2 mg from the different batches showed acceptable UC values regardless of the manufacturing method used (Table 9). For the dosage forms with a target dose of 0.5 mg, the printed ODFs were superior to the OPSs as all ODFs complied with the limits, whereas one batch of OPS failed to comply with the limits as one dosage unit was outside the required ±25 of the average drug content. Another OPSs batch would have required further testing of 20 dosage units as two dosage units were outside ±15%, which was not done in this study and was considered to fail without further testing. For the lowest target dose, i.e., 0.1 mg, two of the three batches fulfilled the UC criteria for all the manufacturing methods. For both printing methods, one batch failed to fulfill the requirement as one dosage unit was outside ±25%, whereas another 20 dosage units should have been analyzed for OPSs as three dosage units were outside ±15%. These results highlight the challenge to prepare low-dose dosage forms with acceptable drug content. For the higher doses, the dose fluctuations were small which is evident from the UC values. Inter-batch variability was observed for all utilized manufacturing

methods. When including all the prepared dosage forms in the three batches printed on different days for the 0.1 mg target dose, the drug content compared to the target dose was 72-140% and 52-112% for the EXT ODFs and IJP ODFs, respectively, and between 36-104% for OPSs. These results show that there is great variability in the administered drug amount for these low-dose dosage units. As the dose increases improved accuracy was observed, i.e., less fluctuation between the single dosage units. For the 2 mg target dose dosage units corresponding values to the ones presented for the 0.1 mg target dose dosage units were 100.5–109.3% for EXT ODFs, 93.1–109.4% for IJP ODFs, and 100.2–116.3% for OPSs.

Table 9. *Drug content, content uniformity, uniformity of dosage units (acceptance value, according to Ph. Eur 9th ed.), and dose accuracy compared to target doses for the various batches prepared by different manufacturing techniques. Drug content is expressed as average ± SD, n = 10, AV and UC are calculated based on 10 dosage forms from each batch. Note that the weight of the OPSs are given without a decimal as that is how it is routinely done when manufacturing OPSs in the hospital pharmacy. The weight of the ODFs are, however, given with one decimal to show differences between the dosage forms. Modified and reproduced with permission from* (Öblom et al., 2019a).

Dosage form; Batch	Weight (mg)	Thickness (mm)	Average drug content (mg)	Maximum deviation (%)	Amount of drug (% of target dose) min / average / max	Acceptance value
EXT ODF						
1	1.5 ± 0.0	0.04 ± 0.00	0.14 ± 0.00	+ 2.9[a]	132.9 / 136.8 / 139.7	41.0[d]
2	1.3 ± 0.1	0.04 ± 0.00	0.11 ± 0.00	+ 1.1[a]	110.0 / 110.7 / 111.9	10.9[c]
3	1.2 ± 0.2	0.04 ± 0.01	0.10 ± 0.02	- 30.0[b]***	71.6 / 102.2 / 116.5	47.1[d]
IJP ODF						
1	2.1 ± 0.1	0.06 ± 0.00	0.07 ± 0.01	+ 25.9[b]***	52.1 / 66.3 / 83.4	55.0[d]
2	2.3 ± 0.2	0.06 ± 0.00	0.09 ± 0.00	- 9.0[a]	82.3 / 90.5 / 95.4	17.6[d]
3	2.2 ± 0.0	0.06 ± 0.00	0.09 ± 0.01	+ 21.4[a]*	84.5 / 92.1 / 111.8	25.4[d]
OPS						
1	200 ± 0	N/A	0.05 ± 0.01	- 22.5[e]***	36.9 / 46.2 / 54.1	67.8[d]
2	200 ± 0	N/A	0.09 ± 0.01	- 23.3[a]*	71.6 / 93.4 / 104.5	29.0[d]
3	200 ± 0	N/A	0.08 ± 0.01	+ 18.3[a]*	69.7 / 82.1 / 97.2	37.6[d]
EXT ODF						
1	6.2 ± 0.1	0.04 ± 0.00	0.59 ± 0.00	+ 1.2[a]	116.1 / 117.2 / 118.5	17.5[d]
2	5.2 ± 0.1	0.04 ± 0.00	0.48 ± 0.01	- 1.8[a]	94.5 / 96.2 / 97.6	4.9[c]
3	5.5 ± 0.1	0.05 ± 0.00	0.52 ± 0.01	- 2.5[a]	100.4 / 103.1 / 104.7	4.5[c]
IJP ODF						
1	8.6 ± 0.1	0.06 ± 0.00	0.51 ± 0.04	- 13.8[a]	87.6 / 101.6 / 108.8	20.8[d]
2	9.3 ± 0.2	0.06 ± 0.00	0.51 ± 0.03	- 13.7[a]	88.7 / 102.8 / 107.8	16.1[d]
3	9.5 ± 0.0	0.06 ± 0.00	0.52 ± 0.02	- 4.6[a]	99.9 / 104.7 / 108.9	11.6[c]
OPS						
1	200 ± 0	N/A	0.47 ± 0.05	- 18.9[e]**	76.0 / 93.7 / 106.6	30.4[d]
2	200 ± 0	N/A	0.54 ± 0.02	+ 5.7[a]	102.6 / 107.9 / 114.1	15.5[d]
3	200 ± 0	N/A	0.48 ± 0.06	- 26.1[b]**	71.1 / 96.2 / 119.2	32.5[d]
EXT ODF						
1	12.2 ± 0.1	0.05 ± 0.00	1.16 ± 0.01	+ 1.2[a]	114.5 / 115.8 / 117.1	16.6[d]
2	10.7 ± 0.1	0.04 ± 0.00	1.01 ± 0.05	- 14.8[a]	86.0 / 100.9 / 106.7	13.7[c]
3	11.5 ± 0.1	0.05 ± 0.00	1.09 ± 0.01	+ 1.3[a]	107.4 / 108.8 / 110.3	9.9[c]

Dosage form; Batch	Weight (mg)	Thickness (mm)	Average drug content (mg)	Maximum deviation (%)	Amount of drug (% of target dose) min / average / max	Acceptance value
IJP ODF						
1	17.0 ± 0.6	0.06 ± 0.00	1.09 ± 0.07	- 11.1[a]	96.9 / 109.0 / 117.4	23.4[d]
2	17.2 ± 0.3	0.06 ± 0.00	1.06 ± 0.07	- 12.0[a]	92.9 / 105.6 / 111.9	21.3[d]
3	18.2 ± 0.6	0.06 ± 0.00	1.05 ± 0.03	- 4.2[a]	101.7 / 104.9 / 108.1	10.3[c]
OPS						
1	200 ± 0	N/A	1.01 ± 0.03	- 6.0[a]	95.2 / 101.2 / 105.5	6.9[c]
2	200 ± 0	N/A	1.10 ± 0.06	+ 8.0[a]	101.9 / 110.1 / 119.0	22.7[d]
3	200 ± 0	N/A	1.11 ± 0.06	+ 7.1[a]	96.9 / 110.7 / 118.6	23.5[d]
EXT ODF						
1	23.0 ± 0.7	0.05 ± 0.00	2.12 ± 0.06	- 5.4[a]	100.5 / 106.2 / 109.3	12.5[c]
2	22.4 ± 0.1	0.05 ± 0.00	2.11 ± 0.01	+ 1.5[a]	104.5 / 105.3 / 106.9	5.4[c]
3	22.7 ± 0.2	0.05 ± 0.00	2.13 ± 0.03	- 2.4[a]	103.8 / 106.3 / 108.4	8.2[c]
IJP ODF						
1	34.7 ± 0.2	0.06 ± 0.00	2.06 ± 0.10	- 9.8[a]	93.1 / 103.2 / 107.5	14.8[c]
2	34.9 ± 0.8	0.06 ± 0.00	2.13 ± 0.10	- 12.7[a]	93.1 / 106.7 / 109.4	17.6[d]
3	40.1 ± 1.2	0.06 ± 0.00	2.10 ± 0.02	+ 1.5[a]	103.8 / 105.0 / 106.6	5.8[c]
OPS						
1	200 ± 0	N/A	2.17 ± 0.07	+ 14.9[a]	100.1 / 108.4 / 114.9	15.98[d]
2	200 ± 0	N/A	2.24 ± 0.03	+ 2.8[a]	108.9 / 112.1 / 114.1	14.32[c]
3	200 ± 0	N/A	2.25 ± 0.05	+ 3.5[a]	108.4 / 112.3 / 116.2	17.14[d]

Number of individual doses outside ± 15% limits: * = 1 dose, ** = 2 doses, *** = 3 doses. [a] = complies with the requirements for UC, [b] = does not comply with the requirements for UC, [c] = complies with the requirements for AV, [d] = does not comply with the requirements for AV, [e] = an additional 20 units should be tested to reveal if the test passed or failed.

The study revealed that based on the fulfillment of AV, EXT was the manufacturing method with the best accuracy and precision of the incorporated drug for most prepared batches and dosage units. Both printing methods were found to be superior to OPSs, which is the method used today at the hospital pharmacy for dose manipulation of warfarin dosage forms for clinical use. EXT was further found to have a linear correlation between the dry weight of the film and the drug content (mg) (R^2 values of 0.9996, 1, and 0.9999 for batch 1, 2, and 3, respectively), which could be an easy quality control that could be used in a hospital pharmacy setting.

The smallest EXT ODFs (0.1 mg) revealed a too high drug content for most prepared dosage units with AV values ≥ 40 for two out of the three prepared batches. For optimization of the drug content compared to the target dose in the EXT ODFs the g-code or the design could be manipulated or alternatively the concentration in the printing ink could have been decreased for this dose strength. IJP has in the literature been reported as a highly accurate printing method suitable for fabrication of low-dose dosage forms. In this study, it was observed that the ink was not stable in the printer before initiating printing of batch 1. This resulted in decreased drug content uniformity as compared to

batch 3 where the printing was trouble-free and printing of all dosage units within the batch could be performed with the same chosen nozzles. The problems encountered during printing of batch 1 were likely related to partial drying of the printhead in a period where the printhead had not been used. This could be seen as droplets not being ejected from some of the nozzles that initially ejected droplets, which correspondingly was reflected in the drug content in these ODFs. Additionally, this study purposely used a large number of printing nozzles (40-60) to decrease the printing time contrary to many other studies where only one or a handful of nozzles have been used (Genina et al., 2012; Jamróz et al., 2017b; Raijada et al., 2013; Sandler et al., 2011). Naturally, an increased number of nozzles used increases the possibility for variation in the droplet volume, although drug content that deviated from the theoretical drug content has been described regardless of the number of nozzles utilized during IJP (Wickström et al., 2015). As droplet volume is one parameter used to calculate the required DPI, a change in the average droplet volume will directly impact the deposited amount of drug in the designated area. To optimize the drug content of the IJP ODFs a structured study evaluating the effect of the various printing parameters on the droplet volume of the developed ink should be performed to enable printing with optimal parameters that result in uniform and stable droplets being ejected during the whole printing process and with minimal day-to-day variability. Furthermore, it should be ensured that the printhead is not allowed to dry out in between printing session in order to avoid that droplets are not being ejected from the nozzles. Lastly, improvement of the content uniformity for OPSs (that would be suitable for preparation in a hospital pharmacy setting) could likely be achieved by formulating pure warfarin together with one or multiple excipients used as a filler. This may result in improved homogeneity of the drug in the powder mixture as the particle size in the mixture would be more similar as compared to the when using a ground commercial tablet as a source of the API. If the commercial tablet however is used, improved grinding of the tablet is required along with a standardized mixing procedure.

Study III

Tailored doses were in study III achieved by subsequent printing of various numbers of layers of the designed 2 x 2 cm QR code on top of each other. The doses attained by imprinting 2-10 layers were between 0.092 ± 0.003 mg and 0.537 ± 0.019 mg for CBD and 0.097 ± 0.002 mg and 0.567 ± 0.021 mg for THC (Figure 12). 1 layer imprinted DEEP could not be analyzed as the concentration was below the limit of quantification. The correlation between the drug content and the number of printed layers was $R^2 = 0.9947$ and $R^2 = 0.9954$ for CBD and THC, respectively. One printed layer resulted on average in 0.051 ± 0.002 mg of CBD and 0.054 ± 0.002 mg of THC, which could be increased by increasing the concentration of the cannabinoids in the printing ink. The cannabinoid concentration in the ink used was fairly low compared to ink concentrations typically aimed for when utilizing IJP. CBD has been shown to have a theoretical solubility beyond 100 mg/ml in the same ink base (1:1 ethanol and PG) as used

in this study (Cape et al., 2017). This would allow for approximately a four-time increase in the amount of drug deposited per printed layer of this design, thus reaching therapeutic cannabinoid doses for the printed DEEP. Other ways to increase the cannabinoid amount in the DEEP is by increasing the printed area (Öblom et al., 2019a), which can be achieved by increasing the dimensions of the QR code (Edinger et al., 2018a) or by completely imprinting the area of the dosage form with a cannabinoid containing ink that is color-free or lightly colored and afterward printing the IRP as a single layer using a drug-free or drug-loaded colored ink with good contrast to the previously printed area.

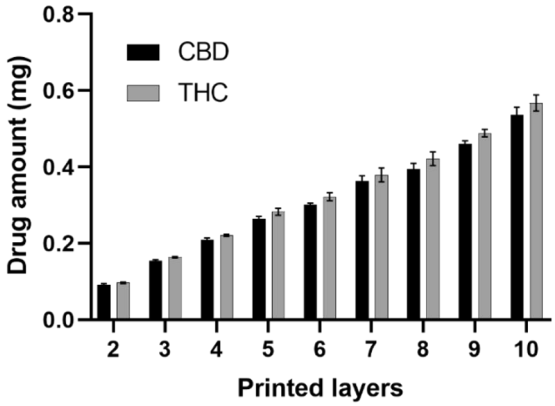

Figure 12. *CBD and THC content in 2-10 layers imprinted DEEP. Reproduced with permission from* (Öblom et al., 2020).

6.1.4.7. In vitro drug release (I-III)

The drug release behavior *in vitro* for the printed oral dosage forms in study I-III was determined utilizing both a manual and an automatic setup depending on the dosage form analyzed. The printed ODFs and OPSs were all found to be immediate release dosage forms, whereas the printed tablets showed a wide range of release profiles.

The dissolution study for the prepared filaments and subsequently printed oral tablets showed that both the formulation as well as the tablet design had an impact on the drug release behavior (I). As no coating was applied, the drug was present on the surface of the tablet and filaments resulting in the drug starting to release immediately as it was placed in the dissolution media. The 8 mm tablets printed with an infill of 90% showed that the time for 80% of the drug to be released varied between 40 to almost 900 min. This confirms that isoniazid tablets with different release characteristics can be 3D-printed according to a patient's need. Tailoring of the drug release can further be done by changing the geometrical design of the printed tablet. The ratio between the surface area and the volume is of importance as an increased surface area to volume ratio for the same formulation has shown to release the drug faster (Goyanes et al., 2015b). This was also evident in this study as all the filaments released the drug faster

than the 3D-printed tablets. When a filament was 3D-printed, which mimicked the geometry of the HME filament a similar drug release was observed, indicating that the printing process conducted at elevated temperatures did not affect the release of the drug. This confirms that the changes seen for filaments that were further processed into tablets originated from the difference in surface area to volume ratio. When different sized tablets were printed with the same formulation only a small difference in the drug release was observed between the tablet sizes. The drug was released faster from the smallest tablets and slowest from the largest (6 mm < 8 mm < 10 mm). This behavior was more prominent for the tablets printed with formulations that displayed sustained release characteristics.

In study I, tablets with two different infills, namely 15% and 90% were printed in addition to the different sized tablets (6 mm, 8 mm, and 10 mm) as infills levels of printed dosage forms has been shown to enable modification of the drug release (Goyanes et al., 2015a; Kadry et al., 2018). In this study, it was expected that the 15% infill level would result in a faster drug release but printing of tablets with two different inner porosities revealed a surprisingly small change in the drug release. This can be explained by the default setting of the printer where only 15% of the tablet was printed with the set infill and the rest was in fact printed with 100% infill i.e., completely solid infill. By manipulating the g-code so that most of the tablet is printed with the desired infill level and thus changing the density of the tablet core it is expected to have a greater impact on the drug release and thus allowing for tuning of the drug release profile.

In the manual release studies, 80% of the drug was released from all the prepared dosage forms (ODFs and OPSs, target dose of 2 mg) within 30 min (II). No prominent differences in the drug release were seen between the different strengths of the prepared dosage forms. The drug release of the printed ODFs was similar regardless of the printing method used. The OPSs showed the fastest drug release, which could be anticipated as the formulation consists of ground tablets with a large surface area that allows the water-soluble drug to rapidly be released. For the ODFs the drug is present on the surface as well as within the polymer network. Although the ODFs disintegrated fast, it was observed that a complete drug release only occurred after approximately 30 min. This suggests that the drug still is embedded in the polymer network in the smaller ODF pieces after disintegration from where it slowly is released based on the nature of the polymer. HPC particles form a viscous gel layer upon hydration resulting in a slower drug release as further wetting of the inside of the dosage form is slowed down due to the viscous layer (Ashland, 2017). The automated setup that was utilized as a comparison to the manual setup for the 2 mg target dose, showed similar drug release for all formulations. The drug was released faster from all formulations using the automated setup, namely 80% drug release within 2 min and 4 min for EXT ODF and IJP ODF, respectively. This can be explained by the increased stirring in addition to a larger volume of dissolution media for the automated setup. This emphasizes the need for a harmonized pharmacopeia

method for studying the drug release behavior of ODFs in order to improve the research conducted in the field of ODFs. The automated setup is preferred due to the robustness of the method and the less tedious process. However, the automated on-line setup was not suitable for the smaller dosage forms containing a low dose of the drug due to the large volume of dissolution media required.

In study III, the release behavior of the marketed product Sativex®, as well as 10 layers, imprinted DEEP was compared. Sativex® showed a faster release than 10 layers imprinted DEEP with a CBD and THC release of 92 ± 2% and 89 ± 4% at 30 min compared to 69 ± 6% and 70 ± 7% for DEEP. The slower release for the printed DEEP originates from the poorly water-soluble cannabinoids being incorporated in the polymer matrix as a result of imprinting the porous foams. For the cannabinoids to be released from the DEEP diffusion through the formed gelling polymer layer is required, which results in slower drug release. However, both the studied formulations are classified as immediate release dosage forms as more than 80% of the drug was released in less than 45 min (European Pharmacopoeia Commission, 2020b).

6.1.4.8. Stability (II-III)

Personalized dosage forms prepared in small quantities on-demand according to a patient's need at a specific time point are envisioned to be administered in a short timeframe after production. In theory, personalized dosage forms thus require shorter stability compared to conventional fixed-dose dosage forms such as tablets where a shelf life of multiple years is needed. In study II and III, brief stability studies of the prepared dosage forms were conducted in order to investigate their stability and recognize potential areas for further improvement of the different dosage forms. The stability studies were also envisioned to indicate possible requirements for the primary and secondary packaging.

In study II, the printed ODFs were stored in Petri dishes (EXT) or loosely packed in foil (IJP) over 4 weeks thus subjecting them to fluctuations in the ambient conditions and was thought to resemble the worst-case scenario at hospital wards where control of the temperature and RH may not always be possible. The OPSs were stored in the same way they would be at the hospital pharmacy, namely packed in waxed powder paper as primary packaging and the sachets were further stored in open ziplock bags that could mimic a secondary packaging. No major changes and thus still acceptable properties of the studied parameters of the prepared dosage forms were observed during the stability study where the temperature and RH fluctuated between 19.6 and 21.5 °C and 13.0 and 32.9%, respectively. No changes were observed in the visual appearance, thermal properties, nor intermolecular interactions. Further, all dosage forms with a target dose of 2 mg (largest dose prepared) showed acceptable UC values at all time points in the stability study. These printed ODFs further showed acceptable AV throughout the stability study, while the OPSs constantly displayed values slightly above the AV limits. Small changes in the mechanical properties of the printed ODFs were noticed over the one-month

follow-up period, which most likely can be attributed to the moisture content in the ODFs. The moisture content can originate from the printing process or fluctuations in the RH. The drug-loaded EXT ODFs showed lower burst strength as well as burst distance after one week of storage suggesting that the ODFs were not completely dry immediately after manufacturing. The drug-loaded IJP ODFs showed a tendency of increased breaking strength and increased brittleness upon storage, which may originate from evaporation of the deposited ink. The changes of the printed ODFs upon storage were, however, small and they could be handled without breaking. The stability study suggests that all prepared dosage forms in study II are stable over one month.

In study III, the stability of DEEP over 8 weeks focused on two parameters, namely drug content and readability of the QR code during storage in either cold and dry (4 °C, over silica) or accelerated stability conditions (40 °C/75% RH). When the DEEP were subjected to cold and dry storage conditions, all DEEP had readable QR codes throughout the stability study, except for a single 1 layer imprinted DEEP that at day 1 was unreadable and also displayed readability problems immediately after preparation. The readability of the QR codes of DEEP subjected to accelerated stability conditions revealed issues already at day 1 for the 5 layers imprinted DEEP and after one week none of the DEEP could be read (1, 3, and 5 layers imprinted DEEP). As seen in Figure 13, the readability problems can be attributed to the migration of the ink that was deposited as a QR code, thus resulting in poor edge definition of the pattern upon storage in accelerated stability conditions. This is likely a result of uptake of moisture from the surrounding air by the hygroscopic components present in the DEEP, namely PG, PEG 4000, Tween 20, and glycerol. This would further explain the decrease in thickness of the DEEP as a result of loss of the porous DEEP structure at these conditions, which was not observed for DEEP stored at cold and dry conditions. A trend where the thickness of the DEEP decreased more the more ink was deposited, i.e., with an increased number of imprinted layers (0.54 ± 0.07 mm and 0.24 ± 0.01 mm for 1 and 5 layers imprinted DEEP, respectively) was seen. A decrease in the thickness of the unprinted foam was not observed in either of the storage conditions, which suggests that the collapse of the porous structure, as well as readability problems of the QR code, mainly is related to the amount of ink printed on the substrate.

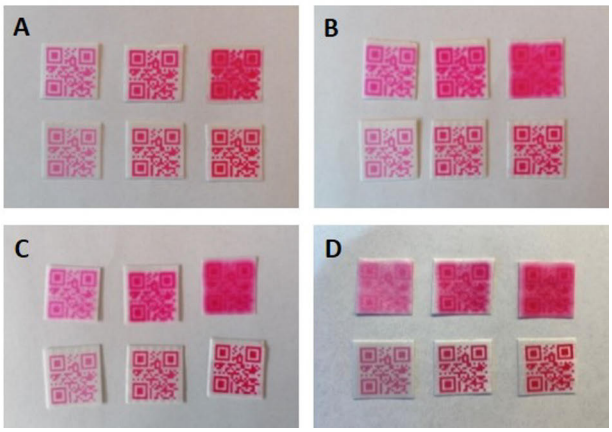

Figure 13. *Photographs of DEEP subjected to different storage conditions. The top row of each picture shows storage at 40 °C/75% RH; 1, 3, and 5 layers imprinted DEEP from left to right, and the bottom row of each picture shows storage at 4 °C and over silica. A) 1 day B) 1 week C) 2 weeks and D) 8 weeks. Reproduced with permission from* (Öblom et al., 2020).

Stability problems regarding the drug content in the DEEP were further observed for the DEEP subjected to accelerated stability conditions. The percent of CBD present in the 3 and 5 layers imprinted DEEP stored at accelerated stability conditions showed a decrease to 68% over 8 weeks compared to the initial content, while the DEEP stored in cold and dry conditions showed a minimum of 94% CBD content. Similar findings were seen for the THC content. Light, heat, and auto-oxidation are all factors known to cause degradation of cannabinoids (Bruni et al., 2018; Fairbairn et al., 1976). In the literature, a loss of 15-20% of CBD and THC during the initial 2 weeks for an oil formulation stored in darkness at 4 °C has been shown, whereafter the formulation was relatively stable (Pacifici et al., 2018). The stability study indicates that the DEEP, similar to the marketed product Sativex®, should be stored in a refrigerator both from a drug content and readability perspective. Furthermore, the DEEP require packaging that prevents moisture uptake from the surroundings. A protective coating could also be applied on the DEEP that could prevent readability issues as a result of moisture uptake and may additionally prevent degradation of the cannabinoids depending on the cause of degradation. This would need to be systematically investigated in future studies.

These stability studies reveal that printed dosage forms may be sensitive especially to changes in the moisture content and great attention should also be paid to the packaging of the on-demand printed dosage forms to ensure the intended quality upon storage. Further studies at different storage conditions should be conducted for an increased understanding of optimal storage conditions for the different printed dosage forms.

6.2. Selecting the most suitable printing technology

As highlighted in this thesis, FDM, EXT, and IJP can all be used to create personalized dosage forms. The processes require different starting materials

and allow for a wide range of drugs to be manufactured into solid oral dosage forms. When it comes to the selection of printing technology it is important to consider the properties of the drug along with the therapeutic application. An example of a decision tree, including some clinically relevant factors, is shown in Figure 14. This decision tree highlights the most suitable printing technology depending on the drug properties as well as the desired dosage form properties. However, the decision tree is not exhaustive and mostly limited to the results obtained in this thesis. Therefore, it must be noted that the printing technologies included may be more versatile than showcased below.

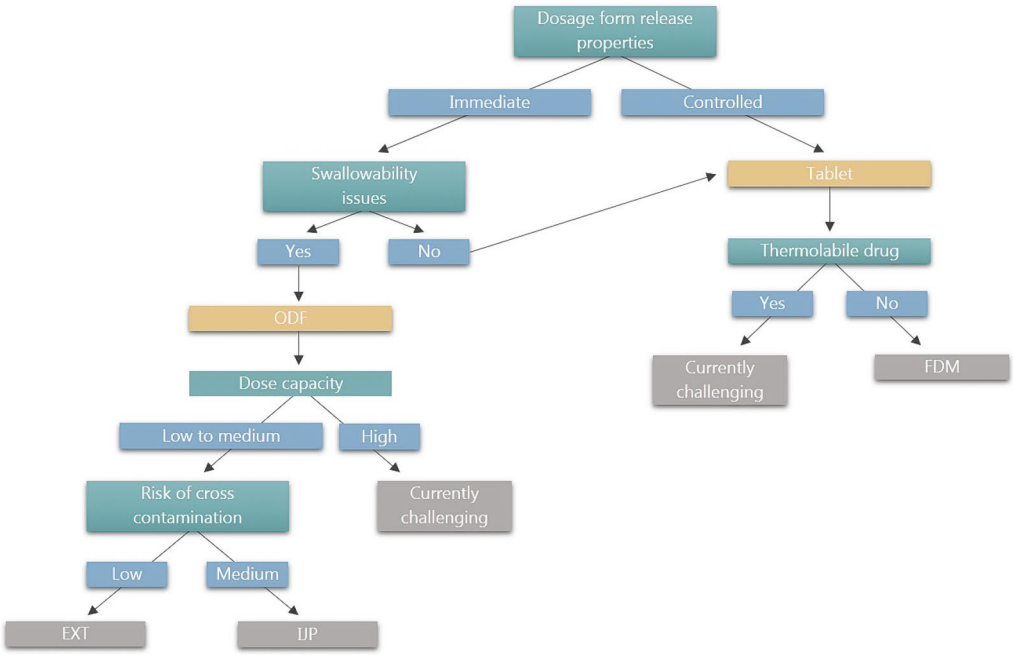

Figure 14. *A decision tree showcasing factors to consider when choosing the optimal printing technology for preparation of solid oral dosage forms based on the results from this thesis.*

Based on the results from this thesis FDM was most suitable for preparation of controlled release dosage forms. It should be noted that the other techniques were not investigated for this purpose in the thesis and it has been shown in the literature that controlled release dosage forms can be produced also by the other technologies, even though FDM remains the most popular. Immediate release dosage forms were successfully prepared by all three printing technologies. The choice of the printing technology is e.g., driven by the need for a dosage form to allow for easy administration due to possible swallowability problems or the required drug content in the dosage form.

IJP is known for achieving high printing resolution making it suitable for personalization in cases where tailoring of the doses (especially of potent drugs) is of importance combined with ease of administration. This is especially of relevance in the case of pediatric treatment where dosing per body weight can

lead to the need for minor dose adjustments in a format that is easy to administer. In this thesis, it was shown that in addition to IJP, also EXT can be used to attain this. FDM was not explored for this purpose but the technology is generally expected to be more suitable for preparation of dosage forms containing a medium to high dose.

Considering the patient needs and dosage form requirements with regards to ease of administration and dosing requirements is the most pragmatic way to select the right printing technology. Selection of the printing technology may today still be influenced by some technical constraints of the technologies. However, these are expected to be solved as printing technologies mature over time and further diversify allowing an increased number of drugs (with varying physicochemical properties) to be manufactured into solid oral dosage forms.

7. Conclusions

This thesis explored the use of three different printing techniques, i.e., FDM, EXT, and IJP, as a means to produce personalized solid oral dosage forms containing one or multiple APIs. Due to the difference in the nature of the utilized printing techniques, they all have distinct requirements for the starting materials and allow for manufacturing of dosage forms with various properties and a wide drug content ranging from low to high. Starting materials for FDM, EXT, and IJP (i.e., solid filaments, semisolid high-viscous inks, and liquid low-viscous inks) were formulated and subsequently successfully used to produce tailored dosage forms of the three model drugs explored in the thesis. Personalization features investigated included tailoring of the dose, drug-release profile, size of the dosage form, incorporation of data, or a combination thereof. Tailoring of the oral printed dosage forms was achieved by e.g., varying the infill level of the printed tablets (FDM), printing various sized dosage forms with the same starting material (FDM, EXT, and IJP), printing multiple subsequent layers to increase the amount of the API(s) being deposited on the substrate (IJP), or imprinting the dosage form with a QR code to enable incorporation of data (IJP). The printed dosage forms were analyzed by established pharmaceutical analytical methods to gain an understanding of the quality of the prepared dosage forms as well as the requirements of the printing materials to enable reliable and successful printing.

In the first study (I), eight of the thirteen HME filaments were successfully printed into various-sized tablets and the HPC-based filaments generally demonstrated good printability. The breaking distance and moisture uptake of the filaments were observed to affect the printability and could thus, in combination with other analyses, be used to predict printability of new formulations. The 3D-printed tablets showed various drug release profiles and isoniazid drug content. The differences in the drug release profiles were mainly affected by the polymers used in the formulation, but also the size and infill level of the tablet were observed to have an impact and may thus be used for modifying the drug release.

In the second study (II), the mechanical properties of the flexible ODFs prepared by means of EXT and IJP were acceptable and allowed handling without damaging the dosage forms. Superior characteristics, e.g., content uniformity and ease of administration, were attained for printed ODFs as compared to OPSs prepared at the hospital pharmacy according to a standard operating procedure. The printed ODFs contained various therapeutic warfarin doses (doses ranging from 0.1 to 2 mg) for pediatrics. The ODFs and OPSs were shown to be stable during the 4-week stability study conducted at room temperature (temperatures and RH ranging from 19.6 to 21.5°C and 13.0 to 32.9%, respectively).

In the third study (III), the concept of data-enriched edible pharmaceuticals (DEEP) was explored. Incorporation of personalized information (in a QR code) on a single dosage unit level while simultaneously tailoring the dose of two cannabinoids was achieved by IJP. The cannabinoid dose was tailored by

imprinting 1-10 layers of the ink. The correlation between the number of printed layers and the deposited amount of cannabinoids was observed to be $R^2 = 0.9947$ and $R^2 = 0.9954$ for CBD and THC, respectively and the 10 layer imprinted DEEP was shown to fulfill the requirements for immediate release oral dosage forms. The novelty of IJP DEEP, namely the possibility to incorporate unique data and tailor the dose in a single step was shown. This is not feasible by means of conventional mass production although generic and identical data (typically an identification label) may be printed on dosage forms or is used to imprint the primary or secondary packaging. Incorporation of personalized information at a single dosage unit level could be used for multiple purposes, e.g., improving patient adherence, traceability, and improved safety, depending on the needs of the specific API.

In study II, therapeutic warfarin doses for the target population were achieved. Therapeutic doses were not achieved for the other studied drugs, i.e., isoniazid (study I) and CBD, and THC (study III). This was due to the low concentration of the APIs in the filament or the ink. Therefore, increasing the drug concentration in the starting material (filament or printing ink) or increasing the size of the dosage form, or in IJP imprinting a larger area, or using a higher print resolution (i.e., DPI) would aid to achieve therapeutic doses in a single dosage unit. How an increased concentration of the drugs studied can be loaded in the starting material, while still ensuring good printability of the starting materials would need to be studied in the future.

Based on the results of this thesis along with a thorough literature review, and the fact that one 3D-printed drug is available on the market today it is evident that current printing technologies are suitable for production of solid oral dosage forms. Whether printing is the most suitable manufacturing technique to prepare solid oral dosage forms needs to be carefully evaluated based on e.g., the personalization need of the API or the size of the targeted population group. As the printing techniques vary in nature and all have their strengths and weaknesses, the printing technique selected for a specific API should take into account the characteristics of the API and the requirements for the final dosage form, i.e., which personalization aspects are needed and what the targeted therapeutic doses are.

This thesis has given an overview of the potential and benefits of printed oral dosage forms and highlighted areas requiring additional development to make printed oral dosage forms available at a larger scale. Although the benefits of such dosage forms from a treatment perspective are evident, a detailed cost-benefit analysis would be required to justify the increased treatment costs which are expected due to higher manufacturing costs and necessary diagnostic tests. This is something that e.g. the government in Sweden started in 2021 when the task was given to the Dental and Pharmaceutical Benefits Agency, TLV (Tandvårds- och läkemedelsförmånsverket, 2021). As it is identified that the traditionally used health economic assessment models are not suitable for personalized medicine, TLV was asked to evaluate and propose new suitable models for personalized medicine and advanced therapies. However, the future

for innovative and personalized medicines is looking promising. This is e.g., highlighted by the pharmaceutical strategy for Europe by The European Commission that was updated to ensure patients have access to innovative and affordable medicines (European Commission, 2020). The strategy further included personalized medicine as it was stated that it will support patient-centered innovations and accommodate digital and technological change. It will remain to be seen if and how fast society will move away from conventional dosage forms and how widely and at which price these promising printed dosage forms will be available for patients in the future.

8. Future perspectives

For 3D-printed oral dosage forms to enter the market on a larger scale it requires new ways of thinking, new regulatory guidelines as well as innovative and modern business models to ensure that these improved drug products efficiently can reach the patients, ideally using a mass customization approach. Various distribution chain scenarios have been proposed for on-demand printed dosage forms. Pharmacoprinting is envisioned to take place at the pharmacy, pharmaceutical company, or patient's home, where the two first are considered the two more likely scenarios (Lind et al., 2017). Good distribution practice as well as guaranteeing safety and efficacy of the on-demand printed personalized dosage forms is crucial regardless of the selected distribution chain. To date, there is a lack of a regulatory framework for oral dosage forms with flexible doses that could be manufactured on-demand by e.g., printing technologies (Vaz and Kumar, 2021). Quality control solutions based on real time release testing for such products also need further development. This makes it challenging and risky for pharmaceutical companies to develop printed oral dosage forms as there are no clear regulatory guidelines ensuring marketing approval. It is still unclear whether the approval of printed dosage forms in the future will involve the entire printing process (from digital design to printed dosage form) or only the final dosage form. Earlier it has been indicated that 3D-printed oral dosage forms would not require a unique regulatory pathway (Khairuzzaman, 2016). This would imply that printed oral dosage forms would need to fulfill the same set of regulatory requirements as comparable oral dosage forms produced in a conventional way (Preis and Öblom, 2017). This may change depending on how printed products are classified and where they are produced. In the future printed products may be classified as a new type of dosage form along with a set of specific regulatory guidelines. Despite these hurdles, the potential of 3D printing in the medical and pharmaceutical fields has been recognized by regulatory bodies. Especially the FDA has been active in this space by issuing guidance for 3D-printed medical devices in 2017 (FDA, 2017). The FDA has also approved numerous 3D-printed medical devices during the past decade as well as the 3D-printed dosage form Spritam®. In 2021 the FDA in addition approved the IND application for the printed T19 dosage form by Triastek, which is envisioned to seek marketing approval in 2023 (Everett, 2021; Khairuzzaman, 2016; Preis and Öblom, 2017; Vaz and Kumar, 2021).

As a thesis is limited with regards to how many things can be explored, it leaves room for further explorations. In addition to the more general outlooks for 3D-printed solid dosage forms mentioned above it would be interesting to explore the possibility to develop one or more standard inks or feedstock materials to which various APIs with different properties could be added. It would be beneficial in e.g., a hospital setting if a standard ink base could be provided and the hospital pharmacy could prepare personalized oral dosage forms by simply adding the desired API(s). Development of such standard ink or feedstock formulations with great printability is additionally expected to

considerably speed up formulation development and may attract more companies and pharmacies to consider printing as a method to manufacturing oral dosage forms.

Another aspect to consider to aid future research on printed dosage forms is the user and patient perspective. This could be elaborated by conducting large interview studies with different population groups (e.g., patients and medical staff). The data collected from these studies would highlight factors essential for printed dosage forms to be widely accepted, which may not be obvious to the researchers developing these novel dosage forms.

9. Acknowledgements

I would like to acknowledge the Finnish Cultural Foundation (Elli Turusen rahasto) and the Board of the Graduate School at Åbo Akademi University for granting personal doctoral research grants enabling me to conduct the PhD studies. Furthermore, NordForsk (the Nordic University Hub project #85352, Nordic POP) is greatly acknowledged for funding the one-year research visit to the University of Copenhagen.

I would like to extend my deepest gratefulness to my supervisors. First, a special appreciation to my main supervisor Professor Niklas Sandler for enabling this journey, and for making me understand that a PhD is as much about personal growth as it is about developing as a scientific researcher. I would like to express my deepest gratitude to my co-supervisor Associate Professor Natalja Genina as well as Professor Jukka Rantanen, and Associate Professor Johan Bøtker at the University of Copenhagen. I greatly appreciate your endless support, enthusiasm, and contribution of scientific knowledge to my project and beyond. I could not have asked for better supervisors during my stay at University of Copenhagen. A special thanks to Associate Professor Genina for always finding time to discuss and give valuable input regarding the daily research activities and at all times having my best interest at heart also on a personal level. Your attention to detail is admirable. A special thank you is also extended to Associate Professor Claus Cornett at the University of Copenhagen for helping with the UPLC method development and many interesting discussions along the way.

I would like to extend my sincerest thank you to all colleagues and co-authors during the years, for your help, support, and discussions allowing me to advance as a researcher. A warm thanks to everyone at PSL, especially Professor Jessica Rosenholm and my colleagues at the Drug-Delivery and Pharmaceutical Technology Research Group; Erica Sjöholm, Dr. Mirja Palo, Dr. Henrika Arnkil, Dr. Hossein Vakili, Dr. Emrah Yildir, and Johan Nyman. To my fellow PhD student and beloved friend, Erica Sjöholm, thank you for always being there. I cannot imagine this journey without you and I will forever cherish the memories we made during these years. Thank you Dr. Maren Preis for your valuable support and guidance during my first year as a PhD student. A special thank you to Dr. Jorrit Water for your scientific support and input as well as interesting scientific discussions throughout my PhD. To my colleagues and friends in the Materials and Manufacturing and Solid State Pharmaceutics group at University of Copenhagen, I truly enjoyed working in the encouraging and dedicated environment. Thank you for making me feel welcome from day one, I sincerely had the best research stay possible thanks to all of you.

A huge thank you to Professor Michael Repka, Dr. Jiaxiang Zhang, and the rest of the research group at the University of Mississippi for sharing your HME expertise and for your overwhelming hospitality during the stay at the university.

I feel honored to have Professor Clive Roberts and Professor João Pinto as reviewers of my PhD thesis. Thank you for your respected comments and for taking the time of your busy schedule to review my thesis.

Finally, I am forever grateful for the unconditional love, support, and understanding from my family, which always has allowed me to pursue all my dreams in life, big and small.

Copenhagen, 2021
Heidi Öblom

10. References

Accenture, 2017. Patients want a heavy dose of digital [WWW Document]. URL https://www.accenture.com/_acnmedia/PDF-8/Accenture-Patients-Want-A-Heavy-Dose-of-Digital-Infographic-v2.pdf (accessed 6.16.17).

Aho, J., Boetker, J.P., Baldursdottir, S., Rantanen, J., 2015. Rheology as a tool for evaluation of melt processability of innovative dosage forms. Int. J. Pharm. 494, 623–642. https://doi.org/10.1016/J.IJPHARM.2015.02.009

Airaksinen, S., 2005. Role of Excipients in Moisture Sorption and Physical Stability of Solid Pharmaceutical Formulations. University of Helsinki.

Aita, I. El, Breitkreutz, J., Quodbach, J., 2020. Investigation of semi-solid formulations for 3D printing of drugs after prolonged storage to mimic real-life applications. Eur. J. Pharm. Sci. 146, 105266. https://doi.org/10.1016/j.ejps.2020.105266

Alhijjaj, M., Belton, P., Qi, S., 2016. An investigation into the use of polymer blends to improve the printability of and regulate drug release from pharmaceutical solid dispersions prepared via fused deposition modeling (FDM) 3D printing. Eur. J. Pharm. Biopharm. 108, 111–125. https://doi.org/10.1016/j.ejpb.2016.08.016

Alhnan, M.A., Okwuosa, T.C., Sadia, M., Wan, K.W., Ahmed, W., Arafat, B., 2016. Emergence of 3D Printed Dosage Forms: Opportunities and Challenges. Pharm. Res. 33, 1817–1832. https://doi.org/10.1007/s11095-016-1933-1

Alomari, M., Mohamed, F.H., Basit, A.W., Gaisford, S., 2015. Personalised dosing: Printing a dose of one's own medicine. Int. J. Pharm. 494, 568–577. https://doi.org/10.1016/j.ijpharm.2014.12.006

Aprecia, 2020. 3D Printing/ZipDose technology [WWW Document]. URL https://www.aprecia.com/zipdose-platform/3d-printing.php (accessed 6.16.20).

Arafat, B., Wojsz, M., Isreb, A., Forbes, R.T., Isreb, M., Ahmed, W., Arafat, T., Alhnan, M.A., 2018. Tablet fragmentation without a disintegrant: A novel design approach for accelerating disintegration and drug release from 3D printed cellulosic tablets. Eur. J. Pharm. Sci. 118, 191–199. https://doi.org/10.1016/j.ejps.2018.03.019

Ashland, 2017. Klucel™ hydroxypropylcellulose- Physical and chemical properties for pharmaceutical applications [WWW Document]. URL https://www.ashland.com/file_source/Ashland/Product/Documents/Pharmaceutical/PC_11229_Klucel_HPC.pdf (accessed 8.22.18).

Awad, A., Trenfield, S.J., Gaisford, S., Basit, A.W., 2018. 3D printed medicines: A new branch of digital healthcare. Int. J. Pharm. https://doi.org/10.1016/j.ijpharm.2018.07.024

Azad, M.A., Olawuni, D., Kimbell, G., Badruddoza, A.Z., Hossain, S., Sultana, T., 2020. Polymers for Extrusion-Based 3D Printing of Pharmaceuticals : A Holistic Materials – Process Perspective. Pharmaceutics 12, 124. https://doi.org/10.3390/pharmaceutics12020124

Boateng, J.S., Stevens, H.N.E., Eccleston, G.M., Auffret, A.D., Humphrey, M.J., Matthews, K.H., 2009. Development and mechanical characterization of solvent-cast polymeric films as potential drug delivery systems to mucosal surfaces. Drug Dev. Ind. Pharm. 35, 986–996. https://doi.org/10.1080/03639040902744704

Boetker, J., Water, J.J., Aho, J., Arnfast, L., Bohr, A., Rantanen, J., 2016. Modifying release characteristics

from 3D printed drug-eluting products. Eur. J. Pharm. Sci. 90, 47–52. https://doi.org/10.1016/j.ejps.2016.03.013

Borges, A.F., Silva, C., Coelho, J.F.J., Simões, S., 2015. Oral films: Current status and future perspectives: I - Galenical development and quality attributes. J. Control. Release 206, 1–19. https://doi.org/10.1016/j.jconrel.2015.03.006

Breitkreutz, J., Boos, J., 2007. Paediatric and geriatric drug delivery. Expert Opin. Drug Deliv. 4, 37–45. https://doi.org/10.1517/17425247.4.1.37

Brion, F., Nunn, A., Rieutord, A., 2010. Extemporaneous (magistral) preparation of oral medicines for children in European hospitals. Acta Paediatr. https://doi.org/10.1111/j.1651-2227.2003.tb00583.x

Bruni, N., Pepa, C. Della, Oliaro-Bosso, S., Pessione, E., Gastaldi, D., Dosio, F., 2018. Cannabinoid delivery systems for pain and inflammation treatment. Molecules 23, 2478. https://doi.org/10.3390/molecules23102478

Cape, S., Mulder, M., Schwartz, S., Chupka, K., Johnson, P., Colagiovanni, D., 2017. Development of Best-In-Class Medical Cannabis Products, in: ICR 2017. p. 47.

Chai, X., Chai, H., Wang, X., Yang, J., Li, J., Zhao, Y., Cai, W., Tao, T., Xiang, X., 2017. Fused deposition modeling (FDM) 3D printed tablets for intragastric floating delivery of domperidone. Sci. Rep. 7, 2829. https://doi.org/10.1038/s41598-017-03097-x

Chen, G., Xu, Y., Chi Lip Kwok, P., Kang, L., 2020. Pharmaceutical Applications of 3D Printing. Addit. Manuf. 34, 101209. https://doi.org/10.1016/j.addma.2020.101209

Cheow, W.S., Kiew, T.Y., Hadinoto, K., 2015. Combining inkjet printing and amorphous nanonization to prepare personalized dosage forms of poorly-soluble drugs. Eur. J. Pharm. Biopharm. 96, 314–321. https://doi.org/https://doi.org/10.1016/j.ejpb.2015.08.012

Clarke, A., Doughty, D., 2017. Development of Liquid Dispensing Technology for the Manufacture of Low Dose Drug Products, in: Kleinbudde, P., Khinast, J., Rantanen, J. (Eds.), Continuous Manufacturing of Pharmaceuticals. 7 John Wiley & Sons Ltd., pp. 551–575. https://doi.org/10.1002/9781119001348.ch17

Clasen, C., Phillips, P.M., Palangetic, L., Vermant, J., 2011. Dispensing of rheologically complex fluids: The map of misery. AIChE J. 58, 3242–3255. https://doi.org/10.1002/aic.13704

Cohen, J.S., 1999. Ways to minimize adverse drug reactions. Postgrad. Med. 106, 163–172. https://doi.org/10.3810/pgm.1999.09.688

Derby, B., Reis, N., 2003. Inkjet Printing of Highly Loaded Particulate Suspensions. MRS Bull. 28, 815–818.

DFE Pharma, 2019. Lactose Some basic properties and characteristics [WWW Document]. URL https://www.dfepharma.com/-/media/documents/technical-documents/technical-papers/lactose-some-basic-properties.pdf (accessed 4.3.19).

DIN, 2003. DIN EN ISO 527-3 Bestimmung der Zugeigenschaften Teil 3: Pruefbedingungen fuer Folien und Tafeln. Beuth Verlag GmbH, Berlin.

DIN, 1996. DIN EN ISO 527-1 Bestimmung der Zugeigenschaften Teil 1: Allgemeine Grundsaetze. Beuth Verlag GmbH, Berlin.

Duran, C., Subbian, V., Giovanetti, M.T., Simkins, J.R., Beyette Jr, F.R., 2015. Experimental desktop 3D printing using dual extrusion and water-soluble polyvinyl alcohol. Rapid Prototyp. J. 21, 528–534.

Edinger, M., Bar-Shalom, D., Rantanen, J., Genina, N., 2017. Visualization and Non-Destructive Quantification of

Inkjet-Printed Pharmaceuticals on Different Substrates Using Raman Spectroscopy and Raman Chemical Imaging. Pharm. Res. 34, 1023–1036. https://doi.org/10.1007/s11095-017-2126-2

Edinger, M., Bar-Shalom, D., Sandler, N., Rantanen, J., Genina, N., 2018a. QR encoded smart oral dosage forms by inkjet printing. Int. J. Pharm. 536, 138–145. https://doi.org/10.1016/j.ijpharm.2017.11.052

Edinger, M., Jacobsen, J., Bar-Shalom, D., Rantanen, J., Genina, N., 2018b. Analytical aspects of printed oral dosage forms. Int. J. Pharm. https://doi.org/10.1016/j.ijpharm.2018.10.030

El Aita, I., Breitkreutz, J., Quodbach, J., 2019. On-demand manufacturing of immediate release levetiracetam tablets using pressure-assisted microsyringe printing. Eur. J. Pharm. Biopharm. 134, 29–36. https://doi.org/10.1016/j.ejpb.2018.11.008

Elbl, J., Gajdziok, J., Kolarczyk, J., 2020. 3D printing of multilayered orodispersible films with in-process drying. Int. J. Pharm. 575, 118883. https://doi.org/10.1016/j.ijpharm.2019.118883

Eleftheriadis, G.K., Ritzoulis, C., Bouropoulos, N., Tzetzis, D., Andreadis, D.A., Boetker, J., Rantanen, J., Fatouros, D.G., 2019. Unidirectional drug release from 3D printed mucoadhesive buccal films using FDM technology: In vitro and ex vivo evaluation. Eur. J. Pharm. Biopharm. 144, 180–192. https://doi.org/10.1016/J.EJPB.2019.09.018

Elkasabgy, N.A., Mahmoud, A.A., Maged, A., 2020. 3D printing: An appealing route for customized drug delivery systems. Int. J. Pharm. 588, 119732. https://doi.org/10.1016/j.ijpharm.2020.119732

European Commission, 2020. Affordable, accessible and safe medicines for all: the Commission presents a Pharmaceutical Strategy for Europe [WWW Document]. URL https://ec.europa.eu/eip/ageing/news/affordable-accessible-and-safe-medicines-all-commission-presents-pharmaceutical-strategy-europe_en.html (accessed 10.31.21).

European Commission, 2019. Falsified medicines [WWW Document]. URL https://ec.europa.eu/health/human-use/falsified_medicines_en (accessed 5.21.19).

European Commission, 2015. Commission delegated regulation (EU) 2016/161. Off. J. Eur. Union.

European Medicines Agency, 2021a. ICH reflection paper on proposed ICH guideline work to advance patient focused drug Development. Amsterdam.

European Medicines Agency, 2021b. Falsified medicines: overview [WWW Document]. URL https://www.ema.europa.eu/en/human-regulatory/overview/public-health-threats/falsified-medicines-overview (accessed 5.21.21).

European Medicines Agency, 2020a. Personalised medicine [WWW Document]. Med. Prod. URL https://ec.europa.eu/health/human-use/personalised-medicine_en (accessed 6.16.20).

European Medicines Agency, 2020b. Personalised medicine [WWW Document]. URL https://www.ema.europa.eu/en/glossary/personalised-medicine%0D (accessed 6.16.20).

European Medicines Agency, 2017. ICH guideline Q8 (R2) on pharmaceutical development.

European Medicines Agency, 2015. Quick Response (QR) codes in the labelling and package leaflet of centrally authorised medicinal products [WWW Document]. URL http://www.ema.europa.eu/docs/en_GB/document_library/Regulatory_and_procedural_guideline/2015/07/WC500190405.pdf (accessed 6.16.17).

European Medicines Agency, 2012a. Guideline on Real Time Release

Testing EMA/CHMP/QWP/811210/2009-Rev1, Committee for Medicinal Products for Human Use (CHMP).

European Medicines Agency, 2012b. Assessment report: Anti-tuberculosis medicinal products containing isoniazid, rifampicin, pyrazinamide, ethambutol, rifabutin: posology in children. London.

European Pharmacopoeia Commission, 2020a. Pharmacopoeia Europea, edition 10.2. European Directorate for the Quality of Medicines & HealthCare (EDQM), Strasbourg, France.

European Pharmacopoeia Commission, 2020b. Pharmacopoeia Europea, edition 10.1. European Directorate for the Quality of Medicines & HealthCare (EDQM), Strasbourg, France.

European Pharmacopoeia Commission, 2017. Pharmacopoeia Europea, edition 9.0. European Directorate for the Quality of Medicines & HealthCare (EDQM), Strasbourg, France.

Everett, H., 2021. Triastek receives FDA IND clearance for 3D printed drug to treat rheumatoid arthritis [WWW Document]. URL https://3dprintingindustry.com/news/triastek-receives-fda-ind-clearance-for-3d-printed-drug-to-treat-rheumatoid-arthritis-184159/

Fairbairn, J.W., Liebmann, J.A., Rowan, M.G., 1976. The stability of cannabis and its preparations on storage. J. Pharm. Pharmacol. 28, 1–7. https://doi.org/10.1111/j.2042-7158.1976.tb04014.x

Fastø, M.M., Genina, N., Kaae, S., Kälvemark Sporrong, S., 2019. Perceptions, preferences and acceptability of patient designed 3D printed medicine by polypharmacy patients: a pilot study. Int. J. Clin. Pharm. 41, 1290–1298. https://doi.org/10.1007/s11096-019-00892-6

FDA, 2017. Technical Considerations for Additive Manufactured Medical Devices Guidance for Industry and Food and Drug Administration Staff Preface Public Comment.

FDA, 2015. Pharmaceutical Quality for the 21st Century A Risk-Based Approach Progress Report.

Fuenmayor, E., Forde, M., Healy, A. V., Devine, D.M., Lyons, J.G., McConville, C., Major, I., 2018. Material considerations for fused-filament fabrication of solid dosage forms. Pharmaceutics 10, 44. https://doi.org/10.3390/pharmaceutics10020044

Garsuch, V., Breitkreutz, J., 2010. Comparative investigations on different polymers for the preparation of fast-dissolving oral films. J. Pharm. Pharmacol. 62, 539–545. https://doi.org/10.1211/jpp.62.04.0018

Garsuch, V., Breitkreutz, J., 2009. Novel analytical methods for the characterization of oral wafers. Eur. J. Pharm. Biopharm. 73, 195–201. https://doi.org/10.1016/j.ejpb.2009.05.010

Genina, N., Boetker, J.P., Colombo, S., Harmankaya, N., Rantanen, J., Bohr, A., 2017. Anti-tuberculosis drug combination for controlled oral delivery using 3D printed compartmental dosage forms: From drug product design to in vivo testing. J. Control. Release. https://doi.org/10.1016/j.jconrel.2017.10.003

Genina, N., Fors, D., Palo, M., Peltonen, J., Sandler, N., 2013a. Behavior of printable formulations of loperamide and caffeine on different substrates—Effect of print density in inkjet printing. Int. J. Pharm. 453, 488–497. https://doi.org/10.1016/J.IJPHARM.2013.06.003

Genina, N., Fors, D., Vakili, H., Ihalainen, P., Pohjala, L., Ehlers, H., Kassamakov, I., Haeggström, E., Vuorela, P., Peltonen, J., Sandler, N., 2012. Tailoring controlled-release oral dosage forms by combining inkjet and flexographic printing techniques. Eur. J. Pharm. Sci. 47, 615–623.

https://doi.org/10.1016/J.EJPS.2012.07.020

Genina, N., Janßen, E.M., Breitenbach, A., Breitkreutz, J., Sandler, N., 2013b. Evaluation of different substrates for inkjet printing of rasagiline mesylate. Eur. J. Pharm. Biopharm. 85, 1075–1083. https://doi.org/10.1016/j.ejpb.2013.03.017

Gioumouxouzis, C.I., Baklavaridis, A., Katsamenis, O.L., Markopoulou, C.K., Bouropoulos, N., Tzetzis, D., Fatouros, D.G., 2018. A 3D printed bilayer oral solid dosage form combining metformin for prolonged and glimepiride for immediate drug delivery. Eur. J. Pharm. Sci. 120, 40–52. https://doi.org/10.1016/j.ejps.2018.04.020

GlaxoSmithKline, 2021. Liquid dispensing technology (LDT) [WWW Document]. URL https://www.gsk.com/media/2758/liquid-dispensing-technology-leaflet.pdf (accessed 1.17.21).

Goole, J., Amighi, K., 2016. 3D printing in pharmaceutics: A new tool for designing customized drug delivery systems. Int. J. Pharm. 499, 376–394. https://doi.org/10.1016/J.IJPHARM.2015.12.071

Govender, R., Abrahmsén-Alami, S., Larsson, A., Folestad, S., 2020. Therapy for the individual: Towards patient integration into the manufacturing and provision of pharmaceuticals. Eur. J. Pharm. Biopharm. 149, 58–76. https://doi.org/10.1016/j.ejpb.2020.01.001

Goyanes, A., Allahham, N., Trenfield, S.J., Stoyanov, E., Gaisford, S., Basit, A.W., 2019. Direct powder extrusion 3D printing: Fabrication of drug products using a novel single-step process. Int. J. Pharm. 567, 118471. https://doi.org/10.1016/j.ijpharm.2019.118471

Goyanes, A., Buanz, A.B.M., Basit, A.W., Gaisford, S., 2014. Fused-filament 3D printing (3DP) for fabrication of tablets. Int. J. Pharm. 476, 88–92. https://doi.org/10.1016/j.ijpharm.2014.09.044

Goyanes, A., Buanz, A.B.M., Hatton, G.B., Gaisford, S., Basit, A.W., 2015a. 3D printing of modified-release aminosalicylate (4-ASA and 5-ASA) tablets. Eur. J. Pharm. Biopharm. 89, 157–162. https://doi.org/10.1016/j.ejpb.2014.12.003

Goyanes, A., Fina, F., Martorana, A., Sedough, D., Gaisford, S., Basit, A.W., 2017. Development of modified release 3D printed tablets (printlets) with pharmaceutical excipients using additive manufacturing. Int. J. Pharm. 527, 21–30. https://doi.org/10.1016/J.IJPHARM.2017.05.021

Goyanes, A., Robles Martinez, P., Basit, A.W., 2015b. Effect of geometry on drug release from 3D printed tablets. Int. J. Pharm. 494, 657–663. https://doi.org/10.1016/j.ijpharm.2015.04.069

Halidi, S.N.A.M., Abdullah, J., 2012. Moisture effects on the ABS used for Fused Deposition Modeling rapid prototyping machine, in: SHUSER 2012 - 2012 IEEE Symposium on Humanities, Science and Engineering Research. pp. 839–843. https://doi.org/10.1109/SHUSER.2012.6268999

Haluza, D., Jungwirth, D., 2018. ICT and the future of healthcare: Aspects of pervasive health monitoring. Informatics Heal. Soc. Care 43, 1–11. https://doi.org/10.1080/17538157.2016.1255215

Han, S., Bae, H.J., Kim, J., Shin, S., Choi, S.-E., Lee, S.H., Kwon, S., Park, W., 2012. Lithographically Encoded Polymer Microtaggant Using High-Capacity and Error-Correctable QR Code for Anti-Counterfeiting of Drugs. Adv. Mater. 24, 5924–5929. https://doi.org/10.1002/adma.201201486

Helmy, S.A., 2015. Tablet splitting: Is it worthwhile? Analysis of drug content and weight uniformity for half tablets of 16 commonly used medications in the outpatient setting. J. Manag. Care Pharm. 21, 76–86.

https://doi.org/10.18553/jmcp.2015.21.1.76

Hemanth, K., Hemamanjushree, S., Abhinaya, N., Pai, R., Girish Pai, K., 2021. 3D Printing : A Review on Technology , Role in Novel Dosage Forms and Regulatory Perspective. Res. J. Pharm. Tech 14, 562–572. https://doi.org/10.5958/0974-360X.2021.00102.5

Hill, S., Varker, A.S., Karlage, K., Myrdal, P.B., 2016. Analysis of Drug Content and Weight Uniformity for Half-Tablets of 6 Commonly Split Medications. J. Manag. Care Pharm. https://doi.org/10.18553/jmcp.2009.15.3.253

Hoffmann, E.M., Breitenbach, A., Breitkreutz, J., 2011. Advances in orodispersible films for drug delivery. Expert Opin. Drug Deliv. 8, 299–316. https://doi.org/10.1517/17425247.2011.553217

Holländer, J., Hakala, R., Suominen, J., Moritz, N., Yliruusi, J., Sandler, N., 2018. 3D printed UV light cured polydimethylsiloxane devices for drug delivery. Int. J. Pharm. 544, 433–442. https://doi.org/10.1016/j.ijpharm.2017.11.016

Homayun, B., Lin, X., Choi, H.J., 2019. Challenges and recent progress in oral drug delivery systems for biopharmaceuticals. Pharmaceutics 11. https://doi.org/10.3390/pharmaceutics11030129

Horvath, J., 2014. A Brief History of 3D Printing, in: Mastering 3D Printing. Apress, Berkeley, CA, pp. 3–10. https://doi.org/10.1007/978-1-4842-0025-4_1

Huanbutta, K., Sangnim, T., 2019. Journal of Drug Delivery Science and Technology Design and development of zero-order drug release gastroretentive fl oating tablets fabricated by 3D printing technology. J. Drug Deliv. Sci. Technol. 52, 831–837. https://doi.org/10.1016/j.jddst.2019.06.004

Huang, Q., Shen, W., Song, W., 2012. Synthesis of colourless silver precursor ink for printing conductive patterns on silicon nitride substrates. Appl. Surf. Sci. 258, 7384–7388. https://doi.org/10.1016/j.apsusc.2012.04.037

Iftimi, L.-D., Edinger, M., Bar-Shalom, D., Rantanen, J., Genina, N., 2019. Edible solid foams as porous substrates for inkjet-printable pharmaceuticals. Eur. J. Pharm. Biopharm. 136, 38–47. https://doi.org/10.1016/J.EJPB.2019.01.004

Jamróz, W., Kurek, M., Łyszczarz, E., Brniak, W., Jachowicz, R., 2017a. Printing techniques: Recent developments in pharmaceutical technology. Acta Pol. Pharm. - Drug Res. 74, 753–763.

Jamróz, W., Kurek, M., Łyszczarz, E., Szafraniec, J., Knapik-Kowalczuk, J., Syrek, K., Paluch, M., Jachowicz, R., 2017b. 3D printed orodispersible films with Aripiprazole. Int. J. Pharm. 533, 413–420. https://doi.org/10.1016/J.IJPHARM.2017.05.052

Jamróz, W., Szafraniec, J., Kurek, M., Jachowicz, R., 2018. 3D Printing in Pharmaceutical and Medical Applications – Recent Achievements and Challenges. Pharm. Res. 35, 176. https://doi.org/10.1007/s11095-018-2454-x

Jang, D., Kim, D., Moon, J., 2009. Influence of fluid physical properties on ink-jet printability. Langmuir 25, 2629–2635. https://doi.org/10.1021/la900059m

Janßen, E.M., Schliephacke, R., Breitenbach, A., Breitkreutz, J., 2013. Drug-printing by flexographic printing technology—A new manufacturing process for orodispersible films. Int. J. Pharm. 441, 818–825. https://doi.org/10.1016/J.IJPHARM.2012.12.023

Kadry, H., Al-Hilal, T.A., Keshavarz, A., Alam, F., Xu, C., Joy, A., Ahsan, F., 2018. Multi-purposable filaments of HPMC for 3D printing of medications with tailored drug release and timed-absorption. Int. J. Pharm. 544, 285–296.

https://doi.org/10.1016/j.ijpharm.2018.04.010

Khairuzzaman, A., 2016. “Click” to “Print”: A Novel Technology to Design and Manufacture Pharmaceutical Drug Products.

Khaled, S., Alexander, M., Wildman, R., Wallace, M., Sharpe, S., Yoo, J., Roberts, C., 2018a. 3D extrusion printing of high drug loading immediate release paracetamol tablets. Int. J. Pharm. 538, 223–230. https://doi.org/10.1016/j.ijpharm.2018.01.024

Khaled, S., Alexander, M.R., Irvine, D.J., Wildman, R.D., Wallace, M.J., Sharpe, S., Yoo, J., Roberts, C.J., 2018b. Extrusion 3D Printing of Paracetamol Tablets from a Single Formulation with Tunable Release Profiles Through Control of Tablet Geometry. AAPS PharmSciTech 19, 3403–3413. https://doi.org/10.1208/s12249-018-1107-z

Khaled, S.A., Burley, J.C., Alexander, M.R., Roberts, C.J., 2014. Desktop 3D printing of controlled release pharmaceutical bilayer tablets. Int. J. Pharm. 461, 105–111. https://doi.org/10.1016/j.ijpharm.2013.11.021

Khaled, S.A., Burley, J.C., Alexander, M.R., Yang, J., Roberts, C.J., 2015a. 3D printing of tablets containing multiple drugs with defined release profiles. Int. J. Pharm. 494, 643–650. https://doi.org/10.1016/j.ijpharm.2015.07.067

Khaled, S.A., Burley, J.C., Alexander, M.R., Yang, J., Roberts, C.J., 2015b. 3D printing of five-in-one dose combination polypill with defined immediate and sustained release profiles. J. Control. Release 217, 308–314. https://doi.org/10.1016/j.jconrel.2015.09.028

Kitson, P.J., Symes, M.D., Dragone, V., Cronin, L., 2013. Combining 3D printing and liquid handling to produce user-friendly reactionware for chemical synthesis and purification. Chem. Sci. 4, 3099–3103. https://doi.org/10.1039/c3sc51253c

Korte, C., Quodbach, J., 2018. Formulation development and process analysis of drug-loaded filaments manufactured via hot-melt extrusion for 3D-printing of medicines. Pharm. Dev. Technol. 23, 1117–1127. https://doi.org/10.1080/10837450.2018.1433208

Krüss GmbH, 2019. Drop Shape Analysis database.

Kyobula, M., Adedeji, A., Alexander, M.R., Saleh, E., Wildman, R., Ashcroft, I., Gellert, P.R., Roberts, C.J., 2017. 3D inkjet printing of tablets exploiting bespoke complex geometries for controlled and tuneable drug release. J. Control. Release 261, 207–215. https://doi.org/10.1016/j.jconrel.2017.06.025

Le, H.P., 1998. Progress and Trends in Ink-jet Printing Technology. J. Imaging Sci. Technol. 42, 49–62.

Li, Q., Guan, X., Cui, M., Zhu, Z., Chen, K., Wen, H., Jia, D., Hou, J., Xu, W., Yang, X., Pan, W., 2018. Preparation and investigation of novel gastro-floating tablets with 3D extrusion-based printing. Int. J. Pharm. 535, 325–332. https://doi.org/https://doi.org/10.1016/j.ijpharm.2017.10.037

Liew, K. Bin, Tan, Y.T.F., Peh, K.K., 2014. Effect of polymer, plasticizer and filler on orally disintegrating film. Drug Dev. Ind. Pharm. 40, 110–119. https://doi.org/10.3109/03639045.2012.749889

Ligon, S.C., Liska, R., Stampfl, J., Gurr, M., Mülhaupt, R., 2017. Polymers for 3D Printing and Customized Additive Manufacturing. Chem. Rev. 117, 10212–10290. https://doi.org/10.1021/acs.chemrev.7b00074

Lind, J., Kälvemark Sporrong, S., Kaae, S., Rantanen, J., Genina, N., 2017. Social aspects in additive manufacturing of pharmaceutical products. Expert Opin. Drug Deliv. 14, 927–936. https://doi.org/10.1080/17425247.2017.1266336

Lion, A., Wildman, R.D., Alexander, M.R., Roberts, C.J., 2021. Customisable Tablet Printing : The Development of

Multimaterial Hot Melt Inkjet 3D Printing to Produce Complex and Personalised Dosage Forms. Pharmaceutics 13, 1679.

Logue, B.A., Kern, J., Altena, S., Petersen, J., Rassmusan, S., Oda, R., Kellar, J.J., 2015. Countering counterfeiting of drugs: unique fluorescent inks for direct printing onto pharmaceuticals, in: NIP & Digital Fabrication Conference. Society for Imaging Science and Technology, pp. 371–374.

Madathilethu, J., Roberts, M., Peak, M., Blair, J., Prescott, R., Ford, J.L., 2018. Content uniformity of quartered hydrocortisone tablets in comparison with mini-tablets for paediatric dosing. BMJ Paediatr. Open 2. https://doi.org/10.1136/bmjpo-2017-000198

Melchels, F.P.W., Feijen, J., Grijpma, D.W., 2010. A review on stereolithography and its applications in biomedical engineering. Biomaterials 31, 6121–6130. https://doi.org/10.1016/J.BIOMATERIALS.2010.04.050

Mira, J.J., Guilabert, M., Carrillo, I., Fernández, C., Vicente, M.A., Orozco-Beltrán, D., Gil-Guillen, V.F., 2015. Use of QR and EAN-13 codes by older patients taking multiple medications for a safer use of medication. Int. J. Med. Inform. 84, 406–412. https://doi.org/10.1016/j.ijmedinf.2015.02.001

Momeni, F., N, S.M.M.H., Liu, X., Ni, J., 2017. A review of 4D printing. Mater. Des. 122, 42–79. https://doi.org/10.1016/j.matdes.2017.02.068

Musazzi, U.M., Selmin, F., Ortenzi, M.A., Mohammed, G.K., Franzé, S., Minghetti, P., Cilurzo, F., 2018. Personalized orodispersible films by hot melt ram extrusion 3D printing. Int. J. Pharm. 551, 52–59. https://doi.org/10.1016/j.ijpharm.2018.09.013

Nair, A.B., Kumria, R., Harsha, S., Attimarad, M., Al-Dhubiab, B.E., Alhaider, I.A., 2013. In vitro techniques to evaluate buccal films. J. Control. Release 166, 10–21. https://doi.org/10.1016/J.JCONREL.2012.11.019

Nørfeldt, L., Bøtker, J., Edinger, M., Genina, N., Rantanen, J., 2019. Cryptopharmaceuticals: increasing the safety of medication by a blockchain of pharmaceutical products. J. Pharm. Sci. 108, 2838–2841. https://doi.org/10.1016/J.XPHS.2019.04.025

Norman, J., Madurawe, R.D., Moore, C.M. V, Khan, M.A., Khairuzzaman, A., 2017. A new chapter in pharmaceutical manufacturing: 3D-printed drug products ☆'☆☆. Adv. Drug Deliv. Rev. 108, 39–50. https://doi.org/10.1016/j.addr.2016.03.001

Öblom, H., Cornett, C., Bøtker, J., Frokjaer, S., Hansen, H., Rades, T., Rantanen, J., Genina, N., 2020. Data-enriched edible pharmaceuticals (DEEP) of medical cannabis by inkjet printing. Int. J. Pharm. 589, 119866. https://doi.org/10.1016/j.ijpharm.2020.119866

Öblom, H., Sjöholm, E., Rautamo, M., Sandler, N., 2019a. Towards printed pediatric medicines in hospital pharmacies: Comparison of 2D and 3D-printed orodispersible warfarin films with conventional oral powders in unit dose sachets. Pharmaceutics 11, 334. https://doi.org/10.3390/pharmaceutics11070334

Öblom, H., Zhang, J., Pimparade, M., Speer, I., Preis, M., Repka, M., Sandler, N., 2019b. 3D-Printed Isoniazid Tablets for the Treatment and Prevention of Tuberculosis—Personalized Dosing and Drug Release. AAPS PharmSciTech 20. https://doi.org/10.1208/s12249-018-1233-7

Oh, B., Jin, G., Park, C., Park, J., Lee, B., 2020. Preparation and evaluation of identifiable quick response (QR)-coded orodispersible films using 3D printer with directly feeding nozzle. Int. J. Pharm. 584, 119405. https://doi.org/10.1016/j.ijpharm.20

20.119405

Okwuosa, T.C., Pereira, B.C., Arafat, B., Cieszynska, M., Isreb, A., Alhnan, M.A., 2017. Fabricating a Shell-Core Delayed Release Tablet Using Dual FDM 3D Printing for Patient-Centred Therapy. Pharm. Res. 34, 427–437. https://doi.org/10.1007/s11095-016-2073-3

Pacifici, R., Marchei, E., Salvatore, F., Guandalini, L., Busardò, F.P., Pichini, S., 2018. Evaluation of long-term stability of cannabinoids in standardized preparations of cannabis flowering tops and cannabis oil by ultra-high-performance liquid chromatography tandem mass spectrometry. Clin. Chem. Lab. Med. 56, 94–96. https://doi.org/10.1515/cclm-2017-0758

Palo, M., Kogermann, K., Laidmäe, I., Meos, A., Preis, M., Heinämäki, J., Sandler, N., 2017. Development of Oromucosal Dosage Forms by Combining Electrospinning and Inkjet Printing. Mol. Pharm. 14, 808–820. https://doi.org/10.1021/acs.molpharmaceut.6b01054

Pardeike, J., Strohmeier, D.M., Schrödl, N., Voura, C., Gruber, M., Khinast, J.G., Zimmer, A., 2011. Nanosuspensions as advanced printing ink for accurate dosing of poorly soluble drugs in personalized medicines. Int. J. Pharm. 420, 93–100. https://doi.org/https://doi.org/10.1016/j.ijpharm.2011.08.033

Park, B.J., Choi, H.J., Moon, S.J., Kim, S.J., Bajracharya, R., Min, J.Y., Han, H.-K., 2019. Pharmaceutical applications of 3D printing technology: current understanding and future perspectives. J. Pharm. Investig. 49, 575–585. https://doi.org/10.1007/s40005-018-00414-y

Pechová, V., Gajdziok, J., Muselík, J., Vetchý, D., 2018. Development of Orodispersible Films Containing Benzydamine Hydrochloride Using a Modified Solvent Casting Method. AAPS PharmSciTech 19, 2509–2518. https://doi.org/10.1208/s12249-018-1088-y

Pereira, B.C., Isreb, A., Forbes, R.T., Dores, F., Habashy, R., Petit, J.-B., Alhnan, M.A., Oga, E.F., 2019. 'Temporary Plasticiser': A novel solution to fabricate 3D printed patient-centred cardiovascular 'Polypill' architectures. Eur. J. Pharm. Biopharm. 135, 94–103. https://doi.org/https://doi.org/10.1016/j.ejpb.2018.12.009

Pietrzak, K., Isreb, A., Alhnan, M.A., 2015. A flexible-dose dispenser for immediate and extended release 3D printed tablets. Eur. J. Pharm. Biopharm. 96, 380–387. https://doi.org/10.1016/J.EJPB.2015.07.027

Preis, M., Knop, K., Breitkreutz, J., 2014. Mechanical strength test for orodispersible and buccal films. Int. J. Pharm. 461, 22–29. https://doi.org/10.1016/J.IJPHARM.2013.11.033

Preis, M., Öblom, H., 2017. 3D-Printed Drugs for Children—Are We Ready Yet? AAPS PharmSciTech 18, 303–308. https://doi.org/10.1208/s12249-016-0704-y

Pryor, C., 2021. Thin Film Gripping and Jaw Face Comparison Pneumatic Side Action Grips for Thin Films Wedge Grips for Thin Films Roller Grips for Thin Films Advanced Screw Side Action Grips for Thin Films [white paper] [WWW Document]. URL https://www.instron.us/-/media/literature-library/whitepapers/2020/04/thin-film-whitepaper.pdf?la=en-us&hash=8FCAE4170C8C307C5FA4838115E322CF67B8DAE5 (accessed 1.6.21).

Rahman, Z., Barakh Ali, S.F., Ozkan, T., Charoo, N.A., Reddy, I.K., Khan, M.A., 2018. Additive Manufacturing with 3D Printing: Progress from Bench to Bedside. AAPS J. 20, 101. https://doi.org/10.1208/s12248-018-0225-6

Raijada, D., Genina, N., Fors, D., Wisaeus, E., Peltonen, J., Rantanen, J., Sandler, N., 2013. A Step Toward Development of Printable Dosage Forms for Poorly

Soluble Drugs. J. Pharm. Sci. 102, 3694–3704. https://doi.org/10.1002/jps.23678

Rathbone, A.L., Prescott, J., 2017. The Use of Mobile Apps and SMS Messaging as Physical and Mental Health Interventions: Systematic Review. J. Med. Internet Res. 19, e295. https://doi.org/10.2196/jmir.7740

Rautamo, M., Kvarnström, K., Sivén, M., Airaksinen, M., Lahdenne, P., Sandler, N., 2020. Benefits and prerequisites associated with the adoption of oral 3D-printed medicines for pediatric patients: A focus group study among healthcare professionals. Pharmaceutics 12. https://doi.org/10.3390/pharmaceutics12030229

Robles-Martinez, P., Xu, X., Trenfield, S.J., Awad, A., Goyanes, A., Telford, R., Basit, A.W., Gaisford, S., 2019. 3D printing of a multi-layered polypill containing six drugs using a novel stereolithographic method. Pharmaceutics 11, 274. https://doi.org/10.3390/pharmaceutics11060274

Rosqvist, E., Niemelä, E., Frisk, J., Öblom, H., Koppolu, R., Abdelkader, H., Soto Véliz, D., Mennillo, M., Venu, A.P., Ihalainen, P., Aubert, M., Sandler, N., Wilén, C.E., Toivakka, M., Eriksson, J.E., Österbacka, R., Peltonen, J., 2020. A low-cost paper-based platform for fast and reliable screening of cellular interactions with materials. J. Mater. Chem. B 8, 1146–1156. https://doi.org/10.1039/c9tb01958h

Sadia, M., Arafat, B., Ahmed, W., Forbes, R.T., Alhnan, M.A., 2018. Channelled tablets: An innovative approach to accelerating drug release from 3D printed tablets. J. Control. Release 269, 355–363. https://doi.org/10.1016/j.jconrel.2017.11.022

Sadia, M., Sośnicka, A., Arafat, B., Isreb, A., Ahmed, W., Kelarakis, A., Alhnan, M.A., 2016. Adaptation of pharmaceutical excipients to FDM 3D printing for the fabrication of patient-tailored immediate release tablets. Int. J. Pharm. 513, 659–668. https://doi.org/10.1016/j.ijpharm.2016.09.050

Sandler, N., Määttänen, A., Ihalainen, P., Kronberg, L., Meierjohann, A., Viitala, T., Peltonen, J., 2011. Inkjet printing of drug substances and use of porous substrates-towards individualized dosing. J. Pharm. Sci. 100, 3386–3395. https://doi.org/10.1002/jps.22526

Sandler, N., Preis, M., 2016. Printed Drug-Delivery Systems for Improved Patient Treatment. Trends Pharmacol. Sci. 37, 1070–1080. https://doi.org/10.1016/j.tips.2016.10.002

Scoutaris, N., Alexander, M.R., Gellert, P.R., Roberts, C.J., 2011. Inkjet printing as a novel medicine formulation technique. J. Control. Release 156, 179–185. https://doi.org/10.1016/j.jconrel.2011.07.033

Scoutaris, N., Ross, S.A., Douroumis, D., 2018. 3D Printed "Starmix" Drug Loaded Dosage Forms for Paediatric Applications. Pharm. Res. 35, 34. https://doi.org/10.1007/s11095-017-2284-2

Shaqour, B., Samaro, A., Verleije, B., Beyers, K., Vervaet, C., Cos, P., 2020. Production of Drug Delivery Systems Using Fused Filament Fabrication: A Systematic Review. Pharmaceutics 12, 517. https://doi.org/10.3390/pharmaceutics12060517

Siiskonen, M., Malmqvist, J., Folestad, S., 2020. Integrated product and manufacturing system platforms supporting the design of personalized medicines. J. Manuf. Syst. 56, 281–295. https://doi.org/10.1016/j.jmsy.2020.06.016

Simões, M.F., Pinto, R.M.A., Simões, S., 2019. Hot-melt extrusion in the pharmaceutical industry: toward filing a new drug application. Drug Discov. Today 24, 1749–1768. https://doi.org/10.1016/j.drudis.2019.05.013

Sjöholm, E., Mathiyalagan, R., Prakash, D.R.,

Lindfors, L., Wang, Q., Wang, X., Ojala, S., Sandler, N., 2020. 3D-Printed Veterinary Dosage Forms—a Comparative Study of Three Semi-Solid Extrusion 3D Printers. Pharmaceutics 12, 1239. https://doi.org/10.3390/pharmaceutics12121239

Sjöholm, E., Sandler, N., 2019. Additive manufacturing of personalized orodispersible warfarin films. Int. J. Pharm. 564, 117–123. https://doi.org/10.1016/j.ijpharm.2019.04.018

Skowyra, J., Pietrzak, K., Alhnan, M.A., 2015. Fabrication of extended-release patient-tailored prednisolone tablets via fused deposition modelling (FDM) 3D printing. Eur. J. Pharm. Sci. 68, 11–17. https://doi.org/10.1016/j.ejps.2014.11.009

Smith, D.M., Kapoor, Y., Klinzing, G.R., Procopio, A.T., 2018. Pharmaceutical 3D printing: Design and qualification of a single step print and fill capsule. Int. J. Pharm. 544, 21–30. https://doi.org/10.1016/j.ijpharm.2018.03.056

Sun, J., Wei, X., Huang, B., 2012. Influence of the viscosity of edible ink to piezoelectric ink-jet printing drop state. Appl. Mech. Mater. 200, 676–680. https://doi.org/10.4028/www.scientific.net/AMM.200.676

Symes, M.D., Kitson, P.J., Yan, J., Richmond, C.J., Cooper, G.J.T., Bowman, R.W., Vilbrandt, T., Cronin, L., 2012. Integrated 3D-printed reactionware for chemical synthesis and analysis. Nat. Chem. 4, 349–354. https://doi.org/10.1038/nchem.1313

Szakonyi, G., Zelkó, R., 2012. The effect of water on the solid state characteristics of pharmaceutical excipients: Molecular mechanisms, measurement techniques, and quality aspects of final dosage form. Int. J. Pharm. Investig. 2, 18–25. https://doi.org/10.4103/2230-973X.96922

Tagami, T., Nagata, N., Hayashi, N., Ogawa, E., Fukushige, K., Sakai, N., Ozeki, T., 2018. Defined drug release from 3D-printed composite tablets consisting of drug-loaded polyvinylalcohol and a water-soluble or water-insoluble polymer filler. Int. J. Pharm. 543, 361–367. https://doi.org/10.1016/j.ijpharm.2018.03.057

Tandvårds- och läkemedelsförmånsverket, 2021. Hur ska vi utvärdera och hur ska vi betala ? Hälsoekonomiska bedömningar och betalningsmodeller för precisionsmedicin och ATMP.

Thabet, Y., Lunter, D., Breitkreutz, J., 2018a. Continuous inkjet printing of enalapril maleate onto orodispersible film formulations. Int. J. Pharm. 546, 180–187. https://doi.org/10.1016/J.IJPHARM.2018.04.064

Thabet, Y., Lunter, D., Breitkreutz, J., 2018b. Continuous manufacturing and analytical characterization of fixed-dose, multilayer orodispersible films. Eur. J. Pharm. Sci. 117, 236–244. https://doi.org/10.1016/J.EJPS.2018.02.030

Tian, Y., Orlu, M., Woerdenbag, H.J., Scarpa, M., Kiefer, O., Kottke, D., Sjöholm, E., Öblom, H., Sandler, N., Hinrichs, W.L.J., Frijlink, H.W., Breitkreutz, J., Visser, J.C., 2019. Oromucosal films: from patient centricity to production by printing techniques. Expert Opin. Drug Deliv. 16, 981–993. https://doi.org/10.1080/17425247.2019.1652595

Trenfield, S.J., Goyanes, A., Telford, R., Wilsdon, D., Rowland, M., Gaisford, S., Basit, A.W., 2018. 3D printed drug products: Non-destructive dose verification using a rapid point-and-shoot approach. Int. J. Pharm. 549, 283–292. https://doi.org/https://doi.org/10.1016/j.ijpharm.2018.08.002

Trenfield, S.J., Tan, H.X., Goyanes, A., Wilsdon, D., Rowland, M., Gaisford, S., Basit, A.W., 2020. Non-destructive dose verification of two drugs within 3D printed polyprintlets. Int. J. Pharm. 577, 119066. https://doi.org/https://doi.org/10.1

016/j.ijpharm.2020.119066

Trenfield, S.J., Xian Tan, H., Awad, A., Buanz, A., Gaisford, S., Basit, A.W., Goyanes, A., 2019. Track-and-trace: Novel anti-counterfeit measures for 3D printed personalized drug products using smart material inks. Int. J. Pharm. 567, 118443. https://doi.org/10.1016/j.ijpharm.2019.06.034

Triastek, 2021. No Title [WWW Document]. URL https://www.triastek.com/indexen.html

Tseng, M.-H., Wu, H.-C., 2014. A cloud medication safety support system using QR code and web services for elderly outpatients. Technol. Heal. Care 22, 99–113. https://doi.org/10.3233/THC-140778

US Food and Drug Administration, 2013. Paving the way for personalized medicine: FDA's role in a new era of medical product development.

Vakili, H., Nyman, J.O., Genina, N., Preis, M., Sandler, N., 2016. Application of a colorimetric technique in quality control for printed pediatric orodispersible drug delivery systems containing propranolol hydrochloride. Int. J. Pharm. https://doi.org/10.1016/j.ijpharm.2016.07.032

Vakili, H., Wickström, H., Desai, D., Preis, M., Sandler, N., 2017. Application of a handheld NIR spectrometer in prediction of drug content in inkjet printed orodispersible formulations containing prednisolone and levothyroxine. Int. J. Pharm. https://doi.org/10.1016/j.ijpharm.2017.04.014

Van Riet-Nales, D.A., Doeve, M.E., Nicia, A.E., Teerenstra, S., Notenboom, K., Hekster, Y.A., Van Den Bemt, B.J.F., 2014. The accuracy, precision and sustainability of different techniques for tablet subdivision: Breaking by hand and the use of tablet splitters or a kitchen knife. Int. J. Pharm. 466, 44–51. https://doi.org/10.1016/j.ijpharm.2014.02.031

Vaz, V.M., Kumar, L., 2021. 3D Printing as a Promising Tool in Personalized Medicine. AAPS PharmSciTech 22, 49. https://doi.org/10.1208/s12249-020-01905-8

Wac, K., 2012. Smartphone as a personal, pervasive health informatics services platform: literature review. Yearb. Med. Inform. 21, 83–93.

Wang, S., Capoen, L., D'hooge, D.R., Cardon, L., 2018. Can the melt flow index be used to predict the success of fused deposition modelling of commercial poly(lactic acid) filaments into 3D printed materials? Plast. Rubber Compos. 47, 9–16. https://doi.org/10.1080/14658011.2017.1397308

Water, J.J., Bohr, A., Boetker, J., Aho, J., Sandler, N., Nielsen, H.M., Rantanen, J., 2015. Three-dimensional printing of drug-eluting implants: Preparation of an antimicrobial polylactide feedstock material. J. Pharm. Sci. 104, 1099–107. https://doi.org/10.1002/jps.24305

Watson, C., Webb, E.A., Kerr, S., Davies, J.H., Stirling, H., Batchelor, H., 2018. How close is the dose? Manipulation of 10 mg hydrocortisone tablets to provide appropriate doses to children. Int. J. Pharm. 545, 57–63. https://doi.org/10.1016/J.IJPHARM.2018.04.054

Wen, H., He, B., Wang, H., Chen, F., Li, P., Cui, M., Li, Q., Pan, W., Yang, X., 2019. Structure-Based Gastro-Retentive and Controlled-Release Drug Delivery with Novel 3D Printing 1–12. https://doi.org/10.1208/s12249-018-1237-3

WHO, 2019. The WHO Member State Falsified Medical Substandard and Mechanism on Products. Geneva.

Wickström, H., Hilgert, E., Nyman, J.O., Desai, D., Sen, D., De Beer, T., Sandler, N., Rosenholm, J.M., 2017a. Inkjet Printing of Drug-Loaded Mesoporous Silica Nanoparticles — A Platform for Drug Development. Molecules 22, 2020. https://doi.org/10.3390/molecules22112020

Wickström, H., Koppolu, R., Mäkilä, E., Toivakka, M., Sandler, N., 2020. Stencil printing—a novel manufacturing platform for orodispersible discs. Pharmaceutics 12, 33. https://doi.org/10.3390/pharmaceutics12010033

Wickström, H., Nyman, J.O., Indola, M., Sundelin, H., Kronberg, L., Preis, M., Rantanen, J., Sandler, N., 2017b. Colorimetry as Quality Control Tool for Individual Inkjet-Printed Pediatric Formulations. AAPS PharmSciTech. https://doi.org/10.1208/s12249-016-0620-1

Wickström, H., Palo, M., Rijckaert, K., Kolakovic, R., Nyman, J.O., Määttänen, A., Ihalainen, P., Peltonen, J., Genina, N., de Beer, T., Löbmann, K., Rades, T., Sandler, N., 2015. Improvement of dissolution rate of indomethacin by inkjet printing. Eur. J. Pharm. Sci. 75, 91–100. https://doi.org/10.1016/j.ejps.2015.03.009

Yang, Y., Wang, H., Li, H., Ou, Z., Yang, G., 2018. 3D printed tablets with internal scaffold structure using ethyl cellulose to achieve sustained ibuprofen release. Eur. J. Pharm. Sci. 115, 11–18. https://doi.org/10.1016/j.ejps.2018.01.005

You, M., Lin, M., Wang, S., Wang, X., Zhang, G., Hong, Y., Dong, Y., Jin, G., Xu, F., 2016. Three-dimensional quick response code based on inkjet printing of upconversion fluorescent nanoparticles for drug anti-counterfeiting. Nanoscale 8, 10096–104. https://doi.org/10.1039/c6nr01353h

Zema, L., Melocchi, A., Maroni, A., Gazzaniga, A., 2017. Three-Dimensional Printing of Medicinal Products and the Challenge of Personalized Therapy. J. Pharm. Sci. 106, 1697–1705. https://doi.org/10.1016/j.xphs.2017.03.021

Zhang, H., Hua, D., Huang, C., Samal, S.K., Xiong, R., Sauvage, F., Braeckmans, K., Remaut, K., De Smedt, S.C., 2020. Materials and Technologies to Combat Counterfeiting of Pharmaceuticals: Current and Future Problem Tackling. Adv. Mater. 32, 1–13. https://doi.org/10.1002/adma.201905486

Zhang, J., Feng, X., Patil, H., Tiwari, R. V, Repka, M.A., 2017a. Coupling 3D printing with hot-melt extrusion to produce controlled-release tablets. Int. J. Pharm. 519, 186–197. https://doi.org/10.1016/j.ijpharm.2016.12.049

Zhang, J., Yang, W., Vo, A.Q., Feng, X., Ye, X., Kim, D.W., Repka, M.A., 2017b. Hydroxypropyl methylcellulose-based controlled release dosage by melt extrusion and 3D printing: Structure and drug release correlation. Carbohydr. Polym. 177, 49–57. https://doi.org/10.1016/j.carbpol.2017.08.058

Zieverink J., 2015. FDA approves the first 3d printed drug product [WWW Document]. https://doi.org/15.10.2015

ISBN 978-952-12-4132-1